

Impact of Future Climate Change on the Building
Performance of a Typical Canadian Single-Family House
Retrofitted to the PassiveHaus

Ali Sehizadeh

A Thesis

In the Department

Of

Building, Civil, and Environmental Engineering

Presented in Partial Fulfillment of the Requirements
for the Degree of Master of Applied Science (Building Engineering) at

Concordia University

Montreal, Quebec, Canada

August 2015

@ Ali Sehizadeh

CONCORDIA UNIVERSITY

School of Graduate Studies

This is to certify that the thesis prepared

By: Ali Sehizadeh

Entitled: **Impact of Future Climate change on the Building Performance of a typical Canadian Residential Building Retrofitted to the PassiveHaus**

and submitted in partial fulfillment of the requirement for the degree of

Master of Applied Science (Building Engineering)

complies with the regulations of the University and meets with the accepted standards with respect to originality and quality.

Signed by the final examining committee:

<u>Dr. R. Zmeureanu</u>	Chair
<u>Dr. B. Lee</u>	Examiner
<u>Dr. Y. Zeng</u>	Examiner
<u>Dr. H. Ge</u>	Supervisor

Approved by Dr. M Zaheeruddin
Chair of Department or Graduate Program Director

12 August 2015

Dr. A. Asef

Dean of Faculty

ABSTRACT

Impact of Future Climate change on the Building Performance of a typical Canadian Residential Building Retrofitted to the PassiveHaus

Ali Sehizadeh

As a response to the global warming, building sector aims to be more energy efficient. The adoption of some energy efficient measures may have potential negative impacts on the building performance under a changing future climate. This study investigates the impact of future climate changes on the building performance of a typical Canadian single-family house built in compliance with current Quebec Energy Code (QEC) and retrofitted to the Passivehaus standard (PH). The building performance is evaluated in terms of energy consumption, thermal comfort, and durability over the current year, 2020, 2050, and 2080. For the energy consumption and the thermal comfort five shading device scenarios are proposed. The thermal comfort is evaluated using an adaptive model for naturally ventilated houses. Durability is also evaluated in terms of the freeze thaw risk on brick and the biochemical risk on plywood. Durability analysis is carried out on two types of above-grade wall assemblies that meet the QEC standards and retrofitted options to the PH. The future weather files are generated using General Circulation Models (GCM) HadCM3 with the IPCC's A2 emission scenario.

Simulation results showed that by upgrading the current typical houses in Canada to the PH standard, compared to the current climate, the overall thermal performance of the PH in terms of the energy consumption and the thermal comfort would decrease by 2080. This study concludes that upgrading the current wall assemblies to the PH standard would increase the freeze thaw risk

of the brick veneer, however, compared to the current climate this risk would decrease under 2080 climate. While the biochemical risk of the plywood sheathing defined by the moisture content criteria would decrease, the risk defined by RHT criteria would increase over future climates. The mold growth risk on the plywood sheathing would likely decrease under the future climates.

ACNOWLEDGEMENT

I would like to express my sincere gratitude to my supervisor Dr. Hua Ge for the continuous support of my research. She is the one who always encouraged me and gave me motivation not only in my research but also in these two years of my life as an international student in Canada. I appreciate her deep knowledge.

Special thanks to my loved ones, my dear family, my mother, my father, my beloved twin brother “Mehdi”, my grandfather, and my grandmother for all the support they have provided me over the years. I will be grateful forever for your love. Words cannot express how indebted I am to all of the sacrifices that you’ve made. Your prayer for me was what sustained me thus far.

Again my deepest gratitude to Mehdi who is not only my brother but also the best friend that I could ever have. He has been always supported me, given me energy and motivation even when he was thousands miles away.

At the end I would like express gratefulness to my friends Mehdi, Amirreza especially to my dear friend Nassim for helping me get through the difficult times.

DEDICATION

I would like to dedicate my thesis to my beloved family, my father, my mother and Mehdi who has always stayed by my side and supported me.

Table of Contents

List of Figures	x
List of Tables	xiii
CHAPTER 1. Introduction	1
1. 1. Research Objectives	2
1. 2. Thesis Organization	2
CHAPTER 2. Literature Review	4
2. 1. 1. Energy Efficient Retrofitting	4
2. 1. 2. Envelope Retrofitting	5
2. 2. Thermal Comfort in Highly Insulated Buildings	7
2. 2. 1. PassiveHaus Standard	7
2. 2. 2. Thermal Comfort Model	8
2. 2. 3. Overheating	10
2. 3. Durability	11
2. 3. 1. Moisture in Material	11
2. 3. 2. Frost Decay Exposure Index (FDEI)	13
2. 3. 3. Frost Damage Risk in Bricks	14
2. 3. 4. Biochemical Risk in Plywood	15
2. 4. Future Climate and the Building Performance	18

2. 4. 1.	Meteorological Data	18
2. 4. 2.	IPCC Scenarios	18
2. 4. 3.	Future Precipitation and Rainfall	20
2. 4. 4.	Impact of Future Climate on the Building Performance	23
2. 5.	Summary and Conclusion.....	28
CHAPTER 3.	Methodology.....	30
3. 1.	Thermal Performance	31
3. 1. 1.	The Case Study House	31
3. 1. 2.	Montreal Future Climate Conditions.....	32
3. 1. 3.	Thermal Comfort.....	35
3. 1. 4.	Whole Building Energy Simulation Using IES >Ve<	36
3. 1. 5.	Natural Ventilation Control.....	37
3. 1. 6.	Shading Strategies.....	38
3. 2.	Durability.....	39
3. 2. 1.	Selection of Base Year for Rain Data	39
3. 2. 2.	Future Rain Data	44
3. 2. 3.	Building Envelope Retrofitting options	48
3. 2. 4.	Performance Indicators	50
3. 2. 5.	Simulation Scenarios and Settings	52

3. 3.	Summary and Conclusion.....	54
CHAPTER 4.		55
4. 1.	Energy Consumption	55
4. 2.	Thermal Comfort	59
4. 3.	Durability.....	64
4. 3. 1.	Frost Decay Exposure Index FDEI: Current V.S. Future	64
4. 3. 2.	Frost Damage Risks for Bricks	65
4. 3. 3.	Biodegradation Risk on Plywood.....	72
CHAPTER 5. Conclusion.....		80
5. 1.	Summary of Research.....	80
5. 2.	Research Contributions and Conclusions	81
5. 2. 1.	Energy Consumption.....	81
5. 2. 2.	Thermal Comfort.....	81
5. 2. 3.	Durability	82
5. 3.	Limitations.....	83

List of Figures

Figure 3-1. Framework of this study.....	30
Figure 3-2. A typical two-storey detached Canadian house (base case) (National Research Council, 2010).....	31
Figure 3-3. Observed changes in global average land and sea surface temperature (Hulme, et al., 2002).....	33
Figure 3-4. Dry bulb temperature at Montreal International Airport in current year, 2020, 2050, and 2080.....	34
Figure 3-5. Ground temperature at Montreal International Airport in current year, 2020, 2050, and 2080.....	34
Figure 3-6. Relative humidity at Montreal International Airport in current year, 2020, 2050, and 2080.....	35
Figure 3-7. Building modeled in IES [VE}	37
Figure 3-8: Shadings Scenarios proposed for this study.....	38
Figure 3-9: Collected rain data from the weather station at Montreal International Airport (Environment Canada's National Climate Services, 2013).....	40
Figure 3-10. Airfield WDR calculated using Montreal International Airport data for year 1953 to 1994.....	42
Figure 3-11. The amount of snowfall in Montreal International Airport between 2009 and 2014; quarter of the year (Environment Canada, 2014)	44
Figure 3-12. The amount of rainfall and precipitation in Montreal International Airport between 2009 and 2014; quarter of the year (Environment Canada, 2014).....	45
Figure 3-13. Proposed linear trend for the seasonal amount of rainfall by 2020, 2050, and 2080.	47
Figure 3-14. Historical and future proposed linear trend for the rainfall intensity in Montreal International Airport	48
Figure 3-15. Wall retrofit strategies: Double Stud Wall.....	49
Figure 3-16. Solid masonry wall retrofit strategies: Sprayed Foam	49

Figure 3-17. Solid masonry wall retrofit strategies: XPS	50
Figure 4-1. Comparison in heating load between the QEC house and the PH retrofitted option over current and future years	55
Figure 4-2: Comparison in cooling load between the QEC and the PH retrofitted option over current and future years	56
Figure 4-3: Impact of shading systems on the monthly heating and cooling loads of the PH retrofitted option in 2013.	57
Figure 4-4: Impact of shading on the monthly heating and cooling loads of the PH retrofitted option in 2080.	57
Figure 4-5. Comparison of heating and cooling loads in QEC and PH retrofitted building with different shading strategies over current and future years.	58
Figure 4-6. Thermal comfort limits as a function of outdoor temperature using adaptive model for naturally ventilated residential buildings and monthly average outdoor temperatures in 2013 and 2080.....	59
Figure 4-7. Internal temperature of specified room in QEC and PH with/without shading in 2013 in comparison to 80% and 90% acceptability limits in 2013.....	60
Figure 4-8. Internal temperature of specified room in QEC and PH with/without shading in 2080 in comparison to 80% and 90% acceptability limits in 2080.....	61
Figure 4-9. Comparison of number of hours in which the internal temperature of the specified bedroom is above 26°C, between the base-case (QEC) and retrofitted to PH building with different shading scenarios	62
Figure 4-10. Comparison of number of hours in which the internal temperature of the specified bedroom is within 90% (Solid color) and 80% (dash-line) thermal comfort acceptability, between base-case (QEC) and retrofitted to PH building with different shading scenarios.	63
Figure 4-11. Comparison of the airfield WDR for the base weather (1973) and by 2020, 2050, and 2080 at Montreal International Airport.	64
Figure 4-12. Comparison of the historical and future FDEI in Montreal International airport for 1day, 2days, 3days, and 4days prior to the freezing point.	65
Figure 4-13. Comparison of the relative humidity and temperature at 5mm into the Calcium Silicate brick of the single stud (base case) and the double stud (retrofitted) under three years of simulation R2=0.35. Based weather data (1973).	66

Figure 4-14. Comparison of the Moisture content of 10mm into the Calcium Silicate in wood-frame assemblies under three years of simulation at Montreal International Airport. R2=0.35. Based weather data 1973 67

Figure 4-15. Comparison of the Moisture content of 10mm into the Calcium Silicate in solid masonry assemblies under three years of simulation at Montreal International Airport. R2=0.35. Based weather data 1973 67

Figure 4-16. RH and T of plywood in the single stud (base) and double stud (retrofitted) assemblies with buff matt clay as the exterior brick. No source, R2=0.07 73

Figure 4-17. Impact of the moisture/air sources on the %MC of plywood in single stud assembly (base) and retrofitted with double stud with Buff Matt clay as exterior brick. R2=0.07..... 73

Figure 4-18. Impact of the moisture/air sources on the %RH and T of plywood in double stud assembly with old brick as the exterior brick. R2=0.07 75

Figure 4-19. Mold growth index of plywood sheeting in double stud assembly over three years of simulation under base weather data (1973) at Montreal International Airport. With decreasing consideration. 78

List of Tables

Table 2-1. PassiveHaus recommended design principles (Passive House Institute, 2012).....	8
Table 2-2. The six ‘storylines’ use in the SRES emissions scenarios in decreasing order of atmospheric CO ₂ concentration at the year 2100; also shown is an: IPCC Special Report on Emission Scenarios (Nakicenovic & Swart, 2007; IPCC, 2007).....	19
Table 2-3. Annual and seasonal precipitation change in Montreal International Airport from 1950 to 2007 and from 2010 to 2050 (Institute for Catastrophic Loss Reduction, 2011).	22
Table 2-4. Change of ratio of snow to total precipitation in Montreal International Airport from 1950 to 2007, and from 2010 to 2050 (Institute for Catastrophic Loss Reduction, 2011).	22
Table 3-1. Building properties and the Quebec Energy Code requirements (CANLII, 2013)	32
Table 3-2. Comparison of the PassiveHaus Standard Requirements with PH Retrofitted Option (Passive House Institute, 2012).....	32
Table 3-3. Components that are varied for different simulation scenarios.....	36
Table 3-4. Comparison of maximum WDR, maximum rainfall intensity and ranking of each year among years between 1953 and 1994	43
Table 3-5. Seasonal solid snowfall, rain, precipitation and liquid snowfall in 2010 at Montreal International Airport (Environment Canada, 2014).....	46
Table 3-6. Basic hygric properties of brick and plywood provided in WUFI database (Fraunhofer IBP, 2013).....	54
Table 3-7. Simulation scenarios.....	54
Table 4-1. Number of crossing point occurs at 5mm of the most exterior layer of bricks over three-year simulation under the current climate (based on 1973) at Montreal International Airport	68
Table 4-2. Impact of orientation on the number of crossing points at 5mm into the brick.	69
Table 4-3. Number of hours that 5mm into the bricks has the both humidity of above 95% and crossing point under the current climate (based on 1973) at Montreal International Airport.	70
Table 4-4. Number of crossing point occurs at 5mm into the most exterior layer of brick under the current climate (based on 1973) and by 2020, 2050, and 2080 at Montreal International Airport. R ₂ =0.35.....	70

Table 4-5. Number of hours that 5mm into the most exterior layer of bricks has the both humidity of above 95% and crossing point under the current climate (based on 1973) and by 2020, 2050, and 2080 at Montreal International Airport. $R^2=0.35$ 71

Table 4-6. Number of hours that plywood in double stud assembly would be within biochemical risk defined by 20% of MC, 30% of MC, and RHT criteria over the second year of simulation under current climatic condition at Montreal International Airport. 74

Table 4-7. Number of hours that plywood would be within biochemical risk defined by 20% of MC, 30% of MC, and RHT criteria over the second year of simulation years under current and future climate of Montreal. 76

Table 4-8. Impact of rain deposition factor on the mold growth index of plywood sheeting over three years of simulation under current climate of Montreal International Airport. 78

Table 4-9. Impact of climate change on the mold growth index of plywood sheeting over three years of simulation under current climate of Montreal International Airport. 79

CHAPTER 1. Introduction

Recent worldwide attention toward energy security and CO₂ emission reduction appeals different sectors to be more energy efficient. There is no doubt that future climate change would impact on the building performance, energy consumption, and occupant comfort (Robert & Kummert, 2012). Potential changes in global climate would increasingly impact the built environment. Perhaps the most remarkable of these changes concerns the influence of higher air temperatures on the thermal performance of buildings (Sajjadian, et al., 2013). Observed weather records demonstrated that the global average near-surface temperature over land and sea has been increased by 0.75 °C over the 20th century (Sharpless, 2009). Sharpless, (2009) also explained that the warming rate has been greater over land regions than over the oceans and has been the greatest in higher northern latitudes. Bill Dunster Architects and Arup R&D (2005) also demonstrated the importance of mitigating climate change effects by designing homes with energy efficiency features to balance the expected increases in air temperatures. They identified that under the UK climate conditions the energy saving of masonry houses with the inherent thermal mass over their life time would be more than the energy saving in a lightweight timber frame house. The study demonstrated that lightweight homes would result in discomfort caused by higher internal temperature (Bill Dunster Architects, 2005). Therefore, it is important to take into account the future climate conditions so that buildings can be designed to be adaptable to their intended future environment.

Currently, the building sector aims to reduce energy consumption by improving building envelope thermal performance. Higher energy efficiency has been set in building codes in Canada and the USA in recent years. Beyond various energy codes that have been set worldwide, the German

standard entitled PassiveHaus (PH), which attempts to reduce energy consumption by 90% within dwellings, is gaining popularity in North America. This high level of energy reduction requires highly insulated building envelopes and high efficiency of heat recovery ventilation systems. While the standard aims to increase both thermal comfort and energy saving, there is a potential risk and uncertainty about the performance of houses built to the PH standard under future climate conditions.

1. 1. Research Objectives

The objective of this study is to assess the performance of a typical Canadian single-family house retrofitted to the PH level under the Montreal's current and future climate conditions in terms of energy consumption and risks of summer overheating in comparison to the same house built to the Quebec Energy Code (QEC). Moreover, the impact of future climate on the thermal comfort of naturally ventilated residential building built in compliance with QEC and retrofitted to the PH is analyzed. The impact of shading devices on the overall energy consumption is also investigated. Furthermore, potential of the freeze thaw and mold growth risk is studied within number of assemblies which meet the requirements of the PH standard under the current and future climate of Montreal.

1. 2. Thesis Organization

This thesis has been structured as follows: Chapter 1 presents an overview of the research topic, the scope and objectives of the research. Chapter 2 reviews the existing literature on energy efficient retrofitting, thermal comfort of highly insulated buildings, future climate change, and the impact of climate change on the building performance. In chapter 3, a typical Canadian single-

family house used as the case study for this research is presented. Moreover, proposed methods for future climate generation, thermal comfort analysis, determination of frost decay risk on bricks and biodegradation risks on plywood, and simulation scenarios are discussed. Simulations and findings of the proposed methods are presented in chapter 4. Chapter 5 concludes this thesis with a summary of findings.

CHAPTER 2. Literature Review

2. 1. 1. Energy Efficient Retrofitting

Globally the building construction and their operation accounts for a large proportion of total energy consumption. According to the report done by IEA Energy Conservation in Building and Community Systems by 2050 in most industrialized countries existing buildings contribute to more than 80% of the energy consumption and less than 20% by the new buildings built from now to 2050 (IEA, 2011; Ma, et al., 2012). Studies done by Three Regions Climate Change Group (TRCCG), Simons, Barlow & Fiala, and Adibi et al demonstrated that the housing stock turnover is low at around 1 to 1.5% worldwide (TRCCG, 2008; Simons, 2008; Barlow & Fiala, 2007; Asadi, et al., 2012).

The Sustainable Development Commission predicted that by 2050 about 70% of the housing stock in the UK has already been built (SDC, 2007). Moreover, Simons (2008) revealed that building sector consumes four times and seven times more energy than the commercial sector and public administration sector, respectively. Therefore, energy efficient retrofitting of the existing buildings, and particularly housing stock, would significantly result in reducing the total energy consumption of building sector worldwide.

In the last decade significant efforts have been made among different countries towards energy efficient retrofitting of existing buildings. According to Department of Energy (DOE, 2009), US government has specified a new \$450 million national-wide program to upgrade existing buildings in U.S which experts estimated that this would annually save \$100 million in utility bills for households and businesses. In Australia, since November 2010 the Commercial Building

Disclosure (CBD) programme has obligated the owners of Australia's large commercial office buildings to provide energy efficiency. Australian government stated that in 2010 around 10% of Australian greenhouse Carbon Dioxide CO₂ emission is because of commercial buildings and this would increase to over 25% by 2020 (Department of Resources, 2010). Moreover, the UK government made a remarkable commitment to increase the energy efficiency of 7.0 million British dwellings by 2020 aiming at reducing carbon emissions by 29% (DOECC, 2010).

Natural resources of Canada (Canada, 2011) also declared that the Eco-Energy retrofit-home program has specified up to \$5000 incentive for each householder to upgrade the efficiency of their dwellings. Preliminary analysis showed that using this program was successful; whereas between 2005 and 2012 only Ontario invested \$2 billion for the program resulted in avoiding more than \$4 billion in new supply costs (Ministry of Energy, 2013).

According to Ma et al (2012) building retrofitting has several challenges and the existence of uncertainties is the main one. Climate change, service change, government policy changes, human behavior change, etc., are uncertainties that would directly impact on the selection of retrofitting strategies. Other challenges would include financial obstacles such as initial investments and payback periods (Ma, et al., 2012; Tobias & Vavaroutsos, 2009). Among all sectors, domestic sector appears to have significant potential for energy saving and CO₂ emission reduction. Study done by Gamtessa & L.Ryan (2007) showed that only by upgrading the building envelope and furnace, 46% of CO₂ emission reduction is achievable in Canada.

2. 1. 2. Envelope Retrofitting

Building envelope retrofitting can be either done from exterior or interior. However, for each method there are various retrofitting options to enhance the energy efficiency and hygrothermal

performance (CMHC, 2012). For historical buildings or buildings with valuable façades in an urban context interior insulation may be the only feasible strategy. However, it may reduce usable interior space. Moreover, it would significantly change the hygrothermal performance of the assemblies, which would result in the increase of condensation risk, mold growth risk, and frost decay (Vereecken, et al., 2015; Haupl, et al., 2003).

According to CMHC, if an interior retrofitting is undertaken, for the above grade walls the existing drywall or gypsum board and vapor barrier have to be removed and another row of wood framing stud has to be added and filled with insulation. Then, new layer of vapor barrier, air barrier and gypsum board have to be installed. Exterior retrofitting also involves removing the existing cladding and installation of an air barrier followed by new insulation and rain screen and new cladding. Usually, extruded polystyrene (XPS) or expanded polystyrene (EPS) are considered as the external insulations (CMHC, 2012).

A study done by Straube & Schumacher (2007) investigated interior insulation retrofits of load bearing masonry walls in terms of moisture control principles in cold climates. Several insulating materials including polyurethane, polystyrene, polyisocyanurate, sprayed foam and XPS were investigated using WUFI. Simulation results showed that closed cell polyurethane with high density would be an acceptable solution for thin applications with about 2” thickness. For the larger thicknesses if the interior humidity is kept low open-celled semi permeable foam was recommended. Moreover, rigid foam board such as expanded/extruded polystyrene or unfaced polyisocyanurate has shown to be a successful approach for interior retrofitting. This method, however, is more difficult to be implemented since it requires firmly contact of the board with the

masonry. This study concluded that among mentioned materials the use of semi-permeable foam insulation is the most successful strategy for interior retrofitting.

2. 2. Thermal Comfort in Highly Insulated Buildings

2. 2. 1. PassiveHaus Standard

Higher energy efficiency has been set in building codes in Canada and the USA in recent years. Among various energy codes that have been set worldwide, the German standard entitled PassiveHaus (PH), which attempts to reduce energy consumption by 90% within dwellings, is gaining popularity in North America (Passive House Institute, 2011; Badea, et al., 2014). Passive house (PH) is a building that demands low energy requirements but maintains appropriate comfort for occupants. Nevertheless, most of the PH certified houses are not completely passive and have active mechanical ventilation system. In order to achieve the PH certification, buildings have to meet the PassiveHaus standard requirements. High insulation, extremely air tight envelope, passive solar gain, heat recovery, day lighting, shading, energy efficient appliances and lighting, and high performing windows are measures that are stringently considered in the PassiveHaus standard (Straube , 2009). If active cooling is required in the PH building, the cooling demand should not exceed 15KWh/m²/year. Also, the total primary energy demand for a passive house should not exceed 120 KWh/m²/year (Passive House Institute, 2012). This high level of energy reduction requires highly insulated building envelopes and high efficiency of heat recovery ventilation systems. While the standard aims to increase both thermal comfort and energy saving, there is a potential risk and uncertainty about the performance of houses built to the PH standard under the future climate conditions.

Table 2-1. PassiveHaus recommended design principles (*Passive House Institute, 2012*)

<i>Component</i>	<i>Passive House Requirements</i>
<i>Insulation</i>	Attic/Roof: Total RSI 9.0-16.0 m ² K/W
	Exterior walls: RSI 7.0–10.5 m ² K/W
	Foundation wall: RSI 5.5–9.0 m ² K/W
<i>Windows</i>	Window U-values of ≤ 0.8 W/m ² k
<i>Air-tightness</i>	0.6 ACH @50 Pa
<i>Heat recovery Ventilator (HRV)</i>	High Efficiency (80%)
<i>Heating load</i>	< 10w/m ²
<i>Cooling Load</i>	< 8w/m ²

2. 2. 2. Thermal Comfort Model

According to ASHRAE, “thermal comfort is the condition of mind which expresses satisfaction with thermal environment” (ASHRAE, 2010). There are typically three thermal comfort approaches including the Predicted Mean Vote PMV method, survey, and the adaptive method (Orosa & Oliveira, 2011). The PMV method is generally used to evaluate the thermal environment in buildings with heating, ventilation and air-conditioning (HVAC) system. For naturally ventilated buildings the adaptive model showed more reasonable predictions (Orosa & Oliveira, 2011; Alfano, et al., 2013). Compared to occupants in centrally air-conditioned buildings, the occupants in naturally ventilated spaces were more responsive to their indoor climate (Dear & Brager, 2001). A few studies investigated the thermal comfort in naturally ventilated residential buildings using adaptive model (Dear & Brager, 2001; Peeters, et al., 2009; Halawa & Van Hoof, 2012). In which the study by Peeters et al. is the most comprehensive listed below.

In recent decade, remarkable number of literatures have been done for air-conditioned buildings using PMV models. Also, there are a number of experimental studies which tried to compare results obtained by PMV method with occupant’s expectations. There are number of literatures

which used adaptive approach to predict thermal comfort. Most of these literatures dealt with commercial, offices and schools and a few of investigations focused on residential buildings. Moreover, studies are mainly done for hot and moderate climates.

Peeters et al. (2009) categorized residential buildings into three different zones including bedrooms, bathrooms and other rooms. For each zone, according to specified metabolic rate, clothing index, relative humidity, air speed, and ranges of outdoor temperature, different neutral temperatures were proposed. Peeters et al. (2009) used the theoretical analysis on psychological and behavioral adaption, body temperature and metabolism of occupants proposed by Maeyens et al. (2001) to estimate the following parameters which results in achieving 90% acceptability for bedrooms:

- Metabolic rate of sleeping: 0.7 met
- Clothing index (sleepwear, sheets, mattress and pillow): 0.8 clo
- Relative humidity: 55%
- Air speed: 0.05 - 1 m/s

Based on these values the course of the bedroom's neutral temperature as a function of the outdoor temperature is as below:

$$T_n = 20.40 + 0.06 \cdot T_{e,ref} \quad T_{e,ref} < 12.5 \text{ }^\circ\text{C} \quad (1)$$

$$T_n = 16.63 + 0.36 \cdot T_{e,ref} \quad T_{e,ref} \geq 12.5 \text{ }^\circ\text{C} \quad (2)$$

Where, T_n stands for neutral temperature and $T_{e,ref}$ for the monthly averaged external temperature.

The acceptable thermal comfort regions for residential buildings are defined using seven points ASHRAE scale (-3 to +3) (Oseland, 1994; van der Linden, et al., 2006; Humphreys & Hancock, 2007) . The equations to calculate upper limit and lower limit of comfort band are as below:

$$T_{\text{upper}} = T_n + w\alpha \quad (3)$$

$$T_{\text{lower}} = T_n - w(1 - \alpha) \quad (4)$$

Where α is a constant equal to 0.7 and the value of w is 5°C and 7°C in case of acceptability of 90% and 80% respectively.

2. 2. 3. Overheating

De Dear et al also presented an adaptive model of thermal comfort for buildings with natural ventilation. Their study showed that when the mean outdoor effective temperature changes from 5°C to 27 °C, the indoor operative temperature varies from 20°C to 25°C (De Dear & Brager, 1998).

Athienethis and Santamouris (2002) indicated that the risk of overheating in highly insulated houses would not only exist in summer but also in winter. Orme et al. (2003) studied the overheating risk in a lightweight highly insulated house using IES >Ve<. They calibrated the dynamic thermal model using on-site measurements. Simulations showed that in a well-insulated free-running house with natural ventilation, an external temperature of 29°C may result in an internal temperature over 39°C.

The application of shading device on buildings in hot climates or subtropical would be an effective solution in terms of reducing cooling loads and improving thermal comfort (Al-Tamimi & Fadzil, 2011; Chan, 2012; Freewan, 2014; Wang, et al., 2014). Application of shading systems for buildings built to the PH standard is essential in warm climates (IPHA, 2010). However, studies have shown that the provision of external shading devices in cold climates would increase the total energy demand of building (Palmero-Marrero & Oliveira, 2010; Nikoofard, et al., 2014). Given the warming of the future climates thus the increase of cooling loads and risks for overheating,

there is a need to investigate the effect of shading for a cold climate under future climatic conditions.

2. 3. Durability

2. 3. 1. Moisture in Material

Study done by Djebbar et al (2002) presented an analytical approach to investigate the effects of building envelope retrofit strategies on the hygrothermal performance of masonry walls in Canada. This study mainly focuses on the moisture related failures in wall assemblies with Brick Veneer and Steel Stud Back-up (BV/SS) using hygrothermal simulation model (*hygIRC*). Three hygrothermal indicators including moisture mass index MMI, freeze thaw index FTI, and relative humidity/temperature index RHT were chosen to predict the potential for moisture damage. As defined in *hygIRC*, the moisture mass index is defined as Equation 5:

$$MMi = (U_{end} - U_{Start}) / U_{Start} \quad (5)$$

Where U_{end} and U_{start} is the daily average of the total moisture in the envelope component considered (kg/m) at the end and start of one year calculation respectively.

Moreover, this study also investigated Freeze Thaw Index to predict the hygrothermal risks caused by repeated free-thaw cycle in every part of the walls. *hygIRC* defines this index as the number of cycles when two indicators are available. First, temperatures fluctuate between freezing and thawing point; and secondly, the envelope component is almost at the moisture saturation level. Equation 6 shows this index.

$$FT(i,j) = \sum_{K=2}^{8760\text{hours}} Cycle(i,j,k) \quad (6)$$

with

$$Cycle(i,j,k)=1 \text{ if } T(i,j,k)*T(i,j,k-1) < 0 \text{ and } \phi(i,j,k) > \phi_{critical}$$

$$Cycle(i,j,k)=0 \text{ if } T(i,j,k)*T(i,j,k-1) > 0 \text{ or } \phi(i,j,k) < \phi_{critical}$$

where

$T(i,j,k)$ calculated temperature (K) within the considered part of the envelope component at a particular time step

$\phi(i,j,k)$ calculated relative humidity (%) within the considered part of the envelope component at a particular time step

$\phi_{critical}$ critical moisture saturation level (%) in the envelope component

i,j spatial indices for the considered part of the envelope component

k considered time step index

Moreover, the critical moisture saturation level, $\phi_{critical}$, is defined based on the nature of construction material. In this study above 95% relative humidity were assumed for frost damage to occur (Djebbar, et al., 2002). Results for the top corner of a 10 storey building with BV/SS assembly in Halifax showed that the only location that frost decay occurred were on the exterior surface of brick veneer.

Furthermore, this study investigated another hygrothermal indicator entitled RHT index, which was used to predict any moisture risk when high moisture levels and warm temperatures occur for a long time. This hygrothermal indicator is commonly used for the sample of corrosion, biomechanical damages, efflorescence, swelling, and expansion (Djebbar, et al., 2002). Equation 7 shows this indicator:

$$RHT(i,j) = \sum_{K=1}^{8760\text{hours}} T_{Potential}(i,j,k) \times \phi_{potential}(i,j,k) \quad (7)$$

with

$$T_{potential}(i,j,k) = T(i,j,k) - T_{critical} \text{ if } T(i,j,k) > T_{critical}$$

$$T_{potential}(i,j,k) = 0 \text{ if } T(i,j,k) < T_{critical}$$

$$\phi_{potential}(i, j, k) = \phi(i, j, k) - \phi_{critical} \text{ if } \phi(i, j, k) > \phi_{critical}$$

$$\phi_{potential}(i, j, k) = 0 \text{ if } \phi(i, j, k) < \phi_{critical}$$

where

$T_{potential}(i, j, k)$	temperature potential for moisture damage (K) within the considered part of the envelope component at a particular time step
$\phi_{potential}(i, j, k)$	moisture potential for moisture damage (%) within the considered part of the envelope component at a particular time step
$T_{critical}$	Critical temperature level (K) above which moisture damage is more likely to occur
$\phi_{critical}$	Critical relative humidity level (%) above which moisture damage is more likely to occur

Moreover, according to IEA Annexe 14 conclusions, typical values of 80% relative humidity for $\phi_{critical}$ and 5°C for $T_{critical}$ were assumed for biochemical risks. Moreover in this study, for corrosion, expansion, and efflorescence 80% relative humidity and 0°C were assumed for $\phi_{critical}$ and $T_{critical}$ respectively (Djebbar, et al., 2002; IEA Annex 14 Final Report, 1991).

2. 3. 2. Frost Decay Exposure Index (FDEI)

Freezing and thawing of porous, mineral materials in combination with large amount of precipitation reflect a significant challenge in designing climate adapted high performance building envelopes. Therefore, it is essential to investigate frost decay risk.

Frost decay risk assessment would be more challenging task for the future climate. Because, there are always uncertainties about future weather conditions. This would add more challenges to investigate future frost decay risk in the building envelope. However, it is predicted that in the future temperature, precipitation and windiness would likely increase. Consequently, facades would likely receive more driving rain (Köliö, et al., 2014).

The frost resistance of a porous, mineral material significantly depends on the material properties and climate impacts. Lis et al (2007) used the climate exposure indices to express the relative

potential of frost decay based on collected rainfall and temperature data from thirteen exemplified stations in Norway and from the reference thirty year period of 1961 to 1990. They investigated the Frost Decay Exposure Index (FDEI) for the accumulated annual average sum of 2-day, 3-day and 4-day rainfall prior to days with freezing points. They concluded that a 4-day spell of rainfall would be a reliable basis for the frost decay risk analysis.

2. 3. 3. Frost Damage Risk in Bricks

Wilkinson et al (2009), Wytrykowska (2012), and Ueno (2013) investigated brick masonry freeze thaw degradation risk using critical saturation threshold measurement. These studies all involved the use of specialized equipment and labour which is costly. Therefore, this method is usually limited to the high value and heritage buildings. Engineers, however, may use the default properties of materials in literature or simulation software database (Wilkinson, et al., 2009; Wytrykowska, et al., 2012; Ueno, et al., 2013; Straaten, 2014).

Due to the time and budget limitation exist in the most typical engineering practices the use of representative material properties is more often preferred rather than sample measurements. Hugh and Bargh (1982) succeeded to establish correlation between the limestone type, building location, and the 'degree of weathering'. However, their attempt to find an approach for brickwork was unsuccessful due to the lack of uniformity in brick manufacturing process (Hughes & Bargh, 1982). Another research done by Laefer et al. (2004) encountered the same obstacle which was assumed to be due to the inconsistency in brick manufacturing processes.

WUFI software does not include critical saturation values which are usually used for the post processing analysis. Therefore it is valuable to compare the measured data with the WUFI material

data base properties. Building science laboratory tested bricks from a number of buildings built between 1830 and 1950 mostly in Northern America to see if the correlation can be found. Four different bricks archived in the WUFI material Northern America database have been tested. Free water saturation, critical saturation and vacuum saturation were included in test results. Results showed that these terms would significantly varies among different bricks (Straaten, 2014; Fraunhofer IBP, 2013).

2. 3. 4. Biochemical Risk in Plywood

Canada Mortgage and Housing Corporation studied and developed recommendations for energy efficient retrofitting strategies applicable on four different housing archetypes across Canada. Energy efficient strategies were investigated on roofs, above grade walls, below grade walls, and windows. Several assemblies were evaluated in terms of feasibility, energy saving potentials, hygrothermal performance, and cost effectiveness under current climate of Vancouver, Halifax, Toronto, and Edmonton. Double stud, Larsen truss, exterior XPS insulation, exterior mineral wool insulation, interior VIPs, and exterior VIPs are assemblies investigated for the above grade wall assemblies. The study also used HOT2000 and WUFI for evaluation of energy usage and hygrothermal performance respectively (CMHC, 2011). For the hygrothermal performance evaluation three moisture/air sources were introduced including “No Source”, exposed to “Air-leakage”, and exposed to a “driving rain leak”. Moreover, moisture content analysis were carried out on the sheathing over two consecutive years. Two percentage of Moisture Content MC of 20% and 30% were considered as limits for the hygrothermal risk on the plywood. Results showed that near net zero retrofits could be technically feasible but might address moisture related performance issues. The study suggested that combination of renewable energy techniques with some of the

most cost effective envelope retrofitting strategies would a cheaper solution to meet overall energy efficiency goals (CMHC, 2011).

Study done by Sedlbauer (2002) indicated that over the last decades the thermal improvement of buildings has affected building performance by creation of micro-organisms such as mold fungi. This issue occurred due to the thermal conduction and air leakage reduction in buildings; which would likely increase as building are being constructed higher insulation and airtightness. The study also defined four main factors as the boundary conditions for mold growth including humidity, temperature, substrate, and time; whereas increase in humidity, temperature, or time would remarkably impact on the mold growth risk.

There are several ways to illustrate the growth conditions for mold. “Isopleth diagrams” are one of the ways which differ for various types of mold and portrait the germination time of growth rate. Time, humidity, and temperature are keys in these models. However, certain temperature have to be set in order to describe the mold risk. “Spore water Content” is another way of illustrating the mold risk. In this model the key condition for germination of the spore is humidity which determines moisture content of the spore. The probability of the mold growth is affected by realistic unsteady boundary conditions. However, in this approach it is assumed that if the moisture content of the spore exceeds specified limit the risk of germination exists (SEDLBAUER, 2002).

The mathematical model of the mold growth on wooden material developed by Hukka and Viitanen (1999) are often used for evaluating mold growth risk (Nik, et al., 2012; Fedorik & Illikainen, 2013; IEA, 2015; Viitanen & Ojanen, 2007). This model calculated the critical relative humidity as a function of temperature shown in *Equation 8*. *Equation 9* shows the mold growth

potential, m , which is the relation between the relative humidity and critical relative humidity.

Whereas values of m greater than 1 were considered as favorable conditions for mold growth.

$$RH_{\text{Critical}} = \{-0.00267T^3 + 0.161T^2 - 3.13T + 100 \text{ when } T \leq 20; 80\% \text{ when } T > \} \quad (8)$$

$$m = \frac{RH}{RH_{\text{critical}}} \quad (9)$$

Exposure time is a critical parameter influencing the mold growth. When a structure remains at favourable conditions for mold growth over a long period of time, the mold growth risk would likely increase. The mold growth index under favourable conditions can be calculated using *Equation 10*. Under unfavourable conditions, mold growth will be slowed down. *Equation 11* can be used for the calculation of mold growth index under unfavourable conditions, where m is less than one.

$$\frac{dM}{dt} = \frac{1}{168 \exp(-0.68 \ln T - 13.9 \ln RH + 0.14W - 0.33SQ + 66.02)} k_1 k_2 \quad (10)$$

$$\frac{dM}{dt} = \begin{cases} -0.00133 & \text{when } t - t_1 \leq 6h \\ -0 & \text{when } 6h < t - t_1 \leq 24h \\ -0.00067 & \text{when } t - t_1 > 24h \end{cases} \quad (11)$$

Where W is timber species, SQ is surface quality, t is time and k_1 and k_2 are coefficients for growth. As suggested by Fedorik et al. (2013), to obtain the safest results $k_1=1$, $k_2=1$, $SQ=0$, and $W=0$ are assumed. The mold growth index has a range of 0 to 7. Whereas, 0 is for no growth, 1 for less than 10% mold coverage (microscopic), 2 for 10% mold coverage (microscopic), 3 for 10-30% mold coverage (visual), 4 for 30-70% mold coverage (visual), 5 for above 70% mold coverage (visual), and 6 for heavy and tight growth with 100% coverage.

2. 4. Future Climate and the Building Performance

2. 4. 1. Meteorological Data

There are several weather stations located inside or in vicinity of cities owned and operated by government bodies. Environment Canada collects, records and archives all meteorological data across Canada. This weather data is organized in different formats including hourly, daily, monthly, and yearly. There are two sets of data for the Canadian climate which are available from the website. The first one is the Canadian Weather Energy and Engineering Data Sets (CWEEDS) which is organized in the ASHRAE Weather Year for Energy Calculation² WYEC² format and contains information of 145 Canadian Locations of the last 51 years starting as early as 1953 (Environment Canada, 2014; Environment Canada, 2008).

Canadian Weather for Energy Calculation (CWEC) is the second type of meteorological data set prepared by Environment Canada. This data set contains 12 months of the highest occurrence data within the 30 years CWEEDS data and it is available for 75 stations across Canada (Environment Canada, 2008).

2. 4. 2. IPCC Scenarios

The first requirement for investigation of any study over the future is the projection of future climate. Atmosphere-Ocean Global Circulation Models (AOGCM) are shown to be the most widespread available models for future climate projections (Wang & Chen, 2014; Solomon, et al., 2007). However, among all GCM models HadCM3 model proposed by Hadley center in the UK has been gained more popularity (Levy, et al., 2004; Johns, et al., 2003). The Intergovernmental Panel on the Climate Change (IPCC) has published an assessment report investigating the future

climate parameters over the different global latitudes (Solomon, et al., 2007). IPCC proposed six ‘storylines’ for future emissions of greenhouse gases and other anthropogenic factors including B1, A1T, B2, A1B, A2, and A1F1. Whereas, B1, B2, A2, and A1F1 are the main scenarios which stand for low-emission, medium-low, medium-high, and high emission scenarios, respectively. A1B and A1T are derived from the combination of main scenarios. These six scenarios are based on the future demographic, economic and technological growth trends. Among IPCC Scenarios, the ‘A’ group assumes the world economic growth is the key driver in a way similar to today. For the other two scenarios- ‘B’ groups, sustainability is the dominant driver (Solomon, et al., 2007; Nakicenovic & Swart, 2007). All of these scenarios project the future warming. For example, IPCC predicted up to 6°C increase in the near-surface temperature over land of Northern latitudes for the period of 2080 to 2099 using A2 scenario. *Table 2-2* shows these six widely used greenhouse emission storylines.

Table 2-2. The six ‘storylines’ use in the SRES emissions scenarios in decreasing order of atmospheric CO₂ concentration at the year 2100; also shown is an: IPCC Special Report on Emission Scenarios (*Nakicenovic & Swart, 2007; IPCC, 2007*)

<i>Scenario</i>	<i>Key drivers</i>	<i>Underlying assumptions</i>	<i>Atmospheric CO₂ /ppm</i>	<i>Total radiative forcing at 2100/W·m⁻²</i>
<i>A1F1</i>	Economic growth Convergent world Fossil fuel energy	A convergent world with substantial reduction in regional differences in per capita income and rapid economic growth; a global population that peaks in mid-century and declines thereafter; rapid introduction of new technologies; energy sources based primarily on continuing use of fossil fuels	970	9.14
<i>A2</i>	Economic growth Heterogeneous world	A heterogeneous world with self-reliance and preservation of local identities; fertility patterns across regions converge very slowly, resulting in continuously increasing global population; economic development is primarily regionally oriented; per capita economic growth and technological change are more fragmented and slower than in other storylines	856	8.07

A1B	Economic growth Convergent world Mixed energy sources	As A1F1 but with energy based on a balance across fossil and non-fossil sources	717	6.05
B2	Sustainability Heterogeneous world	A heterogeneous world with local and regional solutions to economic, social, and environmental sustainability and social equity; continuously increasing global population but at a rate lower than A2; intermediate levels of economic development; less rapid and more diverse technological change than in the B1 and A1 storylines	621	5.71
A1T	Economic growth Convergent world Non-fossil fuel energy	As A1F1 but with energy based on non-fossil fuel sources	582	5.07
B1	Sustainability Convergent world	A convergent world with global solutions to economic, social, and environmental sustainability with an emphasis on improved equity; the same global population as in the A1 storyline but with rapid changes in economic structures toward a service and information economy; reductions in material use intensity; introduction of clean and resource-efficient technologies	549	4.19

2. 4. 3. Future Precipitation and Rainfall

IPCC observed significant increase of precipitation in North and South America from 1900 to 2005 (Solomon, et al., 2007). The study found that the global mean precipitation would increase under A1B scenario, however, the precipitation extremes would be lower than other IPCC scenarios. In addition, they compared the precipitation change of the A2 scenario over ocean and land at various global latitudes for the period of 2080 to 2099 using “precipitation change” and “precipitation change scaled by global temperature” graphs. The study predicted that over the future climates the amount of precipitation would likely increase at high latitudes but decrease in mid-latitude areas. About 20% change in 2100 has been projected under the A1B scenario.

According to Warner (2012) future precipitation at different latitude would vary worldwide. Whereas for a number of locations increase is predicted and in other decrease is forecasted. It also

predicted that in Canada the precipitation would increase by up to 20% by 2020, 40% by 2050 and 60% by 2080. Study done by Jylha et al. (2009) also investigated the projections for the CO₂ level, temperature and precipitation over future climate of Finland for the three CO₂ scenarios of A1, A2 and B1. This study showed that for the Finland latitude based on the A2 scenario the precipitation would likely increase by 3%, 8%, and 12% in 2020, 2050 and 2080 respectively (Jylha, et al., 2009).

The University of Waterloo along with around 80 experts from across the Canada has released a report about the climate change adoption in Canada (University of Waterloo, 2012). According to this report the temperature in Canada will increase by up to 2°C by 2020 and 4°C by 2050. Moreover, this study predicted that precipitation in Canada will increase by up to 20% and 40% in 2020 and 2050 respectively.

Roy et al. (2001) investigated the future climate changes using different GCMs for the southern Quebec area. They concluded that depending on the CO₂ emission Scenario there would be between 1°C to 3.5°C increase in temperature and up to 10% increase in precipitation over the next 100 years. They also used the Canadian CGCM1 model to analyze the amount of rainfall between three different periods of time including 1975-1995, 2020-2040, and 2080-2100. The CGCM1 model uses the observed CO₂ emission data from 1900 to 2000 and for the years after 2000 and it generalized data based on an annual 1% increase in GHG. This study concluded that for the southern Quebec region compared to the precipitation for years 1975-1995, the annual precipitation would decrease by 2.2% for years 2020-2040 and increase by 4.7% for years 2080-2100.

Research done by the Institute for Catastrophic Loss Reduction has provided several future weather parameters, particularly for the year 2050, using CGCM2 model and A2 (high emission) scenario for different locations in Canada (Institute for Catastrophic Loss Reduction, 2011). Annual and seasonal temperature, precipitation, and ratio of snow to the total precipitation are parameters predicted for different locations for 2050. This study showed that the total annual precipitation for Montreal region will increase by 5-15% from 2010 to 2050. The total amount of precipitation in winter, spring, summer, and autumn would increase by 10-15%, 15-20%, 0-10% and 0-10%, respectively at this location. The annual ratio of snow to total precipitation would decrease by 10-20%, and the ratio of snow to total precipitation in winter, spring and autumn would decrease by 15%, 15%, and 5-10%, respectively. Table 2-3 and Table 2-4 show the change of annual and seasonal precipitation and snow to total precipitation ratio for Montreal International Airport from 1950 to 2007 and from 2010 to 2050.

Table 2-3. Annual and seasonal precipitation change in Montreal International Airport from 1950 to 2007 and from 2010 to 2050 (Institute for Catastrophic Loss Reduction, 2011).

	1950-2007	By 2050 from 2010
Annual	5% to 15%	5% to 15%
Winter	-5% to 15%	10% to 15%
Spring	5% to 15%	15% to 20%
Summer	0% to 10%	0% to 10%
Autumn	0% to 15%	0% to 10%

Table 2-4. Change of ratio of snow to total precipitation in Montreal International Airport from 1950 to 2007, and from 2010 to 2050 (Institute for Catastrophic Loss Reduction, 2011).

	1950-2007	By 2050 from 2010
Annual	0% to -10%	-10% to -20%
Winter	0% to -5%	-15%
Spring	0% to -10%	-15%
Autumn	0% to 5%	-5% to -10%

Fenech & Comer (2013) also investigated the future projections of climate change for the Atlantic Region of Canada using 40 GCM models proposed in the fifth Assessment Report (AR5) of IPCC. While providing no guarantee, this study calibrated an ensemble of all GCMs with the historical climatic data and concluded that an ensemble model is likely more accurate in representing future conditions. They also concluded that the amount of precipitation by 2050 in Montreal would likely increase by 9.4%, which is in the precipitation range that the Institute for Catastrophic Loss Reduction has predicted for 2050.

IPCC in their Fourth Assessment Report projected the precipitation change of different latitudes for the period of 2080 to 2099 under the A2 scenario (Solomon, et al., 2007). For the latitude of 45.4° N at the Montreal International Airport, the A2 scenario projected an increase of about 6% in the precipitation over the land, which is within the predicted range of increase by the Institute of Catastrophic Loss Reduction (Institute for Catastrophic Loss Reduction, 2011). The seasonal projections of the future precipitation for Montreal provided by the Institute of Catastrophic for Loss Reduction using IPCC's A2 (medium-high emission) scenario is used for future rain data generation.

2. 4. 4. Impact of Future Climate on the Building Performance

The impact of future climates on the building performance have been investigated in recent years with the majority of studies focused on the future heating and cooling demand of buildings (Jentch, et al., 2008; Gaterell & McEvoy, 2005; Wang, et al., 2010; de Wilde, et al., 2008; Lomas & Giridharan, 2012; Chowa, et al., 2013; Bjorsell, et al., 1999; Nijland, et al., 2009; Grossi, et al., 2007; Wan, et al., 2012) . For example, the study done by Berger et al (Berger, et al., 2014)

investigated the impact of future climate change on the cooling and heating energy demand of office buildings in Austria using IPCC's A1B emission scenario. This study used the German database entitled as REMO-UBA for the future climate generation (Jacob, et al., 2008). Investigations were carried out for four categories of office buildings including buildings built before World War I (ONB), buildings built after WWI (BGN), highly glazed buildings built after 2000 (STG), and buildings built to the PassiveHaus standard after 2000 (SOL4). Results showed that with varying constructions cooling demand would likely increase and heating demand would decrease over future climates. Whereas by 2050 the cooling demand of ONB, BGN, STG, and SOL4 would increase by 92%, 39%, 28%, and 41% respectively. Moreover the heating demand for these building types would decrease by 30%, 26%, 11%, and 56% respectively. Zmeureanu and Renaud (2008) investigated the impact of climate change on the heating energy use of existing domestic buildings in Montreal area using A2 scenario and GCM2 model. They concluded that from 1961 to 1990, which represents the current climate, and from 2040 to 2069, which represents the future climate, the heating energy use would likely reduce by 7.9% and 16.9% respectively. Jylha et al. (2009) assessed the energy demands of houses over future climate conditions of Finland using a dynamic simulation tool entitled IDA Indoor Climate and Energy (IDA-ICE) program (Bjorsell, et al., 1999; Sahlin, et al., 2004). The study concluded that the heating demand would decrease between 20% and 40% by 2100. However, the cooling demand would increase by 40-80%. The authors attributed the wide ranges to the uncertainty of the future greenhouse emission evolution. The annual overall energy use of a typical detached house in Finland was predicted to decrease by 20-35% by 2100. This study also did a long-term economic analysis indicating that because of the climate change by 2100 the net value of household's energy costs would decrease by 5-10% compared to the current year.

Aguiar et al. (2002) evaluated the energy consumption of Portuguese buildings at three different locations including North, Centre, and South between 2070 and 2099 using monthly and daily data generated by HadCM3 and HadRM models. The study concluded that while from north to south the heating demand would decrease between 34% and 60%, from north to centre the cooling demand would increase between 130% and 525%.

Nik and Kalagasidis also investigated the impact of future climates on the energy performance of 153 statically selected buildings built in Stockholm. This study covered 12 different scenarios for generation of the future climate. Three cooling strategies including natural ventilation, mechanical ventilation and hybrid system were used in simulations using a dynamic building energy simulator programme developed in MATLAB software. The study concluded that by 2100 the heating demand would decrease by 30% compared to 2011. Results showed that the heating demand would vary for about 30% between different climate scenarios and even more for the cooling demand. Moreover, this study demonstrated that the natural ventilation would be an appropriate solution for mitigating the future overheating risk (Nik & Kalagasidis, 2013).

Study done by Karimpour et al. (2015) also evaluated the impact of future climate on the energy efficient building envelopes design philosophy under the current climate and by 2070. Heating and cooling demands were studied on a building with various combination of wall assemblies, roof assemblies, reflected foil, and different floor coverings under the climate of Adelaide, Australia. The study concluded that over the future climates in well insulated buildings cooling demand would be significantly more important than heating demands. Moreover, it resolved that for the heating dominated climates like Adelaide design approaches should be more focused on the cooling design strategies.

Several studies also evaluated the building indoor temperature and thermal comfort under future climates (Gaterell & McEvoy, 2005; Coley , et al., 2012; Coley & Kershaw, 2010; Wan, et al., 2012; Ren, et al., 2011; Lomas & Giridharan, 2012; Gupta & Gregg, 2012; Mavrogianni, et al., 2012; Haojie & Chen, 2014) . For example, Haojie and Chen (2014) evaluated the thermal comfort and heating and cooling energy use of buildings in the United States (US) using HadCM3. This study generated weather data for 15 cities of the US under three CO2 emission scenarios of IPCC's B1, A2, and B1F1. For each city two types of residential building and seven types of commercial buildings were simulated using EnergyPlus Software. They concluded that by 2080 natural ventilation would not be an appropriate solution for San Diego but it would be acceptable for San Francisco and Seattle.

Study by Gupta & Gregg (2012) showed that over future climate changes the comfort temperature would increase in the summer while remains the same in the winter. Using the adaptive approach, Van Hoof, J et al investigated the indoor thermal comfort as a function of outdoor temperature. Results showed that the acceptable indoor temperature within thermal comfort zone for cold climates such as Canada varies between 20°C to 25°C (Halawa & Van Hoof, 2012).

Jenkins D.P et al (2013) investigated the overheating risks of a typical residential building over future years at different locations in the UK using Integrated Environmental Solutions Virtual Environment >IES Ve< and SAP. Simulation results from IES indicated that while the risk of indoor overheating in London would increase by about 5% between 2005 and 2030, there would be no indoor overheating risk in Edinburgh between these years. The increase in summer temperature over the future climates would increase the risks of overheating as well as the cooling energy consumption, especially in highly-insulated buildings

These existing studies mainly focused on investigating the impact of future climates on the energy performance of buildings and indoor thermal environment, there are limited studies on the impact of future climates on the durability of buildings, especially for North American. Given the global warming and the climate change, a few studies predicted the building durability based on the possible changes in climate parameters of European countries (Nijland, et al., 2009; Grossi, et al., 2007; Nik, et al., 2012). For example, Nijland et al. (2009) investigated the impact of climate change on the durability of porous materials (brick and natural masonry stone) used in building envelopes under the Netherlands climate. This study used four scenarios of climate change developed by the Royal Netherlands Meteorological Institute to generate the future climates (Van Den, et al., 2006). They found that under all four scenarios the future climate of Netherlands would likely experience an increase in temperature, extreme amount of precipitation, intensity of severe rain in summer, and solar radiation. However the total number of rainy days in summer, relative humidity, and the soil moisture content would decrease over the future climates. Their study concluded that the higher temperature and higher precipitation under future climate would decrease the number of freeze thaw cycles on porous materials, however, these conditions would likely speed up the biocolonization and biodegradation for timber, stony materials, and coatings. The study by Grossi et al. (2007) investigated the freeze thaw risk in Europe under the future climates. This study Used HadCM3 model with IPCC's A2 scenario to generate the future European weather data. This study also concluded that the frost damage on the porous stone used in monuments of temperate areas would remarkably decrease over the future climate. Kolio et al. (2014) predicted that in the future temperature, precipitation and windiness would likely increase. Consequently, facades would likely receive more driving rain. Lis et al (2007) used the climate exposure indices to express the relative potential of frost decay based on collected rainfall and

temperature data from thirteen exemplified stations in Norway and from the reference thirty year period of 1961 to 1990. They investigated the Frost Decay Exposure Index (FDEI) for the accumulated annual average sum of 2-day, 3-day and 4-day rainfall prior to days with freezing points. They concluded that a 4-day spell of rainfall would be a reliable basis for the frost decay risk analysis.

Nik et al. (2012) assessed the impact of future climate on the mould growth risk in ventilated attics under the Sweden climate through hygrothermal simulations for the period of 1961 to 2100 using RCA3 regional climate model (RMC) and the IPCC's A2, A1B, and B1 emission scenarios. The study concluded that the potential risk of mould growth would increase over the future climates. However, changing the emission scenarios would not change the mould growth risk of the attic.

2. 5. Summary and Conclusion

So far, beside these reviewed literatures many other studies were found with the focus on the future heating and cooling demand of buildings (Jentch, et al., 2008; Gaterell & McEvoy, 2005; Wang, et al., 2010; de Wilde, et al., 2008; Lomas & Giridharan, 2012). Moreover, several studies also evaluated the building indoor temperature and thermal comfort under future climates (Gaterell & McEvoy, 2005; Coley , et al., 2012; Coley & Kershaw, 2010; Wan, et al., 2012; Ren, et al., 2011; Lomas & Giridharan, 2012; Gupta & Gregg, 2012; Mavrogianni, et al., 2012). These studies mainly investigated the impact of future climates more on the thermal performance of the buildings in the Europe, US, Australia and Asia and less for the North America's climate. Moreover, there are a few literatures on the impact of future climate on the durability of buildings in North America or elsewhere. Therefore, a question arises that can energy efficient retrofitting of the building

envelope be a robust approach to address energy consumption reduction, thermal comfort improvement, and durability enhancement under the Northern America's future climate?

CHAPTER 3. Methodology

This study investigates the impact of climate change on the performance of a typical building in compliance with the Quebec Energy Code (QEC) retrofitted to the PassiveHaus (PH) standard. The term “performance” is assessed by three different topics including energy consumption, thermal comfort, and durability. For the energy consumption and the thermal comfort simulations are carried out on a whole house as the case study. However, for the durability analysis investigations are narrowed into the assembly itself. Moreover, while energy consumption and thermal comfort analysis are done using typical hourly weather data provided by the US Department of Energy (DOE), durability analysis requires more detailed weather data which includes rain data (U.S. Department of Energy, 2012). Therefore, methodology chapter is divided into two subsections and the methodology for the energy consumption/thermal comfort and durability is presented separately. The framework of this study is summarized in Figure 3-1.

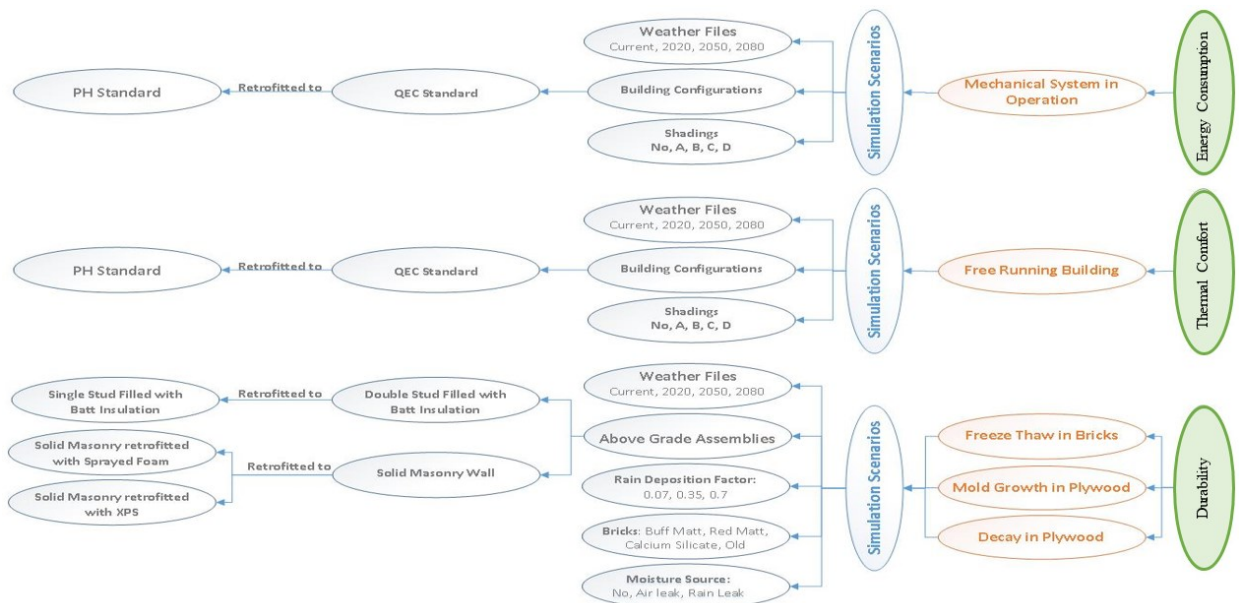


Figure 3-1. Framework of this study

3. 1. Thermal Performance

3. 1. 1. The Case Study House

A typical two-storey detached single-family house is considered for energy consumption/thermal comfort analysis shown in *Figure 3-2*. This house, which represents a typical Canadian residential house, was built in 1998 as a research facility at the National Research Council of Canada and it is south oriented. The house is a two story detached building with a hipped roof, a two-car garage and a full basement with livable area of 210 m² (2260 ft²). The total windows area is 35.0 m² (377 ft²) (15% of the total wall surface area) and with 16.2 m² (174 ft.²) South facing windows. This house is used to investigate two scenarios. The first scenario assumes that the house is built in compliance with the Quebec Energy Code (QEC) and the actual properties of the building are used in simulations. The second scenario assumes that the house is retrofitted to the PassiveHaus (PH) standard. *Table 3-1* compares the QEC requirements with the actual thermal performance of the house (National Research Council, 2010). *Table 3-2* also compares properties of the retrofitted option with the PH standard.

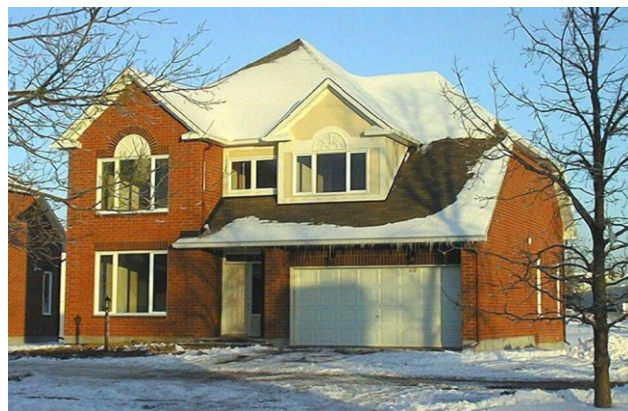


Figure 3-2. A typical two-storey detached Canadian house (base case) (National Research Council, 2010)

Table 3-1. Building properties and the Quebec Energy Code requirements (CANLII, 2013)

<i>Component</i>	<i>QEC Requirements</i>	<i>Building Properties Description</i>
<i>Insulation</i>	Attic/ceiling: Minimum R Value: 5.3 m ² k/W	Attic/Ceiling: Total R Value: 6.98 m ² k/W (Asphalt shingles, Roofing felt, Plywood, Cavity, 260mm glass wool insulation, polyethylene, Gypsum board)
	Exterior wall: Minimum R Value: 3.4 m ² k/W	Exterior Wall: Total R Value: 3.89 m ² k/W (Brick veneer, 19mm air space, Tyvak, Plywood, 140mm Batt insulation, Polyethylene, Gypsum Board)
	Foundation wall: Minimum R Value: 4.7 m ² k/W	Foundation wall: Total R-Value: 4.7 m ² k/W (Compacted soil, Plastic drainage with cementitious coating, 89mm Expanded polystyrene rigid board, damproofing, Concrete foundation wall, 89mm Batt insulation, polyethylene, Gypsum board)
<i>Windows</i>	Maximum U-Value: 2.85 W/m ² k	Total U-Value: 2.34 W/m ² K Small Double glazing windows- Low e-coating, 30% Glazed frame
<i>Air-tightness</i>	2.5 ACH @50 Pa	2.5 ACH @50 Pa
<i>Heat recovery Ventilator (HRV)</i>	Minimum 40% Efficiency	High Efficiency (67%)

Table 3-2. Comparison of the PassiveHaus Standard Requirements with PH Retrofitted Option (Passive House Institute, 2012)

<i>Component</i>	<i>Passive House Requirements</i>	<i>Passive house Retrofitted Option</i>
<i>Insulation</i>	Attic/Roof: Total R-value: 9.0-16.0 m ² K/W	Attic/Roof: Total R-Value: 14.40 m ² K/W (Asphalt shingles, Roofing felt, Plywood, Cavity, 500mm Glass wool, 40mm Polyurethane, Polyethylene, Gypsum Board)
	Exterior walls: RSI 7.0–10.5 m ² K/W	Exterior Wall: Total R-Value: 10.38 m ² K/W (Brick veneer, 19mm air space, Tyvak, Plywood, 140mm Polyurethane, 140 mm Expanded Polystyrene, Polyethylene, Gypsum Board)
	Foundation wall: RSI 5.5–9.0 m ² K/W	Foundation wall: Total R-Value: 8.39 m ² K/W (Compacted soil, Plastic drainage with cementitious coating, 89mm Expanded polystyrene rigid board, damproofing, Concrete foundation wall, 140mm polyurethane closed cell insulation, polyethylene, Gypsum board)
<i>Windows</i>	Window U-values of ≤ 0.8 W/m ² k	Window U-values of ≤ 0.8 W/m ² k Low-E Triple Glazing SC=0.65
<i>Air-tightness</i>	0.6 ACH @50 Pa	0.6 ACH @50 Pa
<i>Heat recovery Ventilator (HRV)</i>	High Efficiency (80%)	High Efficiency (80%)
<i>Heating load</i>	< 10w/m ²	-----
<i>Cooling Load</i>	< 8w/m ²	-----

3. 1. 2. Montreal Future Climate Conditions

In this study future weather data files are generated using the CCWeatherGen program. This program was developed by the Sustainable Energy Research Group at the University of Southampton. The software uses the current Montreal weather file to generate future weather files

by using HadCm3 model and A2 emission scenario. Among all IPCC scenarios, A2 is more widely used, which is categorized by a heterogeneous world with regionally oriented economic development; self-reliant nations; continuously increasing population; and slower and more fragmented technological changes (Robert & Kummert, 2012). Figure 3-3 shows the observed and predicted changes in global sea surface temperature. As mentioned B1, B2, A2, and A1F1 are main scenarios which stand for low emission, medium-low, medium-high, and high emission scenarios respectively. In this study to prevent overestimating and underestimating analysis B1 and A1F1 are not considered. Moreover, since the study investigates the risk of climate change on the building performance A2 which is a medium-high scenario is used. *Figure 3-4, Figure 3-5, and Figure 3-6* plot the dry bulb temperature, ground temperature and relative humidity at the Montreal International Airport under the current and future years.

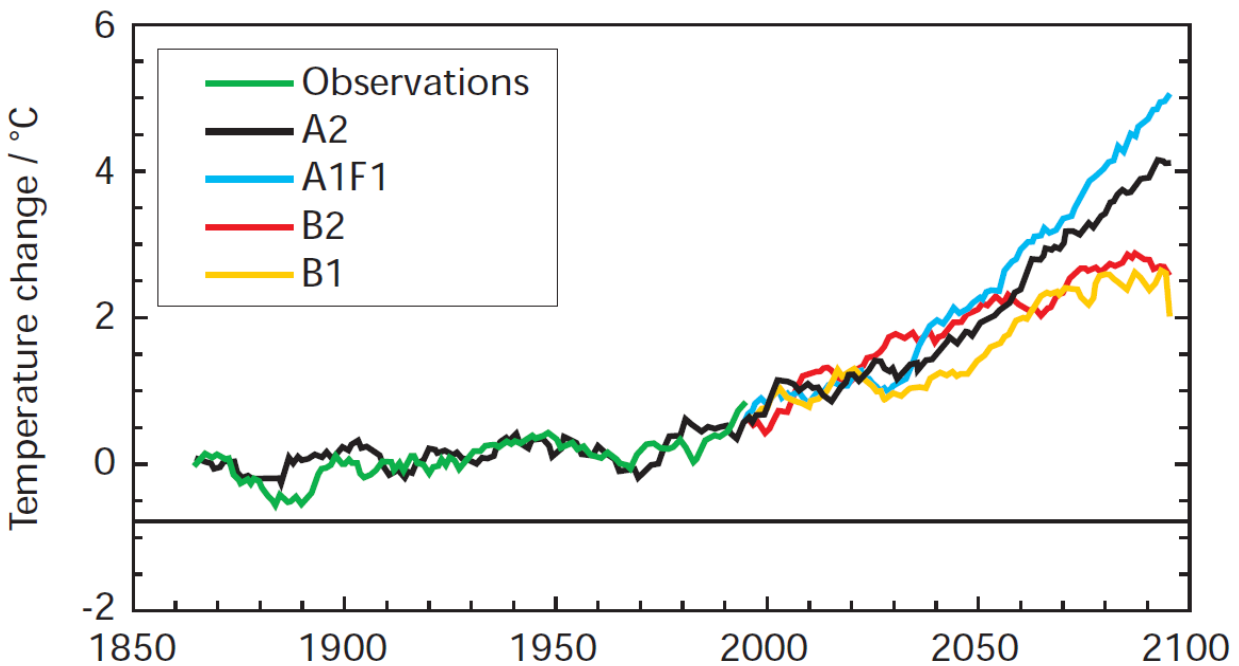


Figure 3-3. Observed changes in global average land and sea surface temperature (Hulme, et al., 2002)

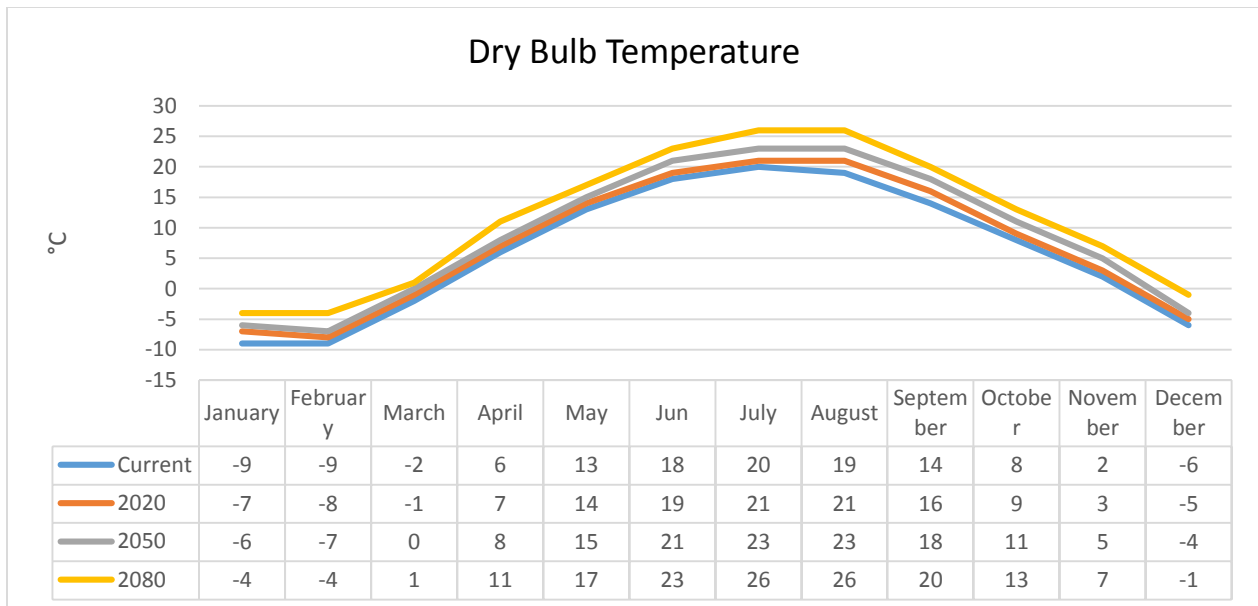


Figure 3-4. Dry bulb temperature at Montreal International Airport in current year, 2020, 2050, and 2080.

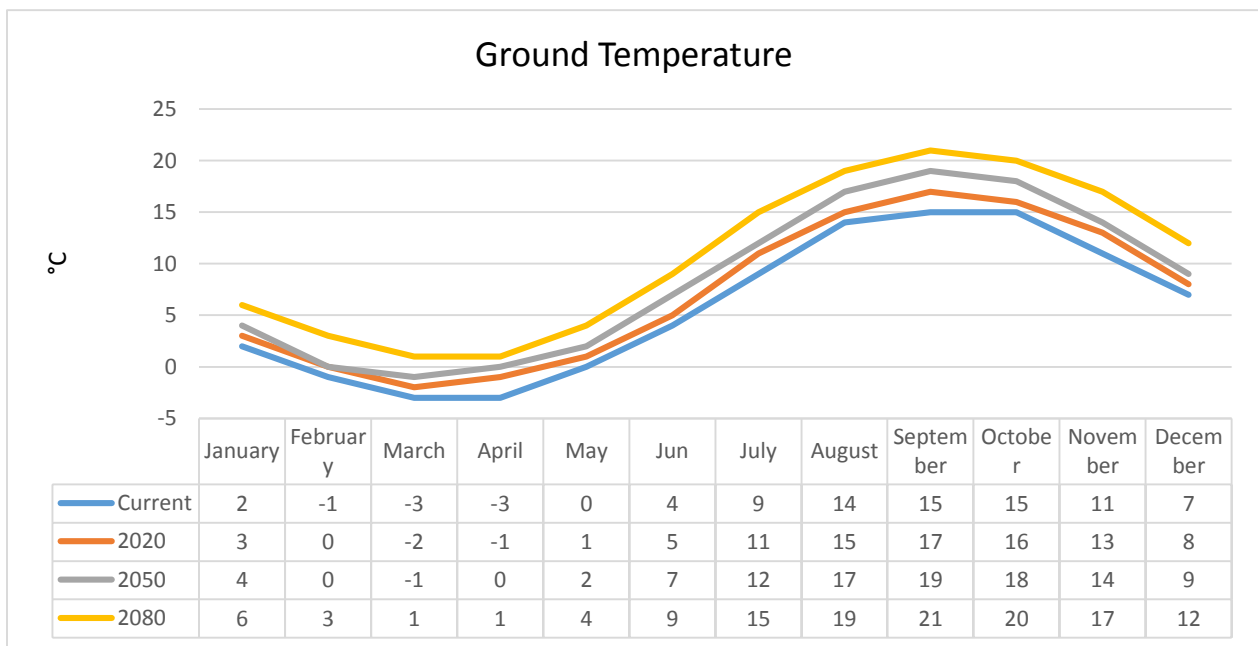


Figure 3-5. Ground temperature at Montreal International Airport in current year, 2020, 2050, and 2080

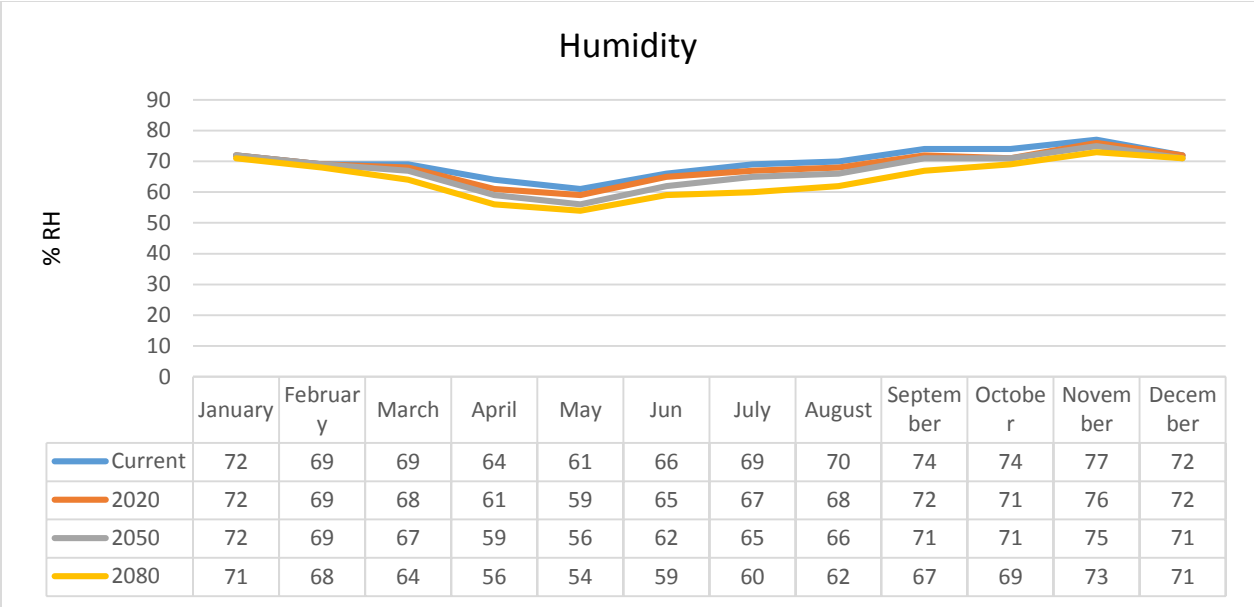


Figure 3-6. Relative humidity at Montreal International Airport in current year, 2020, 2050, and 2080.

As shown in *Figure 3-4* and *Figure 3-5*, the dry bulb temperature and ground temperature in Montreal would increase over future years. Therefore, the risk of overheating within buildings would potentially increase in the future. *Figure 3-6* shows that in summer the relative humidity would decrease over the future climate. Increase of the temperature and decrease of the relative humidity would likely impact on the building performance and particularly on the hygrothermal issues and requires further investigations.

3. 1. 3. Thermal Comfort

While thermal comfort is a complex term defined by different parameters, taking all these parameters into account is out of the scope of this research. In this study, two different methods are considered. The first method is a simplified approach, which considers an indoor air temperature of 26°C or greater as overheating (McLeod, et al., 2013; Sajjadian, et al., 2013; Kwong, et al., 2014). The Second method is the adaptive model proposed by Peeters et al. (2009)

mentioned in section 2. 2. 2. , in which the bedroom’s neutral temperature is defined as a function of outdoor temperature defined in the literature review.

3. 1. 4. Whole Building Energy Simulation Using IES >Ve<

Several computational software have been developed to analysis the building thermal performance. Integrated Environment Solutions Virtual Environment IES >Ve< is a well-developed dynamic software used for the building performance analysis based on the hourly weather data. In this study, IES >Ve< is used to analysis the building thermal performance. The excessive number of corners on the north and south facades and roof have been eliminated in building the model to shorten simulation time. *Table 3-3* shows the components that are varied for different simulation scenarios.

Table 3-3. Components that are varied for different simulation scenarios

<i>Components</i>	<i>Description</i>
<i>Weather files</i>	Current year, 2020, 2050 and 2080
<i>Opaque building envelope thermal characteristic</i>	QEC house and retrofitted option to PH (refer to <i>Table 3-1</i> and <i>Table 3-2</i>)
<i>Maximum infiltration rate</i>	2.5ACH for QEC, 0.6ACH for retrofitted option to PH
<i>Solar shading components</i>	1m overhang, 0.5m overhang, 30° angled louver shading, and 30° angled shading with 0.5m overhang

Solar radiation is the main parameter that influences the variation of indoor temperatures in different rooms in the building and contributes to the overheating. To simplify simulations only one bedroom located at the south west of the second floor is considered for indoor temperature analysis. This room is highlighted in the model shown in *Figure 3-7*. As for heating and cooling loads and the total energy consumption, the whole building is considered.

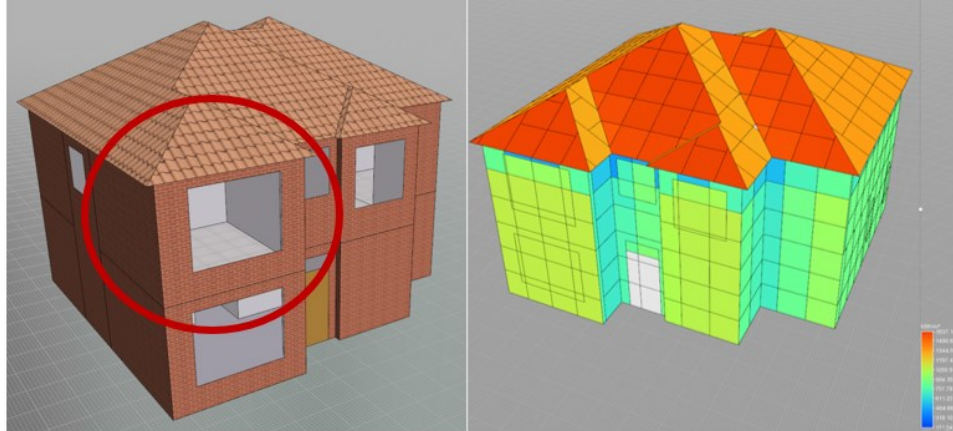


Figure 3-7. Building modeled in IES [VE}

This model has been specified to have central natural gas-fired furnace system with efficiency of 89%. Furthermore, Energy Efficiency Ratio (EER) of 3.6 has been specified for the cooling system. Moreover, sum of sensible cooling load and dehumidification plant load are considered as cooling load. Also, maximum sensible gain of 10.76W/m^2 , including single-family florescent lighting profile, single family equipment profile and 5 persons family, has been set as internal gain. The heating set point of 20°C and cooling set point of 25°C are specified in simulations, which means that when the internal temperature is lower than 20°C or higher than 25°C , the mechanical system will be turned on to maintain the desired indoor temperature range.

3. 1. 5. Natural Ventilation Control

Windows are adjusted to have 30% openable area. Windows are side hung with maximum opening angel of 20° . Also, the opening threshold of 20°C has been considered to control the natural ventilation. Which means that they will be opened when the outdoor temperature is 20°C or more.

3. 1. 6. Shading Strategies

As mentioned in the literature review, several literatures demonstrated that over the future climate the cooling demand of highly insulated buildings would increase. Therefore climate change approaches need to dramatically focus more on cooling strategies. Implementation of shading systems could be one these strategies which requires further investigation for various locations. Therefore, in this study the impact of shading systems on the internal temperature and energy consumption is also investigated by considering five different shading scenarios including no shading, typical shading with 1m overhang (shading A), typical shading with 0.5m overhang (shading B), 30° angled louver shading (shading C), and 30° angled shading with 0.5m overhang (shading D). To be able to investigate the indoor internal temperature building is considered as a free running model. Energy consumption, however, is studied when the HVAC system is in operation to maintain acceptable conditions. Figure 3-8 illustrates these scenarios.

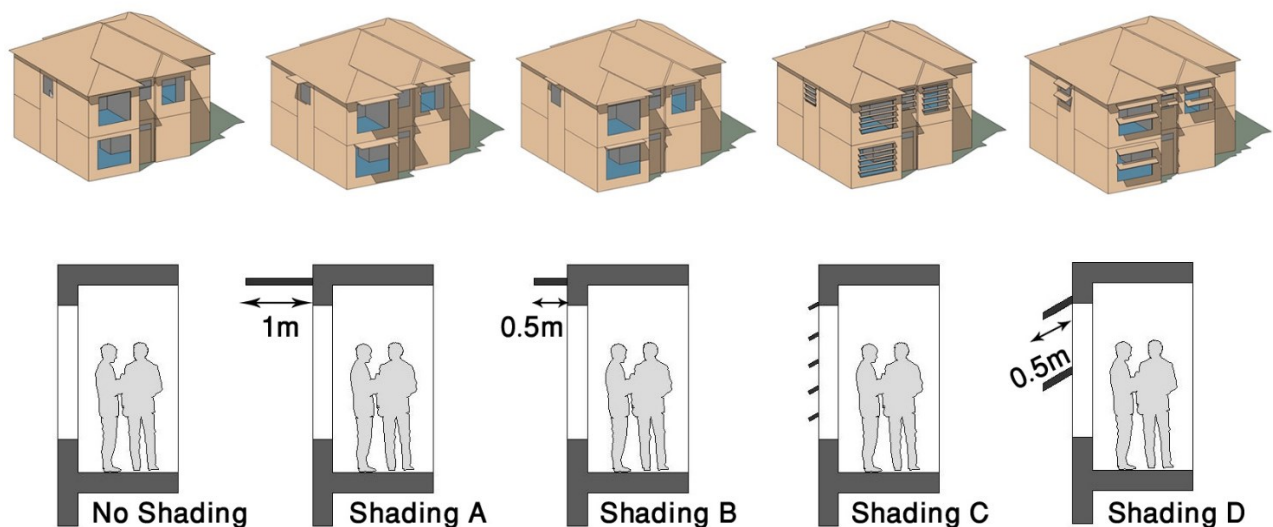


Figure 3-8: Shadings Scenarios proposed for this study

3. 2. Durability

The objective is to evaluate the durability of retrofitted building envelopes under future climates. Two existing above grade exterior wall assemblies are considered as the base assemblies for retrofitting. One assembly is the common Pre-World War II solid masonry construction and the second is the common Post-War 2x4 wood frame construction. The solid masonry is retrofitted from the interior using two types of insulations, i.e. Sprayed Polyurethane foam and Extruded Polystyrene board to achieve an effective thermal resistance of 6.49 m²k/W. The 2x4 wood frame wall is retrofitted using double stud with 89mm gap between studs filled with batt insulation to achieve an effective thermal resistance of 8.18 m²k/W. Durability is investigated in terms of the freeze thaw risk of the brick and biodegradation of the plywood sheathing in wood-frame assemblies. The Frost decay Exposure index (FDEI) and relative humidity of above 95% and the existence of crossing point RHCP are considered as the performance indicators for brick. The biodegradation of plywood is assessed using three criteria: 1) percentage of moisture content level above 20%; 2) relative humidity above 80% with temperature above 5°C, RHT, and 3) mold growth index of m. The hygrothermal simulations are carried out using WUFI PRO 5.1. Detailed hourly weather data is generated for 2020, 2050, and 2080 using Montreal International Airport data.

3. 2. 1. Selection of Base Year for Rain Data

As mentioned in the section 3. 1. 2. , future weather data used for energy simulation is generated by CCWeatherGen programme based on the hourly weather file provided by the US Department of Energy for the Montreal international airport (U.S. Department of Energy, 2012). CCWetherGen programme does not project the future amount of rainfall, however, the hourly

rainfall data is an essential element of the detailed hygrothermal analysis for assessing durability performance of building envelopes. Future rainfall data is created based on literatures predicting future precipitation for Montreal region. The detailed procedure of generating hourly rainfall data is provided in this section and section 3. 2. 2.

Among mentioned software above, only WUFI climate files have included rain data. WUFI has an archive of the climate files for the number of locations in WAC format. Nevertheless, it is not possible to extract rain data from these files. Therefore for this study, the amount of rain data at Montreal International Airport is chosen based on the available rain data collected by the Environment Canada. *Figure 3-9* shows the total annual rainfall amount collected at the Montreal International Airport from 1953 to 1994.

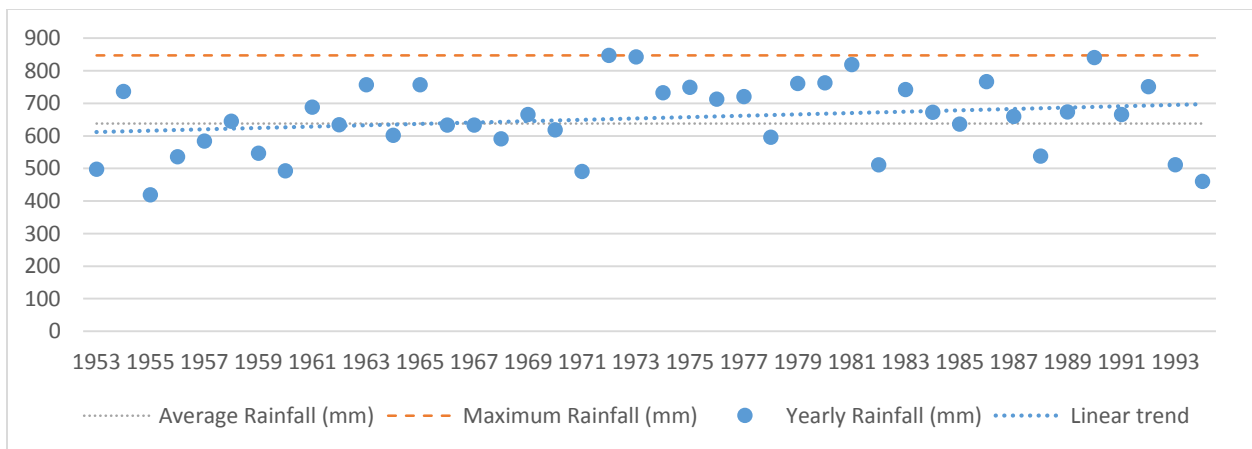


Figure 3-9: Collected rain data from the weather station at Montreal International Airport (Environment Canada's National Climate Services, 2013).

As illustrates, while the amount of rainfall for each two consecutive years varies significantly, the linear trend of rainfall between 1953 and 1994 is upward. To choose the most reasonable year as the base year data for future rain data generation, all available WYEC2 hourly weather data between 1953 and 1994 collected by the Environment Canada (Environment Canada, 2008) are

compared in terms of the annual rainfall amount and annual airfield Wind Driven Rain (WDR). Airfield WDR is an indication of the level of exposure of building façade to wetting, which is a significant parameter influencing the durability performance of wall assemblies. The annual airfield WDR is calculated from the collected data by Environment Canada using the ISO standard shown in *Equation 12* (ISO, 2009).

$$I_A = \frac{2 \sum vr^{8/9} \cos(D - \theta)}{9N} \quad (12)$$

The airfield WDR is calculated for twenty five orientations between 0 to 345° with an interval of 15° and the maximum airfield WDR at a specific orientation is identified for each year. *Figure 3-10* shows the airfield WDR calculated between 1953 and 1994 for Montreal International Airport. As shown in *Figure 3-10*, the airfield WDR varies significantly with orientation over different years. The prevailing wind-driven rain direction is more towards the south west and the north east.

Table 3-4 lists the maximum amount of WDR and maximum annual rainfall for each year and the corresponding ranking between 1953 and 1994. As shown in Table 3-4, year 1973 has a high annual rainfall amount of 842mm (2nd rank among all the years) and high amount of airfield WRD 406.1 (5th rank among all the years) at 60° orientation, therefore, it is chosen as the base year for generating future rain data. Historically, at the Montreal International Airport the prevailing WDR orientation is from South West, however, since the real collected rain data of 1973 will be used, in this study 60° is defined as the wall orientation in hygrothermal simulations.

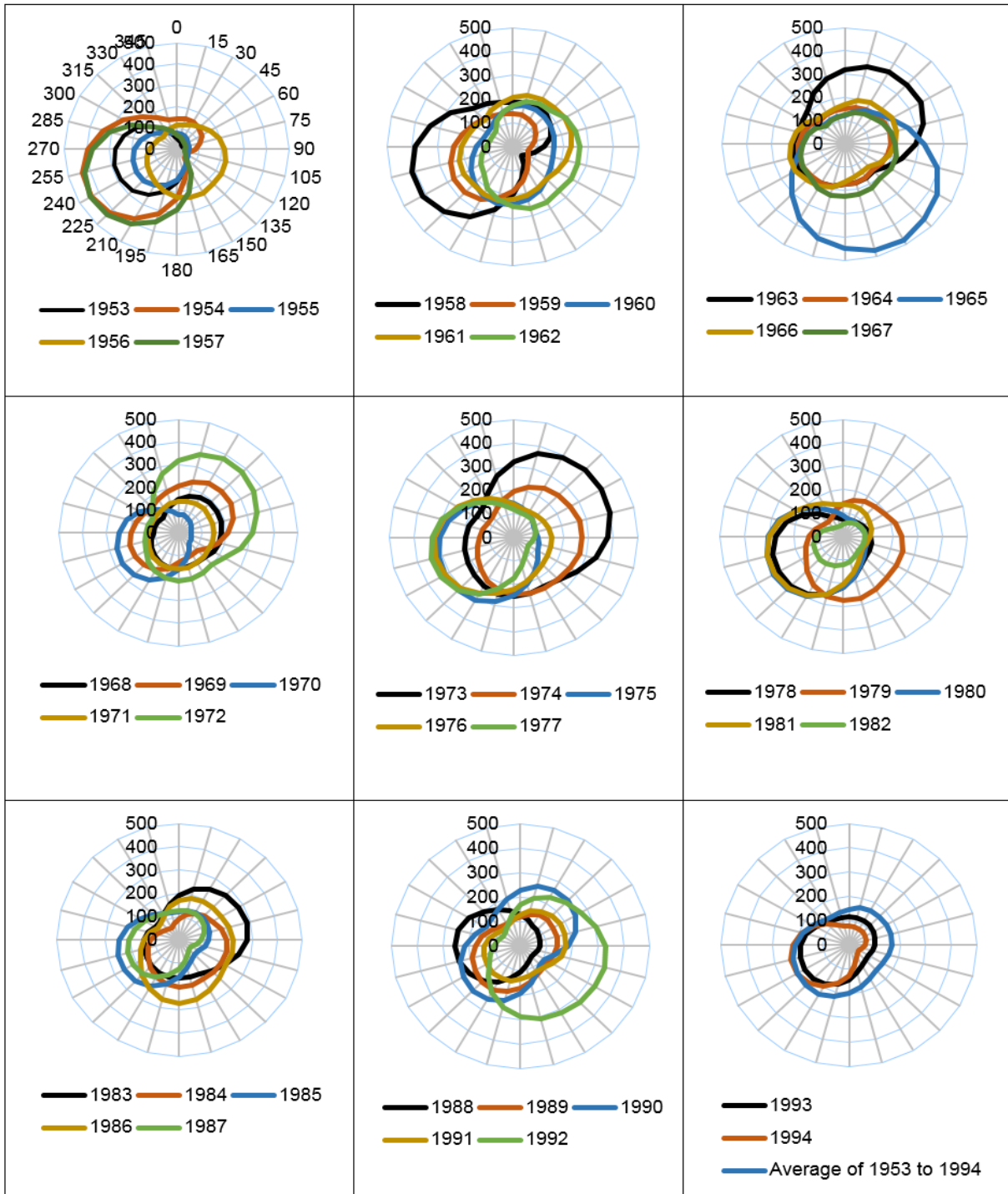


Figure 3-10. Airfield WDR calculated using Montreal International Airport data for year 1953 to 1994.

Table 3-4. Comparison of maximum WDR, maximum rainfall intensity and ranking of each year among years between 1953 and 1994

	Orientation of the Max WDR	Max Value of the WDR	Ranking of the Max WDR	Annual Rainfall amount (mm)	Ranking of the Rainfall mm
1953	240	287.4	15	497.8	38
1954	240	441.6	3	736.3	13
1955	225	208.1	35	418.7	42
1956	150	236.3	29	535.3	35
1957	240	443.3	2	584.4	32
1958	255	414.2	4	644.7	23
1959	240	268.7	22	546.5	33
1960	195	244.1	27	492.4	39
1961	75	240.7	28	687.9	17
1962	150	270.1	21	633.6	25
1963	45	359.3	7	756.5	9
1964	240	197.9	38	601.7	29
1965	150	477.7	1	757.3	8
1966	255	232.2	31	633.1	26
1967	195	227.9	32	633	27
1968	60	189.6	39	590.4	31
1969	45	257.7	25	665.2	21
1970	240	272.0	19	618.8	28
1971	195	158.4	41	490.8	40
1972	45	377.4	6	847.1	1
1973	60	406.1	5	842.6	2
1974	90	275.1	17	732.5	14
1975	225	319.5	13	748.9	11
1976	225	325.6	10	712.4	16
1977	225	343.0	8	721	15
1978	240	302.4	14	595.8	30
1979	180	273.0	18	761.2	7
1980	240	323.8	11	762.5	6
1981	240	321.2	12	819.3	4
1982	225	136.5	42	511.1	36
1983	75	285.1	16	741.8	12
1984	180	203.8	36	672.5	19
1985	240	258.4	24	636.2	24
1986	180	271.5	20	766.7	5
1987	255	216.7	33	659.5	22
1988	270	253.1	26	537.6	34
1989	225	210.8	34	673.1	18
1990	30	264.1	23	840.6	3
1991	75	179.8	40	665.8	20
1992	120	337.9	9	751.1	10
1993	240	200.9	37	510.7	37
1994	255	234.7	30	460.1	41

3. 2. 2. Future Rain Data

Since the future climate predictions done by Institute for Catastrophic Loss Reduction are generated based on the A2 (medium-high emission) scenario and it has been specified for the Montreal Location, in this thesis the future rainfall trends are predicted based on the predictions of this organization mentioned in the literature review.

However, in the table provided by the Institute for Catastrophic Loss reduction the amount of rainfall has not been predicted directly and only the precipitation and the ratio of snow to precipitation has been considered. Therefore, to be able to calculate predictions for the rainfall the amount of snowfall and precipitation by 2010 is essential. Environment Canada has provided these seasonal parameters for the Montreal International Airport from 2009 to 2014 shown in Figure 3-11. *Figure 3-12* also compares the seasonal amount of rainfall and precipitation for this location and this period of time.

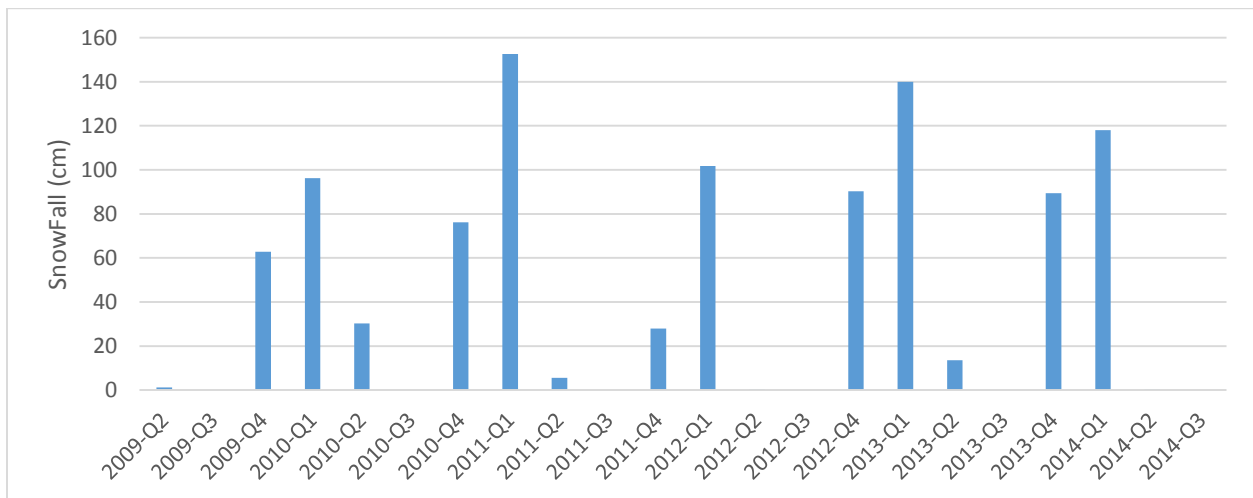


Figure 3-11. The amount of snowfall in Montreal International Airport between 2009 and 2014; quarter of the year (*Environment Canada, 2014*)

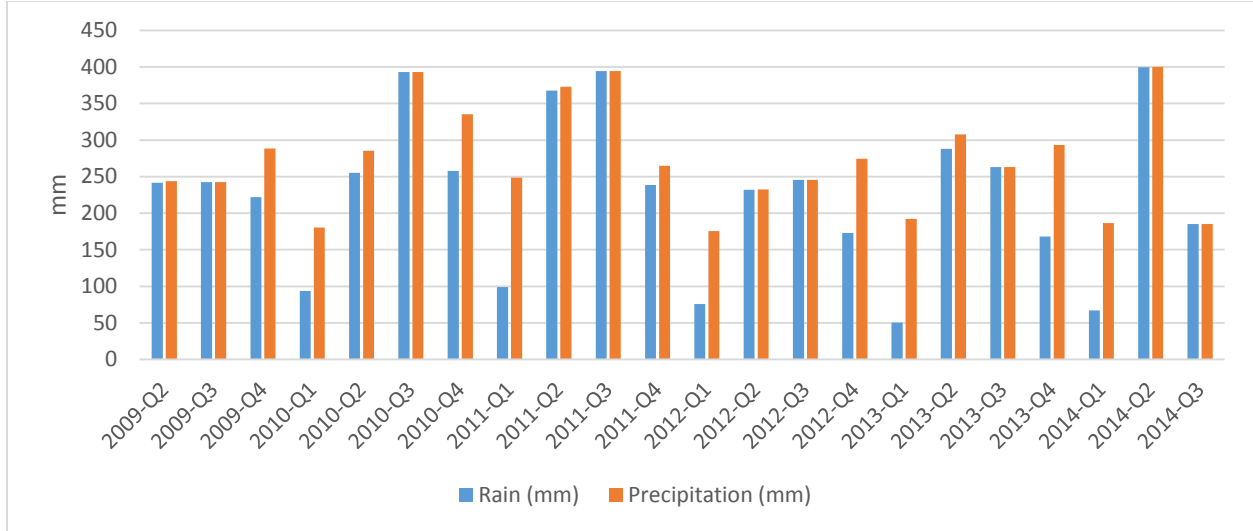


Figure 3-12. The amount of rainfall and precipitation in Montreal International Airport between 2009 and 2014; quarter of the year (Environment Canada, 2014)

Table 3-5 lists the breakdown of seasonal rainfall, total precipitation, and snow fall in liquid recorded for 2010 by Environment Canada for Montreal International Airport. Using the predictions by the Institute of Catastrophic Loss Reduction for 2050 (Table 2-3 and Table 2-4) and the data collected for 2010 by Environment Canada (Environment Canada, 2014), the seasonal amount of rainfall is predicted for year 2020, 2050 and 2080.

To simplify the calculations the average of the predicted ranges and is used, therefore, it is assumed that by 2050 the precipitation will increase by 12.5%, 17.5%, 5%, and 5% for winter, spring, summer and autumn, respectively. The ratio of snow to total precipitation is also assumed to decrease by an average of 15%, 15%, and 7.5% respectively for winter, spring and autumn by year 2050 for Montreal.

Table 3-5. Seasonal solid snowfall, rain, precipitation and liquid snowfall in 2010 at Montreal International Airport (*Environment Canada, 2014*)

	Rain (mm)	Precipitation (mm)	Snow Fall (mm) Liquid
2010-Winter	93.6	180.4	86.8
2010-Spring	255.2	285.4	30.2
2010-Summer	393	393	0
2010-Autumn	258	335.2	77.2

According to Table 2-3, Table 2-4, and *Table 3-5* the amount of rainfall in winter 2050 can be calculated using the following equations:

$$\text{Precipitation}_{\text{Winter2050}} = 1.125 \text{ Precipitation}_{\text{Winter2010}}$$

$$\text{Snow}_{\text{Winter2050}} / \text{Precipitation}_{\text{Winter2050}} = 0.85 \text{ Snow}_{\text{Winter2010}} / \text{Precipitation}_{\text{Winter2010}}$$

$$\text{Snow}_{\text{Winter2050}} = 0.9563 \text{ Snow}_{\text{Winter2010}}$$

$$\text{Rain}_{\text{Winter2050}} + 0.9563 \text{ Snow}_{\text{Winter2010}} = 1.125 \text{ Precipitation}_{\text{Winter2010}}$$

$$\text{Rain}_{\text{Winter2050}} + 0.9563 \text{ Snow}_{\text{Winter2010}} = 1.125 \text{ Rain}_{\text{Winter2010}} + 1.125 \text{ Snow}_{\text{Winter2010}}$$

$$\text{Rain}_{\text{Winter2050}} = 0.1687 \text{ Snow}_{\text{Winter2010}} + 1.125 \text{ Rain}_{\text{Winter2010}}$$

$$\text{Rain}_{\text{Winter2050}} = 0.1687 \times 86.8 + 1.125 \times 93.6 = 119.94316$$

$$\text{Rain}_{\text{Winter2050}} = 1.2814 \text{ Rain}_{\text{Winter2010}}$$

Similar to the above calculation considered for the prediction of rainfall in winter 2050, the amount of rainfall in spring, summer and fall 2050 would be 1.06, 1.05, and 1.07 times of the amount of rainfall in related seasons of the year 2010 respectively.

Since no meaningful reference about the predicted amount of rainfall in the Montreal International Airport by 2020 and 2080 was found, seasonal values for 2020 and 2080 are estimated based on the linear trend from 2010 to 2080 shown in *Figure 3-13*. To create future climatic data required for hygrothermal analysis, all parameters for year 1973 is imported into the CCweatherGen programme. Then the hourly rainfall data of 1973 was multiplied by the seasonal increase value estimated to generate hourly rainfall data for year 2020, 2050 and 2080. The extracted future

climate files from the CCweatherGen and the future hourly rain data are manually imported into the WUFI's Weather Creator programme. This programme is a conversion tool that exports Excel's spreadsheets in the WAC format (IBP, 2011).

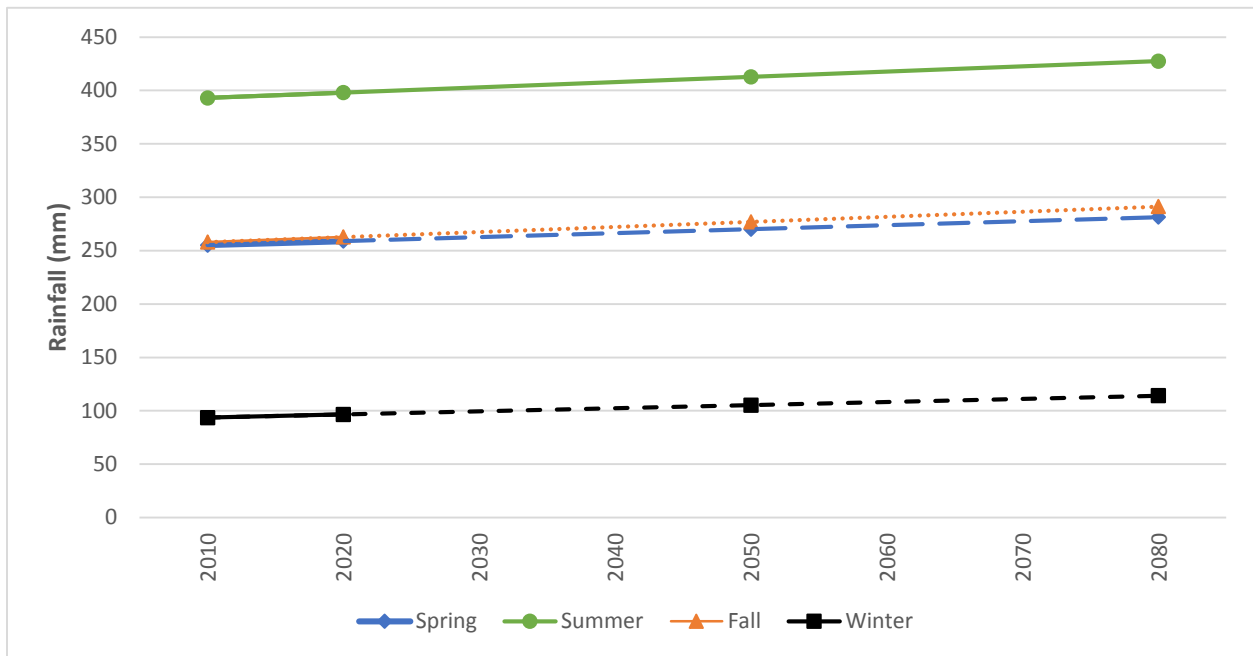


Figure 3-13. Proposed linear trend for the seasonal amount of rainfall by 2020, 2050, and 2080.

As shown in *Figure 3-13*, for this study it is assumed that the seasonal amount of rainfall in Montreal International Airport from 2010 to 2080 would have linear upward trend. Consequently, compared with the year 2010 there would be 1.4%, 1.2%, 1.8%, and 3.1% increase by 2020; 5.7%, 5%, 7.3%, and 12.5% increase by 2050; and 10%, 8.7%, 12.8%, and 21.8% increase by 2080 for spring, summer, and fall respectively. To create future climatic data required for hygrothermal analysis, all parameters for year 1973 is imported into the CCweatherGen programme. Then the hourly rainfall data of 1973 was multiplied by the seasonal increase value estimated to generate hourly rainfall data for year 2020, 2050 and 2080. The extracted future climate files from the CCweatherGen and the future hourly rain data are manually imported into the WUFI's Weather

Creator programme. This programme is a conversion tool that exports Excel's spreadsheets in the WAC format (IBP, 2011). Figure 3-14 compares the historical and the future annual amount of rainfall in Montreal international Airport.

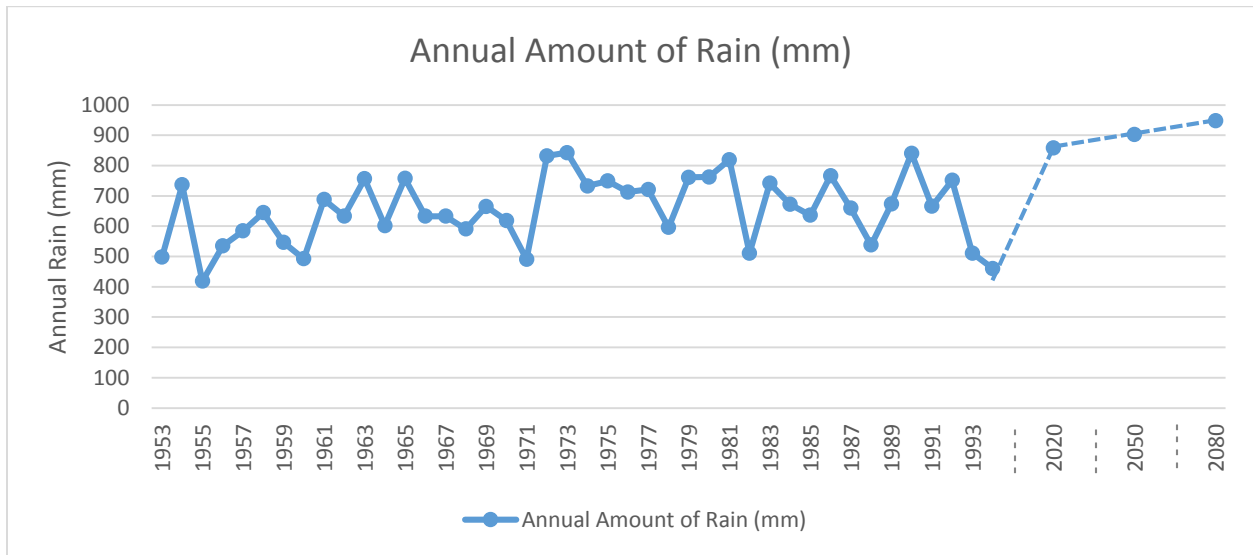


Figure 3-14. Historical and future proposed linear trend for the rainfall intensity in Montreal International Airport

3. 2. 3. Building Envelope Retrofitting options

Canada Mortgage and Housing Corporation (2004) investigated the potential energy saving from retrofitting the existing Canadian residential buildings in different provinces of Canada. The study divided the common housing stock into eleven categories. The report concluded that among all categories the potential energy savings of retrofitting Pre-World War II houses and Post-War 1½-Storey homes will be greater than other types of houses in Quebec. Therefore, a solid masonry wall commonly used in the existing pre-world War II houses and a typical Post-War 2×4 wood frame construction are chosen as the base wall assemblies. As shown in *Figure 3-15*, the 2x4 wood-frame wall is comprised of a 100mm brick veneer, 25mm air space, asphalt impregnated

building paper as water resistive barrier, plywood sheathing and 89mm existing stud filled with fibre glass batt insulation, and polyethylene vapor barrier (1perm), and gypsum board. The base wall is retrofitted to a double-stud assembly by adding an additional 89mm stud from the interior and filled with a 89mm gap with fiber glass insulation. An effective thermal resistance of $6.82\text{m}^2\text{k/W}$ is achieved. This retrofitting strategy is one of the successful common configurations proposed by CMHC (CMHC, 2011).

For the solid masonry wall, two interior retrofitting strategies are considered, one with 140mm closed-cell sprayed foam (Figure 3-16) and the other with 140mm XPS board (Figure 3-17). An effective thermal resistance of $6.49\text{ m}^2\text{k/W}$ is achieved.

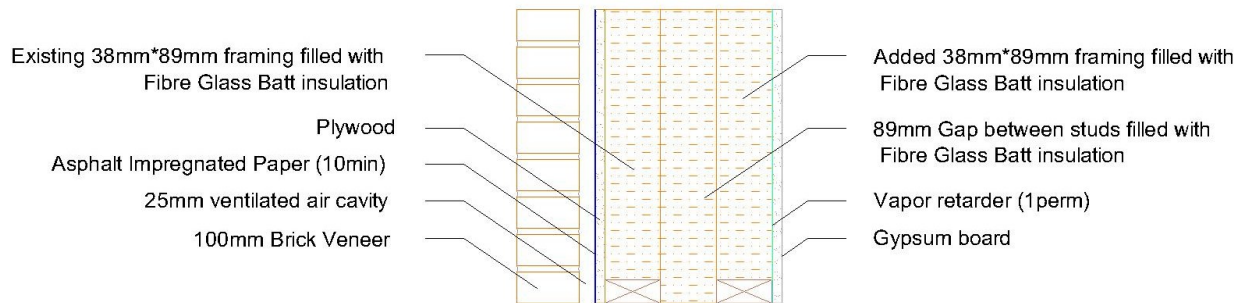


Figure 3-15. Wall retrofit strategies: Double Stud Wall

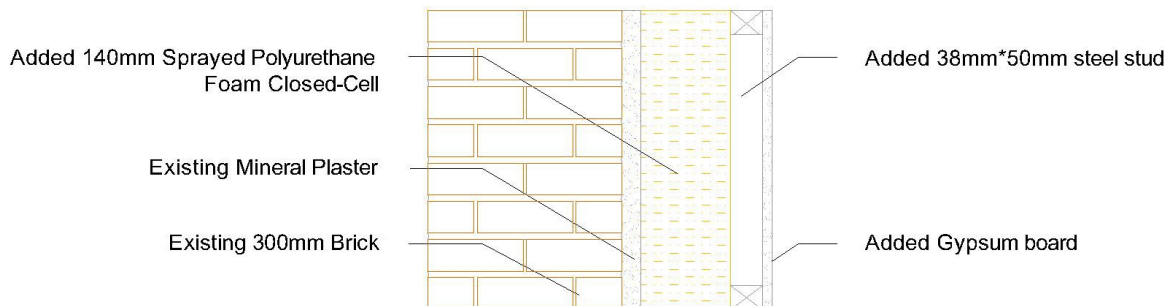


Figure 3-16. Solid masonry wall retrofit strategies: Sprayed Foam

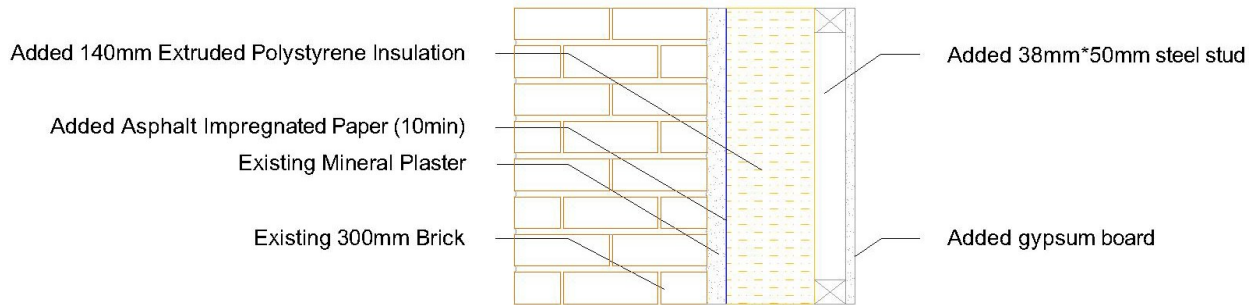


Figure 3-17. Solid masonry wall retrofit strategies: XPS

3. 2. 4. Performance Indicators

In this study freeze thaw risk of brick and biodegradation of plywood are investigated to assess the durability of mentioned assemblies.

Frost Damage Risk

The potential of frost damage risk on brick is investigated using Frost Decay Exposure Index and the Relative Humidity of above 95% with the existence of crossing points on brick (RHCP). FDEI is an index indicating the potential for frost damage and influenced by the climatic data only. FDEI can be calculated based on the accumulated annual average sum of 2-day, 3-day and 4-day rainfall prior to days with freezing points. The FDEI for accumulated 4-day sums of rainfall is defined as the annual accumulated precipitation in the form of rainfall during the 96 hours (4 days) prior to each freezing point (Lis, et al., 2007).

Frost damage is caused by the repeat freeze/thaw cycles. The RHCP approach is to evaluate the frost damage risk of the brick itself. The relative humidity and the temperature at 5mm from the exterior surface of the brick are obtained from the hygrothermal simulations. The frost damage most likely occur when the brick is wet while there is a freezing/thaw cycle. Therefore the co-

occurrence of high relative humidity of 95% and crossing points is used to evaluate the frost damage potential for brick for current and future climates. Frost damage most likely occur at 3-5mm into the brick from the exterior surface (Straube, et al., 2010). In this study, the hygrothermal conditions at 5mm from the exterior surface of the brick are used for the analysis.

Biodegradation of Plywood

Biodegradation on plywood risk is assessed using three criteria including the occurrence of moisture content above 20% (CMHC, 2011), relative humidity of above 80% with temperature above 5°C (RHT) (Djebbar, et al., 2002; IEA Annex 14 Final Report, 1991) and the mold growth index (Hukka & Viitanen, 1999; Viitanen & Ojanen, 2007). The RHT index approached proposed by Djebbar et al. (2002) was explained earlier in Equation 7 section 2.3.1. The mathematical mold growth model developed by (Hukka & Viitanen, 1999) is used for mold growth investigations on plywood. As described in section 2.3.4. The model calculates the critical relative humidity as a function of temperature shown in *Equation 8*. The mold growth potential (m) were shown in *Equation 9*, which is the relation between the relative humidity and the critical relative humidity. When m is greater than one, favorable conditions for mold growth are assumed. Otherwise, decreasing conditions for growth are considered. During the favorable conditions (m greater than one) the mold growth index is calculated using *Equation 10*. During the unfavorable conditions (m less than one) Equation 6 is used. The index is evaluated based on the 0 to 7 index. Whereas, Whereas, 0 is for no growth, 1 for less than 10% mold coverage (microscopic), 2 for 10% mold coverage (microscopic), 3 for 10-30% mold coverage (visual), 4 for 30-70% mold

coverage (visual), 5 for above 70% mold coverage (visual), and 6 for heavy and tight growth with 100% coverage.

3. 2. 5. Simulation Scenarios and Settings

In this study, frost decay analyses are carried out for both solid masonry and wood-frame assemblies while biodegradation analysis is carried out only for wood-frame assembly. The frost damage risk is evaluated for four different types of bricks, namely, Red Matt Clay brick, Buff Matt Clay brick, Calcium Silicate brick, and Old brick available in WUFI database. Buff Matt Clay, Red Matt Clay, and Calcium Silicate are the commonly used brick types in Eastern Canada (George Brown College, 2013). As shown in Table 5, the water absorption coefficient, A-value, has a wide range from 0.0012 to 2 kg/m²s^{0.5}. For the Old brick no A-value has been specified in WUFI's database, however, according to studies done by Straaten the A-value of the old brick defined in WUFI PRO would be around 2 kg/m²s^{0.5} (Fraunhofer IBP, 2013; Straaten, 2014). A-value is directly related to the wetting of brick due to wind-driven rain.

Three different “air/moisture source” scenarios are assumed in the simulations including “no air/rain source”, “rain leak” with 1% fraction, and “air leakage” with air change rate of 0.8 ACH. For single and double-stud wood frame assemblies, a cavity ventilation rate of 7.5ACH is assumed. Since initial simulations showed that “air leak” and “rain leak” moisture loads do not have significant impact on the frost decay risk of brick, for the frost decay analysis only “No Source” scenario is simulated. For the biodegradation risk of plywood, all three moisture loads are considered.

The default rain deposition factor (R2) in WUFI PRO is set to be 0.07s/m for a typical low-rise building (IBP, 2011). To investigate the impact of wind-driven rain and runoff on the frost damage risks of brick, more severe rain conditions are considered by setting R2 by 5 and 10 times of the default value. The indoor moisture load is set as “high moisture load” category according to EN15026 standard (2007) to represent a worst condition.

Hygrothermal simulations are carried out for three consecutive years under the current and year 2020, 2050, and 2080 climatic conditions. However, to eliminate the influence of the initial conditions, only the second year’s results are used for the biodegradation analysis of the plywood. The simulation scenarios are listed in *Table 3-7*.

Table 3-6. Basic hygric properties of brick and plywood provided in WUFI database (*Fraunhofer IBP, 2013*)

	<i>Buff Matt Clay</i>	<i>Red Matt Clay</i>	<i>Calcium Silicate</i>	<i>Brick (old)</i>	<i>Plywood high</i>
<i>Bulk Density [Kg/m³]</i>	1719	1935	1973	1670	600
<i>Porosity [m³/m³]</i>	0.351	0.217	0.272	0.196	0.96
<i>A-Value [kg/m²s^{0.5}]</i>	0.0012	0.0268	0.181	≈2	0.0026
<i>Specific Heat Capacity [J/kgk]</i>	800	800	800	840	1880
<i>Water Vapour Diffusion Resistance Factor</i>	29.3	137.8	182.5	16	383.2

Table 3-7. Simulation scenarios

<i>Assemblies</i>		<i>Bricks</i>	<i>Moisture sources</i>	<i>R2</i>	<i>Weather file</i>
<i>Pre-World War II construction</i>	<i>Post-War construction</i>				
Solid masonry (Base Case)	Single stud (Base Case)	Buff Matt Clay	No Moisture/Air	0.07	1973 (Base weather data)
Retrofitted with Sprayed Foam (Retrofitted option).	Double stud (Retrofitted Option)	Red Matt Clay	Rain Penetration 1% fraction	0.35	2020
Retrofitted with XPS (Retrofitted option)		Calcium Silicate	Infiltration 0.8ACH	0.7	2050
		Brick (old)			2080

3. 3. Summary and Conclusion

This study aims to investigate the impact of future climate on the building performance of a typical Canadian house in compliance with QEC and retrofitted to PH at Montreal International Airport. Building performance is evaluated in terms of the energy consumption, thermal comfort, and durability. While energy consumption and thermal comfort simulations are carried out for the whole building, durability analysis are done only for above grade assemblies. This approach attempts to evaluate the performance of energy efficient retrofitting under the current climate and future climate of Northern America.

CHAPTER 4.

4. 1. Energy Consumption

To maintain the indoor temperature within 20°C and 25°C, the mechanical system will be turned on when the internal temperature is lower than 20°C or higher than 25°C. *Figure 4-1* and *Figure 4-2* compare the heating and cooling loads of the base case to the PH retrofitted option, respectively. It is observed that the heating load of the base case (QEC) and the PH retrofitted house would decrease by 45.1% and 34.1% between current year and 2080, respectively. Although the internal temperature of the PH retrofitted house under free running scenario is higher than that in the house built to QEC, the cooling load of PH retrofitted house would be lower than that in the QEC house; particularly by 2050 onward.

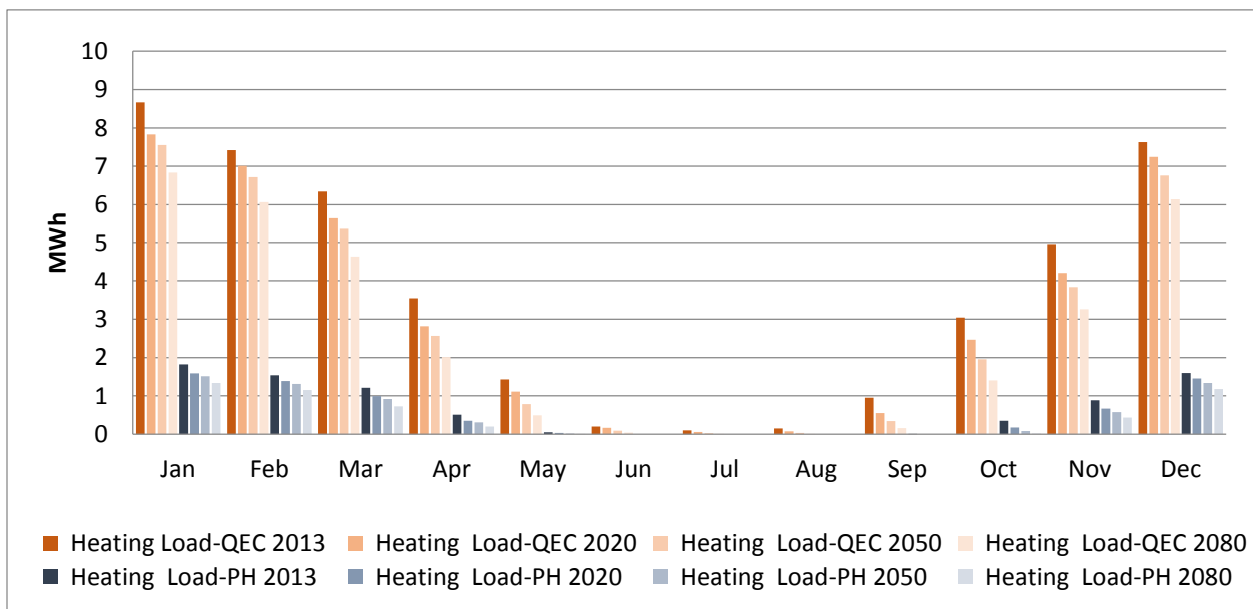


Figure 4-1. Comparison in heating load between the QEC house and the PH retrofitted option over current and future years

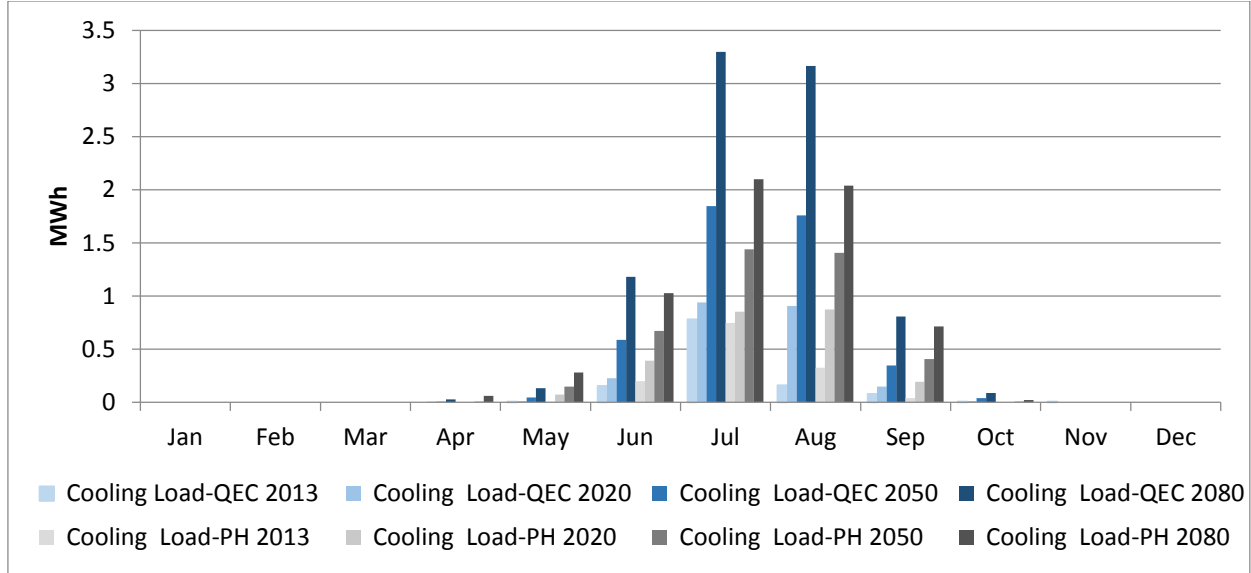


Figure 4-2: Comparison in cooling load between the QEC and the PH retrofitted option over current and future years

In this study, the impact of five simplified shading systems including shading systems with 1m overhang (shading A), typical shading with 0.5m overhang (shading B), 30° angled louver shading (shading C), and 30° angled shading with 0.5m overhang (shading D) on the heating load and the cooling load are investigated. Figure 4-3 and Figure 4-4 compare the monthly heating and cooling loads between different shading systems added to the PH retrofitted house for the year 2013 and 2080, respectively. Results show that while the cooling loads of the PH option with 1m overhang is 12.6% lower than that in the PH option with no shading in 2013, the heating load would be 1.9% higher. By 2080 these values would be 7.2% and 2.3% respectively. However, the total energy consumption of both scenarios in current year and 2080 are likely the same.

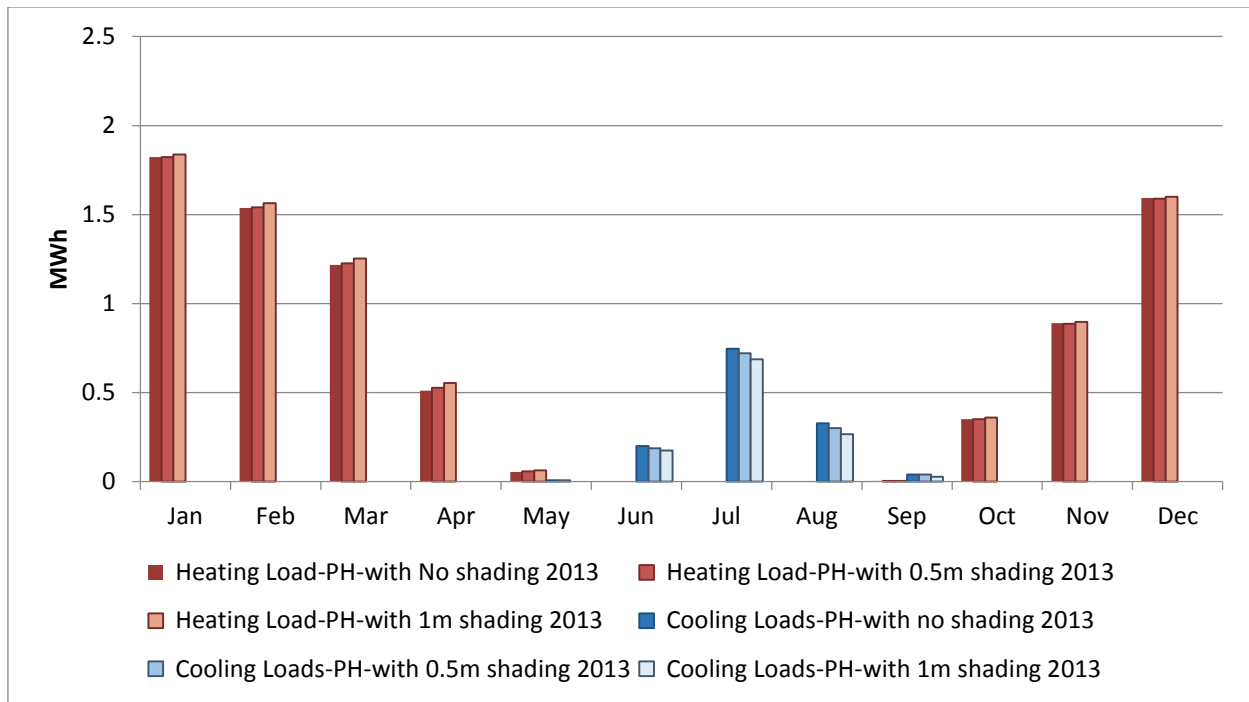


Figure 4-3: Impact of shading systems on the monthly heating and cooling loads of the PH retrofitted option in 2013.

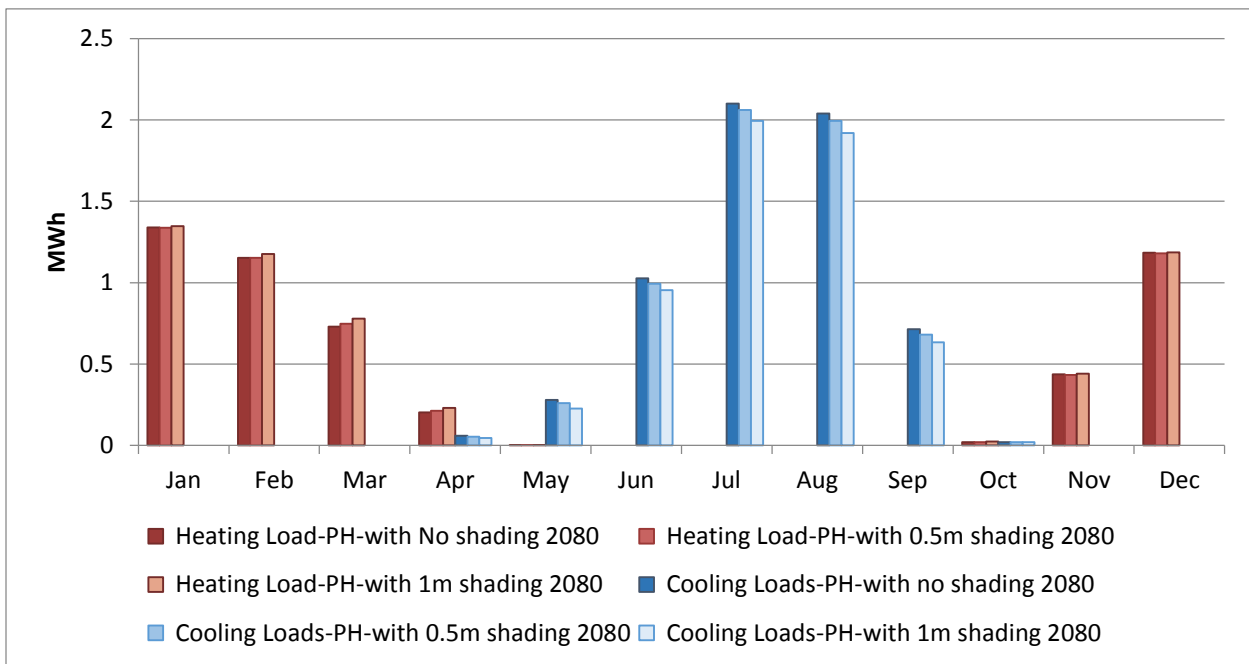


Figure 4-4: Impact of shading on the monthly heating and cooling loads of the PH retrofitted option in 2080.

Figure 4-5 shows the total energy consumption of QEC house and PH with different shading scenarios over current and future climates. The internal temperature is set at 20°C for heating and 25°C for cooling.

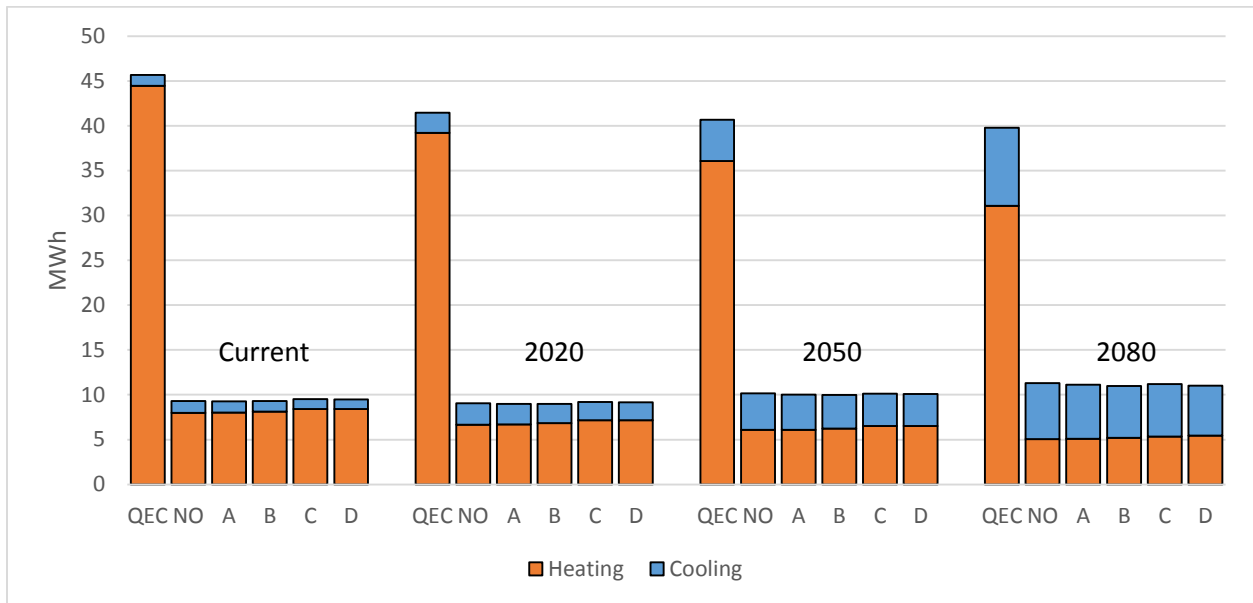


Figure 4-5. Comparison of heating and cooling loads in QEC and PH retrofitted building with different shading strategies over current and future years.

As shown in Figure 4-5, PH houses consume significantly less energy than QEC house. Due to the warming of the climate, the total energy consumption in QEC house would decrease from the current year to 2080. For PH houses, the total energy consumption in 2020 is the lowest compared to other years. It is concluded that in order to moderate the internal temperature within 20°C and 25°C PH with shading C and D would slightly consume more energy than scenarios including PH with no shading, PH with shading A, and PH with shading B by around 3% over years.

4. 2. Thermal Comfort

As mentioned in the methodology, the term “thermal Comfort” in the free running base case model and the free running retrofitted to the PassiveHaus model is investigated under the current and future climates using 2 methods. First, the number of hours that the interior temperature is above 26°C and the second, number of hours that the interior temperature is in the limits of comfort defined by Peeters et al (Peeters, et al., 2009). The thermal comfort limits defined by Peeters et al and the outdoor temperatures at Montreal International Airport in 2013 and 2080 are shown in

Figure 4-6.

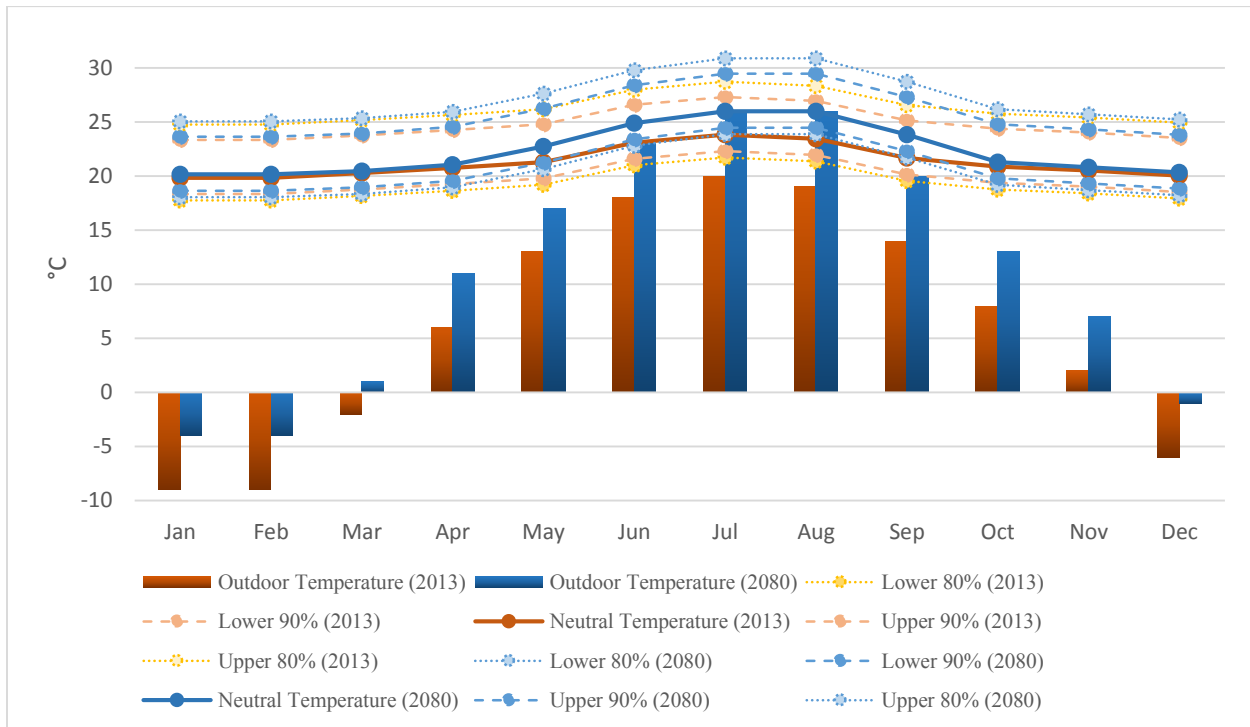


Figure 4-6. Thermal comfort limits as a function of outdoor temperature using adaptive model for naturally ventilated residential buildings and monthly average outdoor temperatures in 2013 and 2080.

It can be seen that the outdoor temperature in Montreal would likely increase by 2080, and the neutral temperature, lower limits and upper limits would significantly increase by summer 2080. However, in winter the lower and upper acceptable limits would not change much. *Figure 4-8* and *Figure 4-8* plot the internal temperature in the south-west room for QEC, PH with/without shading, in 2013 and 2080 respectively.

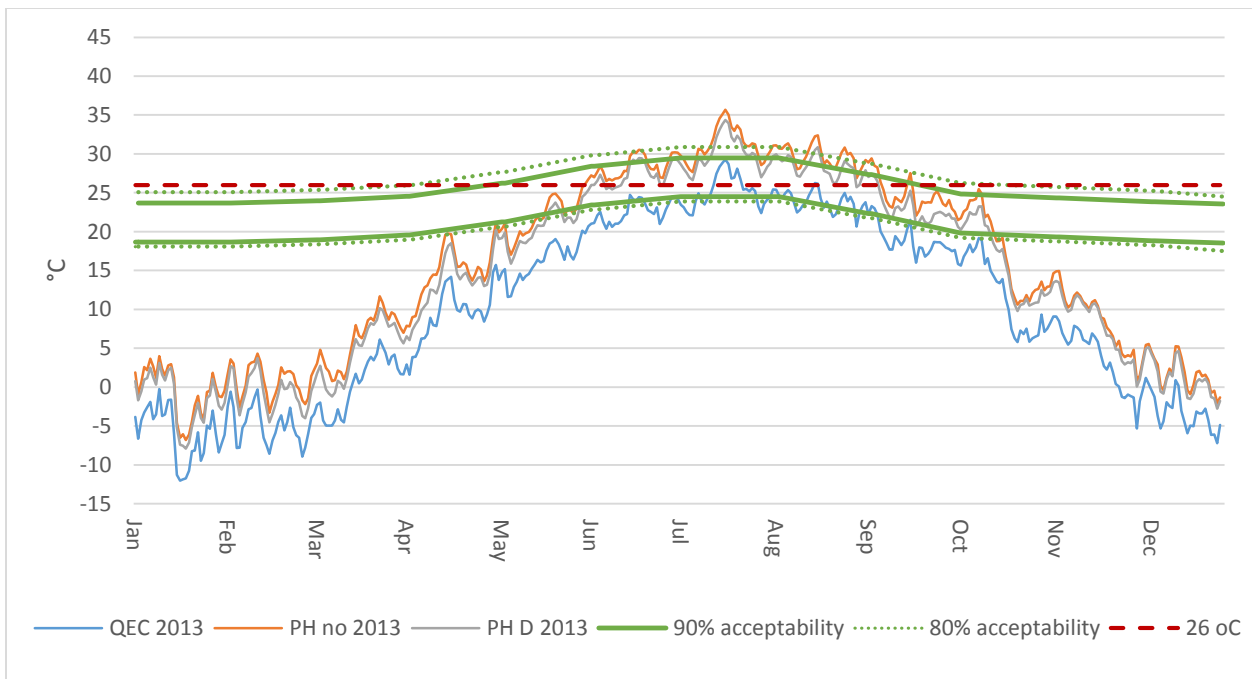


Figure 4-7. Internal temperature of specified room in QEC and PH with/without shading in 2013 in comparison to 80% and 90% acceptability limits in 2013.

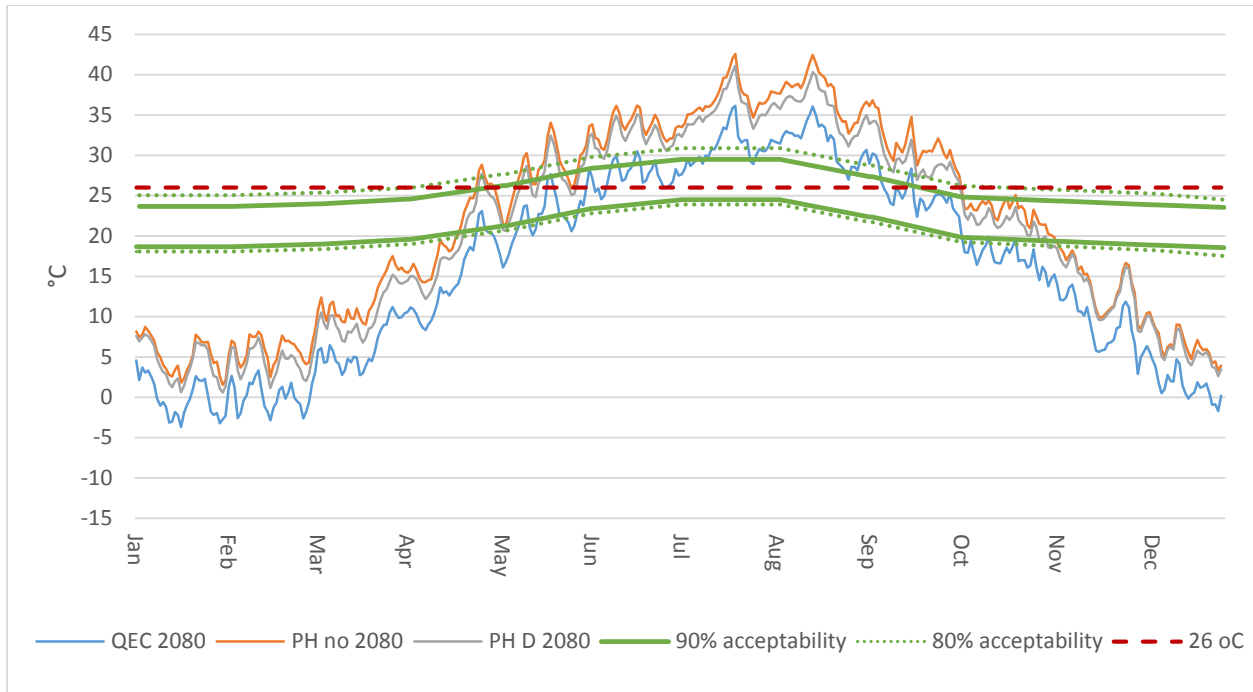


Figure 4-8. Internal temperature of specified room in QEC and PH with/without shading in 2080 in comparison to 80% and 90% acceptability limits in 2080.

Results show that the internal temperature in PH house is higher than that in QEC house with PH-no shading having the highest temperature. Whereas, the indoor air temperature will reach as high as 36°C in the QEC house while about 43°C in the PH- No by 2080. In 2013, the periods in PH house with acceptable indoor temperatures are from May to mid-June and from Sept. to Mid-Oct. while the period in QEC house with acceptable indoor temperatures is from June to Sept. In 2080 with the increasing of outdoor temperature, the periods in PH house with acceptable indoor temperatures are from mid-April to mid-May and from Oct. to Nov. while in QEC house with acceptable indoor temperature from May to June and from Sept. to Oct. *Figure 4-9* shows the total number of hours that the internal temperature of the specified room in the different scenarios is above 26°C.

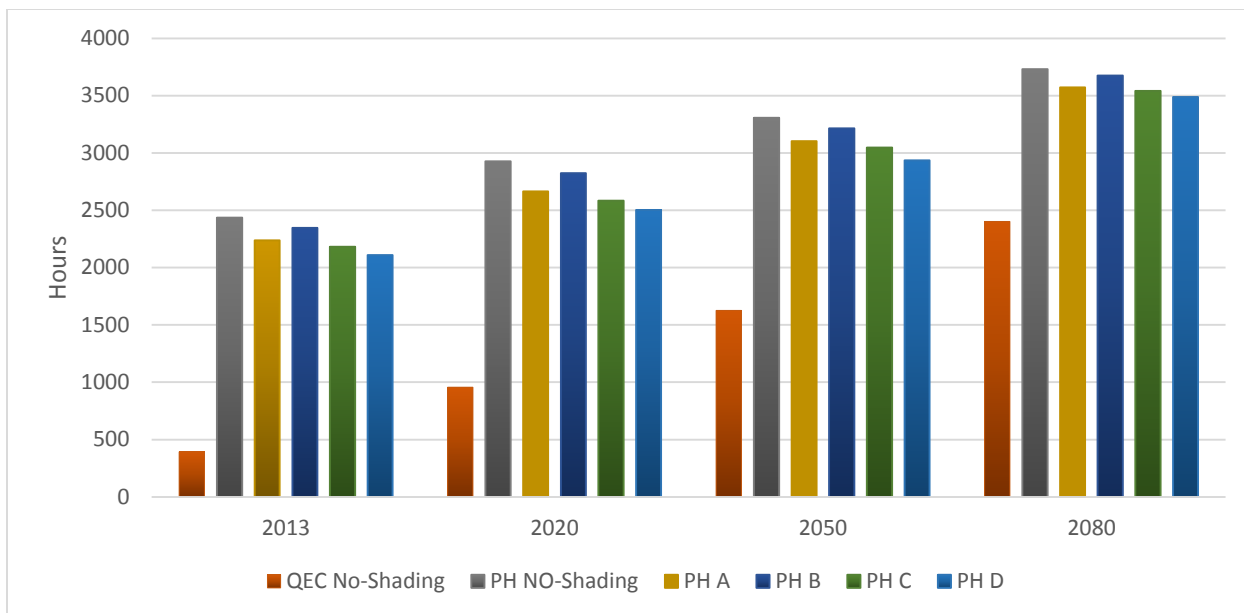


Figure 4-9. Comparison of number of hours in which the internal temperature of the specified bedroom is above 26°C, between the base-case (QEC) and retrofitted to PH building with different shading scenarios

Figure 4-9 shows that the overheating risk of the PH retrofitted option is likely higher than a typical QEC building over future years under free running conditions with natural ventilation. Result shows that the difference of the overheating risk from 2013 to 2080 in Quebec would be more than the PH. From 2013 to 2080, the percentage of time within a year that the internal air temperature is over 26°C for the QEC house and for the PH retrofitted option with no shading would increase by 509% and 65%, respectively.

Moreover, simulation shows that the risk of overheating risk defined by 26°C criteria on the PH with shading D would be likely less than other PH scenarios. Whereas the number of hours in overheating risk defined by 26°C criteria in PH D would be 13% and 6% less than the PH with No shading in 2013 and 2080 respectively. *Figure 4-10* shows the total number of hours that the

internal temperature of the specified room in the various scenarios is within 90% and 80% thermal comfort acceptability range.

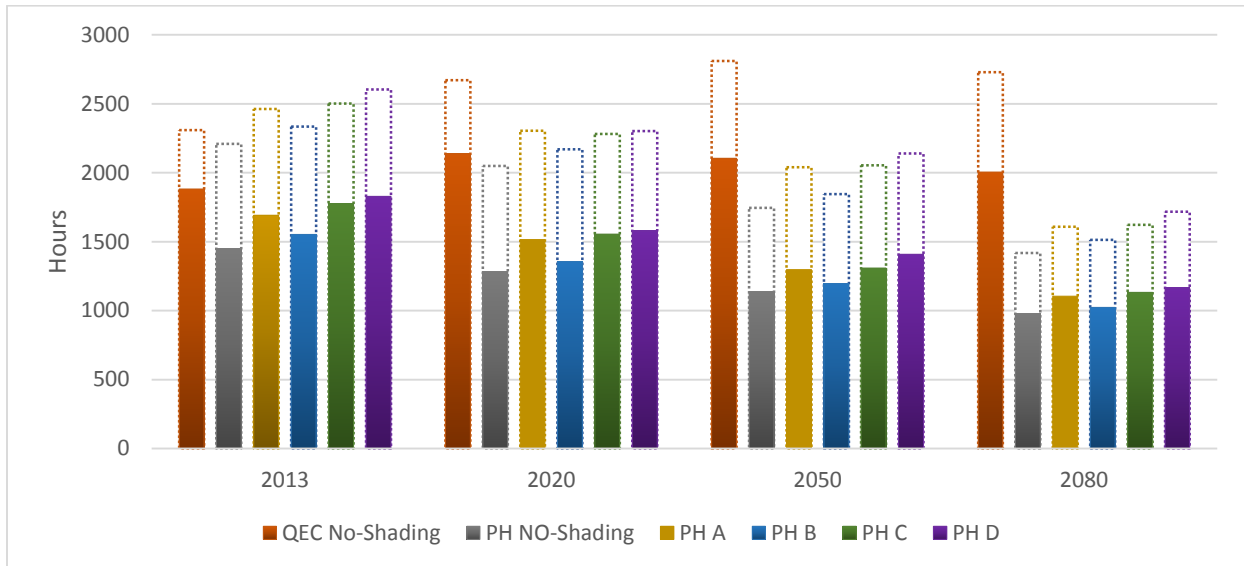


Figure 4-10. Comparison of number of hours in which the internal temperature of the specified bedroom is within 90% (Solid color) and 80% (dash-line) thermal comfort acceptability, between base-case (QEC) and retrofitted to PH building with different shading scenarios.

It can be seen that in 2013, QEC has the highest number of hours in the 90% acceptability zone while PH with shading configuration D has the highest number of hours in the 80% acceptability zone. However, the number of hours in 90% and 80% acceptability zone for PH with any shading device would likely decrease over the future climate while the number of hours in 90% and 80% acceptability zone for QEC house would increase. Results also indicate that having any of the shading configurations A, B, C and D would provide more hours of acceptability for PH, among which shading D provides the most.

It is observed that the total hours of QEC in compliance with 90% acceptability would be 1883 hours which is 23% and 3% higher than PH with no shading and PH with shading D in 2013

respectively. However, this difference would respectively change to 51% and 42% by 2080. The number of hours in compliance with 90% acceptability in PH with shading D would be higher than that in PH with no shading by around 21% and 16% by 2013 and 2080 respectively.

4. 3. Durability

4. 3. 1. Frost Decay Exposure Index FDEI: Current V.S. Future

Figure 4-11 shows the airfield WDR for the base year 1973 and the future year 2020, 2050, and 2080. Year 2050 has the highest amount of airfield WDR.

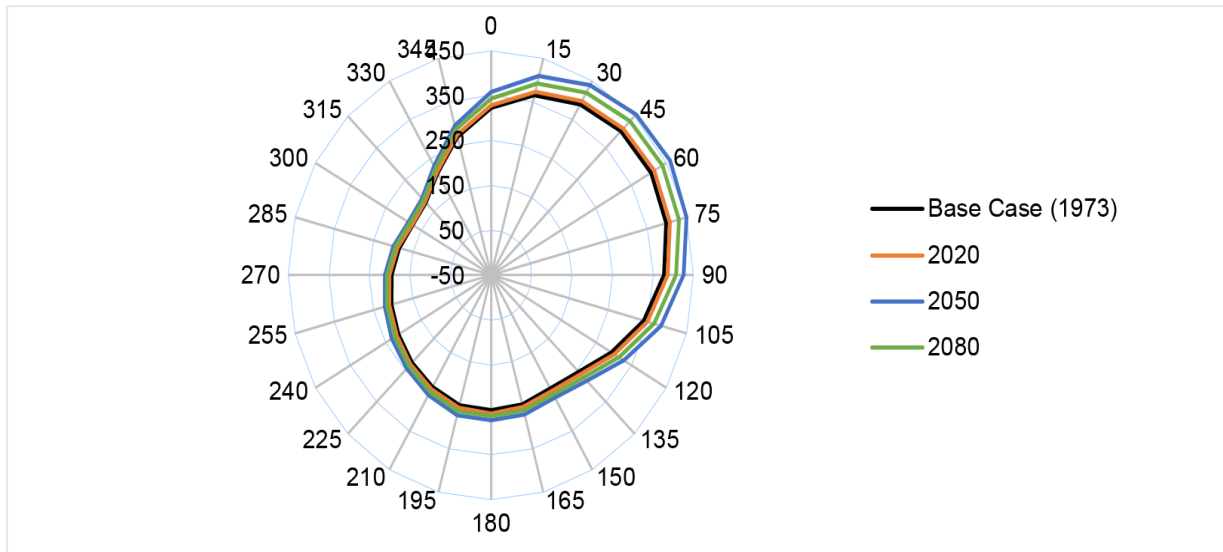


Figure 4-11. Comparison of the airfield WDR for the base weather (1973) and by 2020, 2050, and 2080 at Montreal International Airport.

The potential of the freeze thaw for the current and future climate in Montreal using FDEI for 4days, 3days, 2days, and one day prior to days with freezing points is shown Figure 4-12.

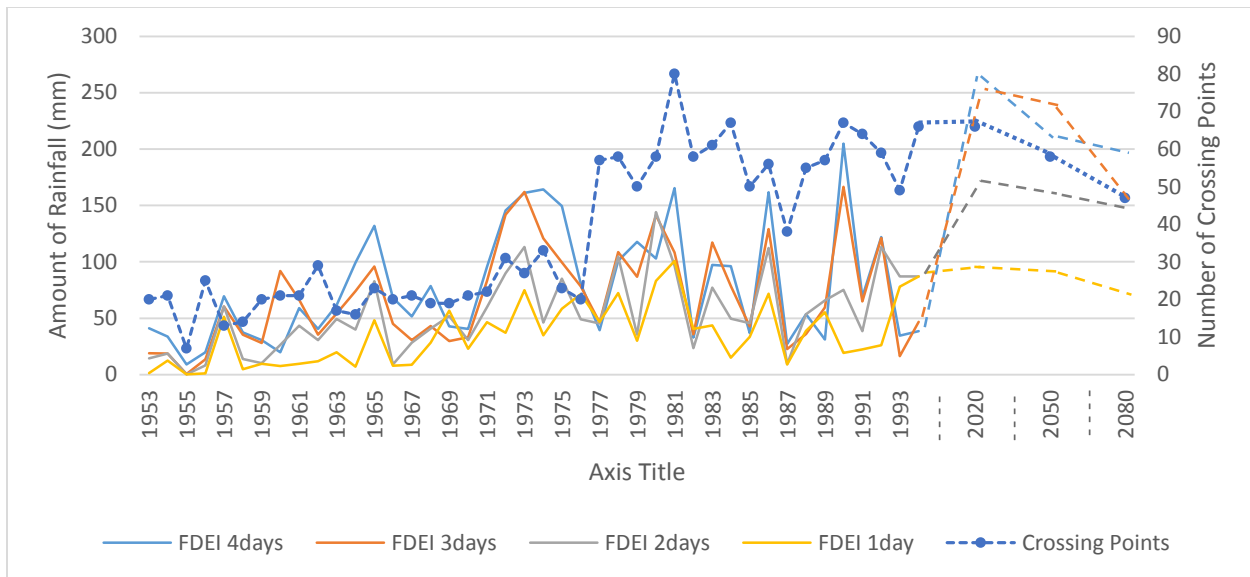


Figure 4-12. Comparison of the historical and future FDEI in Montreal International airport for 1day, 2days, 3days, and 4days prior to the freezing point.

The frost decay exposure potential would likely increase from 1993 to 2020 while from 2020 onward this risk would likely decrease. Although the amount of rainfall would likely increase in the future, this downward trend of frost decay exposure index is due to the decrease in the number of crossing points in the future. As shown in Figure 4-12, the number of crossing points increases from 1953 to current year with a significant increase in 1977. The number of crossing points decreases from 2020 to 2080. In general, the FDEI follows the pattern of number of crossing points. The decrease in the number of crossing points is probably due to the increase in temperature and solar radiation.

4. 3. 2. Frost Damage Risks for Bricks

Frost damage risks of bricks are evaluated by the number of crossing points and the co-occurrence of crossing points at high RH level of 95%. Since the frost damage of brick typically occurred within 3.5-7mm into the brick (Aarle, et al., 2015) , in this study, the RH and temperature at 5mm

into the brick are evaluated. *Figure 4-13* compares temperature and relative humidity at 5mm of calcium silicate brick in single stud (base case) and double stud (retrofitted) over three years of simulation using WUFI pro. It is observed that in general the brick in the retrofitted double-stud assembly has higher RH than the base case and experiences greater fluctuation of temperature. *Figure 4-14* and *Figure 4-15* show the moisture content averaged over the first 10mm into the calcium silicate brick for the wood-frame and the solid masonry assemblies respectively. Higher MC is observed in the brick in retrofitted options, which indicates potentially greater frost damage risk for bricks in retrofitted options.

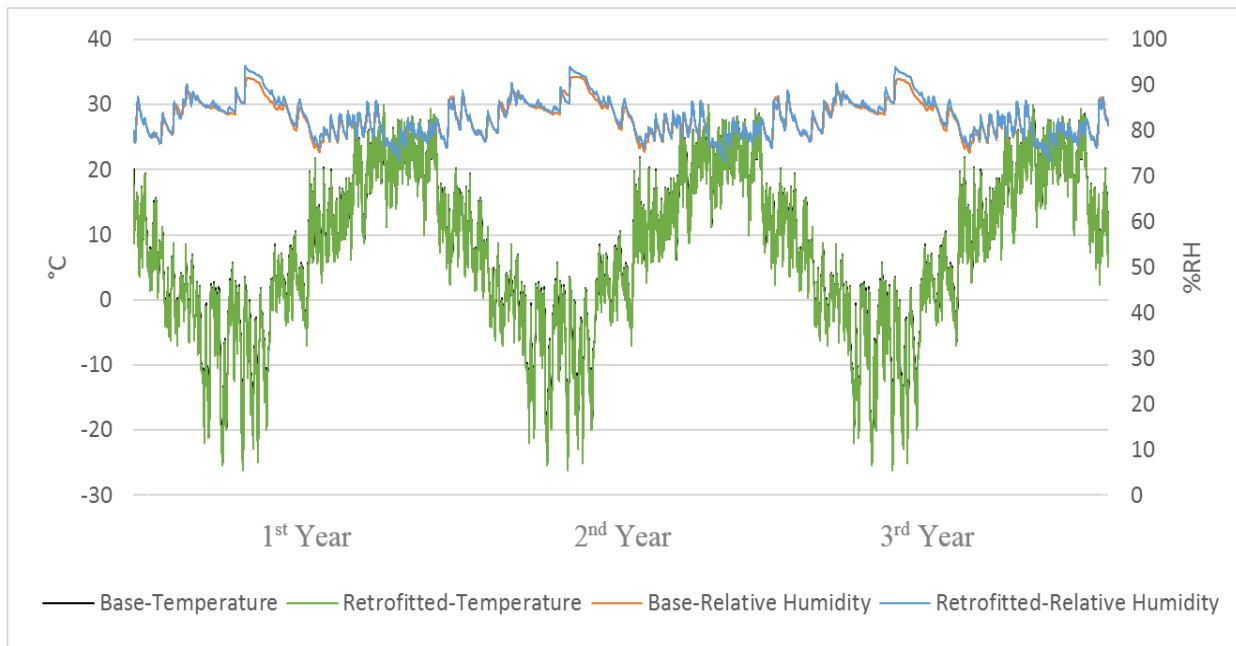


Figure 4-13. Comparison of the relative humidity and temperature at 5mm into the Calcium Silicate brick of the single stud (base case) and the double stud (retrofitted) under three years of simulation R2=0.35. Based weather data (1973).

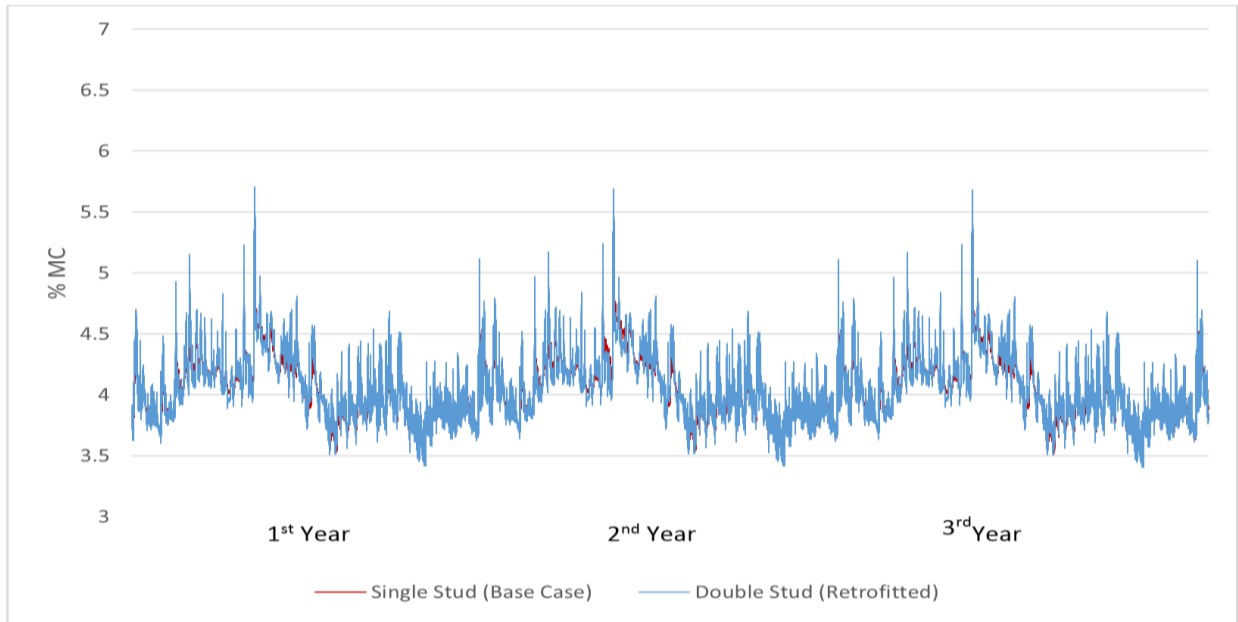


Figure 4-14. Comparison of the Moisture content of 10mm into the Calcium Silicate in wood-frame assemblies under three years of simulation at Montreal International Airport. $R^2=0.35$. Based weather data 1973

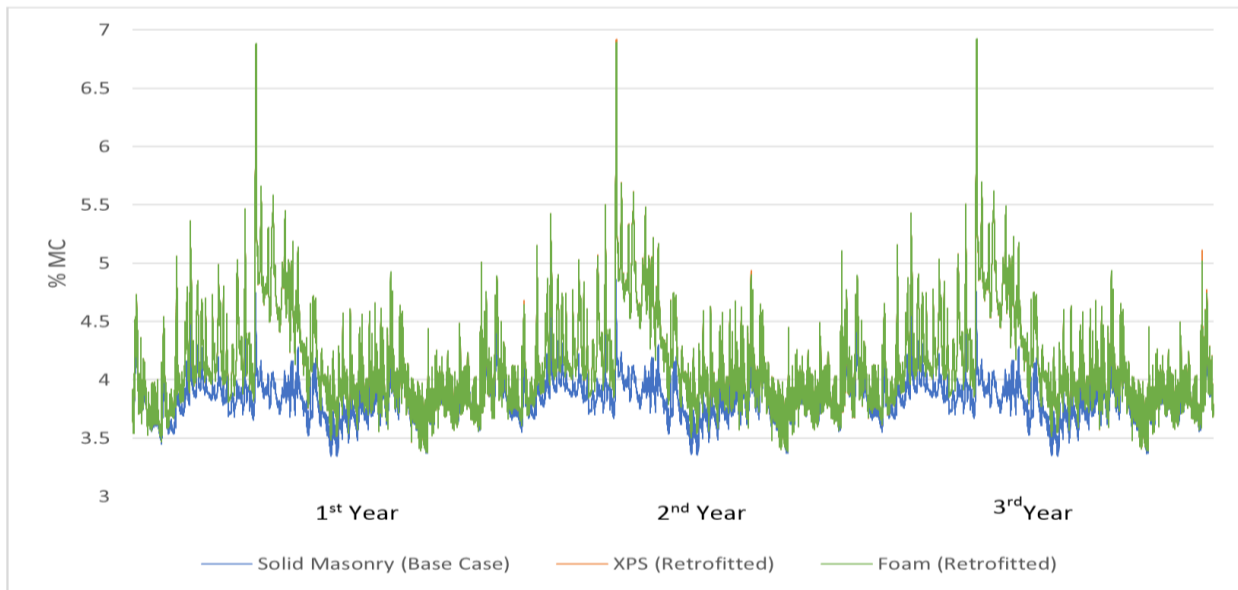


Figure 4-15. Comparison of the Moisture content of 10mm into the Calcium Silicate in solid masonry assemblies under three years of simulation at Montreal International Airport. $R^2=0.35$. Based weather data 1973

Table 4-1 lists the number of crossing points for both base and retrofitted cases using the temperature calculated at 5mm into the brick for the current climatic conditions with three rain deposition factors (R2) of 0.07, 0.35, and 0.7. In general, adding insulation to the base case would increase the number of crossing points; rain deposition factor does not have much impact on the number of crossing points except for the old brick; and as expected the different insulation added to the solid masonry have little impact on the number of crossing points.

Table 4-1. Number of crossing point occurs at 5mm of the most exterior layer of bricks over three-year simulation under the current climate (based on 1973) at Montreal International Airport

	<i>Rain Deposition</i>	<i>Single Stud</i>	<i>Retrofitted Double Stud</i>	<i>Solid Masonry</i>	<i>Retrofitted XPS</i>	<i>Retrofitted Foam</i>
<i>Buff Matt Clay</i>	<i>0.07</i>	137	159	139	153	160
	<i>0.35</i>	137	160	138	157	162
	<i>0.7</i>	137	159	141	159	162
<i>Red Matt Clay</i>	<i>0.07</i>	136	142	136	148	148
	<i>0.35</i>	136	142	134	148	148
	<i>0.7</i>	136	142	136	148	148
<i>Calcium Silicate</i>	<i>0.07</i>	118	150	138	157	156
	<i>0.35</i>	118	150	139	157	160
	<i>0.7</i>	118	150	138	157	160
<i>Brick (old)</i>	<i>0.07</i>	143	137	137	149	147
	<i>0.35</i>	100	115	115	102	102
	<i>0.7</i>	102	130	130	109	110

Table 4-2 shows the impact of wall orientation on the number of crossing points occurs at 5mm into the brick for both base and retrofitted assemblies. NE has the highest WDR while SW orientation receives higher solar radiation, which may increase the freeze/thaw cycles. The number of crossing points is also calculated for year 2080 and a rain deposition factor of 0.35 is used. For wood-frame assembly, there is little difference in the number of crossing points between SW and NE orientation for the base case except for the old brick. For the old brick, the number of crossing points is greater at the SW than that in the NE orientation. When the single-stud assembly is retrofitted to double-stud, the number of crossing points increases and walls facing the NE

orientation has greater number of crossing points except for the old brick, which has higher number of crossing points at the SW orientation. For the solid masonry assembly, in general wall facing the SW orientation has higher number of crossing points. Adding insulation in the retrofitted assembly increases the number of crossing points more for the NE orientation and results in little difference between SW and NE except for the old brick. For the old brick, the number of crossing points decreases in the retrofitted assembly. For the future climate 2080, the number of crossing points decreases except for the retrofitted solid masonry in the NE orientation.

Table 4-2. Impact of orientation on the number of crossing points at 5mm into the brick.

		<i>Single Stud</i>		<i>Retrofitted Double stud</i>		<i>Solid Masonry</i>		<i>Retrofitted XPS</i>		<i>Retrofitted Foam</i>	
		<i>SW</i>	<i>NE</i>	<i>SW</i>	<i>NE</i>	<i>SW</i>	<i>NE</i>	<i>SW</i>	<i>NE</i>	<i>SW</i>	<i>NE</i>
<i>Buff Matt Clay</i>	1973	139	137	142	160	157	138	152	157	161	162
	2080	100	101	97	100	76	76	95	95	95	95
<i>Red Matt Clay</i>	1973	136	136	134	142	139	134	148	148	148	148
	2080	97	97	97	97	64	64	86	86	86	86
<i>Calcium Silicate</i>	1973	118	118	136	150	147	139	157	157	155	160
	2080	91	91	91	90	62	62	90	93	93	99
<i>Brick (old)</i>	1973	134	100	156	115	154	115	159	102	160	102
	2080	106	100	101	96	95	91	116	123	114	120

Table 4-3 shows the number of hours with RH above 95% when crossing points exist at 5mm into the brick (RHCP) under the current climate. The RHCP is a more direct indicator of potential frost damage risk for brick. For wood-frame assemblies, adding insulation in the retrofitted assembly would not increase the risk for frost damage except for the old brick, in which the frost damage risks slightly increases. For the solid masonry assembly, adding insulation slightly increases the frost damage risks except for buff matt clay brick, which has the lowest water absorption coefficient. For all the cases, the old brick assembly has the highest occurrence of high RH and crossing points, which is an indication of higher potential of frost damage.

Table 4-3. Number of hours that 5mm into the bricks has the both humidity of above 95% and crossing point under the current climate (based on 1973) at Montreal International Airport.

	<i>Rain Deposition</i>	<i>Single Stud</i>	<i>Retrofitted Double stud</i>	<i>Solid Masonry</i>	<i>Retrofitted XPS</i>	<i>Retrofitted Foam</i>
<i>Buff Matt Clay</i>	<i>0.07</i>	0	0	0	0	0
	<i>0.35</i>	0	0	0	0	0
	<i>0.7</i>	0	0	0	0	0
<i>Red Matt Clay</i>	<i>0.07</i>	0	0	0	7	9
	<i>0.35</i>	0	0	0	63	56
	<i>0.7</i>	0	0	0	65	51
<i>Calcium Silicate</i>	<i>0.07</i>	0	0	0	6	6
	<i>0.35</i>	0	0	0	8	8
	<i>0.7</i>	0	0	3	9	10
<i>Brick (old)</i>	<i>0.07</i>	131	126	126	144	142
	<i>0.35</i>	96	109	109	99	99
	<i>0.7</i>	98	124	124	106	107

Table 4-4 shows the number of crossing points at 5mm into the brick for the current and future years. In general, the number of crossing points increases from now to year 2020 and then decreases from 2020 to year 2080 except for the old brick assemblies, The number of crossing points peaks in year 2050 and then decreases in old brick assemblies. The number of crossing points in year 2080 is less than that for the current year for all assemblies.

Table 4-4. Number of crossing point occurs at 5mm into the most exterior layer of brick under the current climate (based on 1973) and by 2020, 2050, and 2080 at Montreal International Airport. R2=0.35.

	<i>Year</i>	<i>Single Stud</i>	<i>Retrofitted Double Stud</i>	<i>Solid Masonry</i>	<i>Retrofitted XPS</i>	<i>Retrofitted Foam</i>
<i>Buff Matt Clay</i>	<i>Current</i>	137	160	138	157	162
	<i>2020</i>	151	155	133	148	148
	<i>2050</i>	133	136	109	132	130
	<i>2080</i>	101	100	76	95	95
<i>Red Matt Clay</i>	<i>Current</i>	136	142	134	148	148
	<i>2020</i>	145	151	139	148	148
	<i>2050</i>	124	129	97	133	133
	<i>2080</i>	97	97	64	86	86
<i>Calcium Silicate</i>	<i>Current</i>	118	150	139	157	162
	<i>2020</i>	132	163	112	126	127
	<i>2050</i>	124	119	91	126	121
	<i>2080</i>	91	90	62	93	99
<i>Brick (old)</i>	<i>Current</i>	100	115	115	102	102

2020	122	125	150	130	129
2050	152	150	115	158	157
2080	100	96	91	123	120

Table 4-5 shows the number of hours with RH above 95% when crossing points exist at 5mm into the brick (RHCP) under the current and future years. For wood-frame assemblies, there is no frost damage risk defined by the RHCP criteria for both the base and retrofitted assemblies under current and future climates except for the old brick assemblies. The frost damage risk increases from now to year 2050 and then decreases for the old brick assemblies. For the solid masonry assembly, adding insulation slightly increases the frost damage risks under current and future climates except for buff matt clay brick, which has no frost damage risk. For red matt clay brick, the frost damage risk decrease from now to year 2080. For the calcium silicate brick, the future climates have little impact on the frost damage risk. The frost damage risk is lower in year 2080 then current year for all assemblies except for the old brick. The retrofitted solid masonry assemblies have slightly higher risk in the old brick under year 2080 than the current year.

Table 4-5. Number of hours that 5mm into the most exterior layer of bricks has the both humidity of above 95% and crossing point under the current climate (based on 1973) and by 2020, 2050, and 2080 at Montreal International Airport. R2=0.35.

	<i>Year</i>	<i>Single Stud</i>	<i>Retrofitted Double Stud</i>	<i>Solid Masonry</i>	<i>Retrofitted XPS</i>	<i>Retrofitted Foam</i>
Buff Matt Clay	Current	0	0	0	0	0
	2020	0	0	0	0	0
	2050	0	0	0	0	0
	2080	0	0	0	0	0
Red Matt Clay	Current	0	0	0	13	16
	2020	0	0	0	12	14
	2050	0	0	0	5	15
	2080	0	0	0	0	0
Calcium Silicate	Current	0	0	0	8	8
	2020	0	0	0	6	6
	2050	0	0	0	9	9
	2080	0	0	0	5	5
Brick (old)	Current	96	109	109	99	99
	2020	116	120	145	125	125

2050	146	144	110	153	152
2080	93	93	87	116	113

4. 3. 3. Biodegradation Risk on Plywood

Biodegradation risk of plywood sheathing in the wood-frame assemblies is evaluated under current and future climatic conditions using Moisture Content (MC), Relative Humidity-Temperature (RHT), and Mold Growth Index (m).

Figure 4-16 shows the relative humidity and temperature of the plywood sheathing over the three-year simulation period for the base and retrofitted assemblies with buff matt clay brick under “no air/rain source” loading conditions for the current year. As expected, adding insulation lowers the temperature of plywood sheathing and results in higher relative humidity during the cold periods and will increase the MC of the plywood. *Figure 4-17* shows the MC of plywood sheathing over the three-year simulation period under three moisture load conditions, i.e. no air/rain source, with air leakage and with 1% rain leakage for both the base and retrofitted assemblies with buff matt clay brick. Due to the higher RH in plywood in the retrofitted double-stud assemblies, the MC level of plywood is higher than the base-case under all the three moisture load conditions. The introduction of air leakage increases the MC of plywood, however, the MC is still within the safe range under 20%. The introduction of 1% rain leakage elevates the MC of plywood sheathing above 20% for the base-case and above 30% for the double-stud case during the second-year. The MC keeps increasing, which indicates that the wood-frame assemblies may not be able to handle the continuous rain leakage deposited directly to the plywood sheathing. The double-stud assembly would experience higher risk for moisture damage.

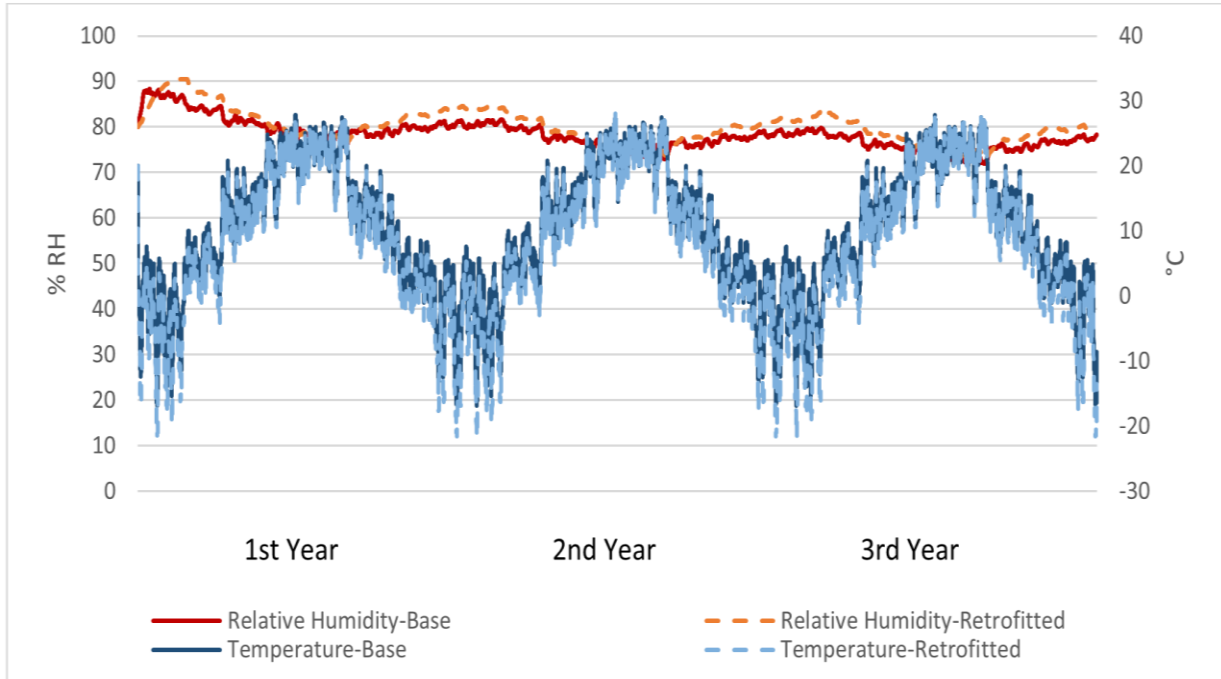


Figure 4-16. RH and T of plywood in the single stud (base) and double stud (retrofitted) assemblies with buff matt clay as the exterior brick. No source, R2=0.07

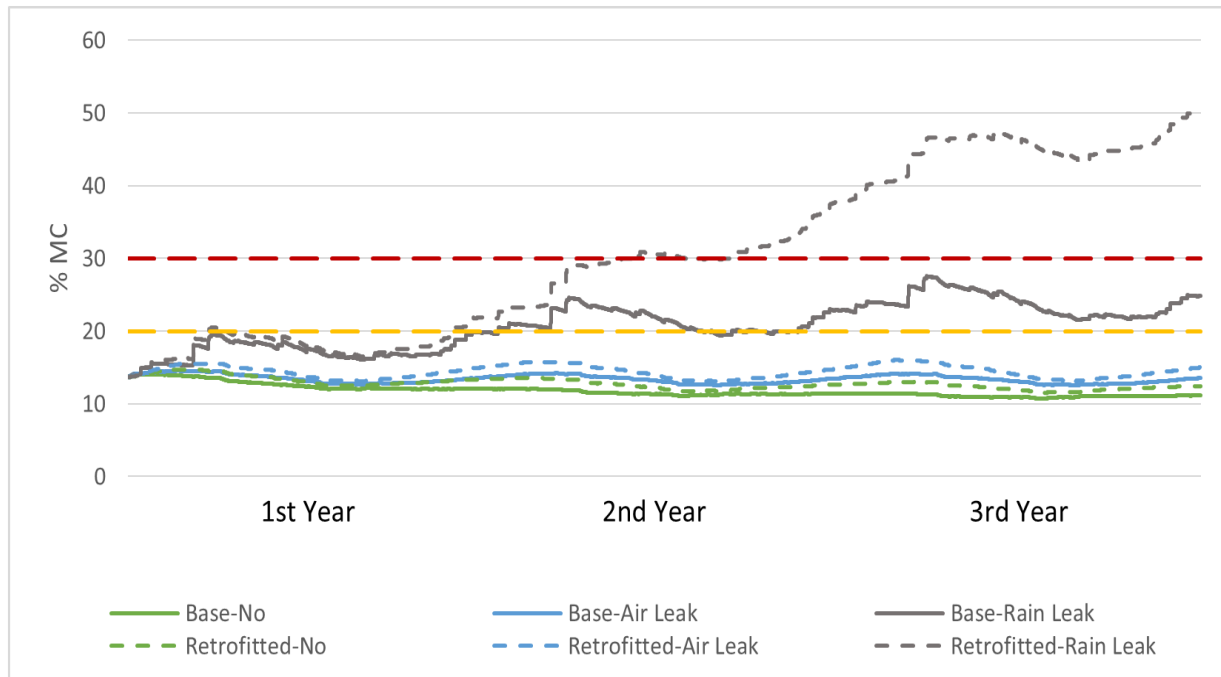


Figure 4-17. Impact of the moisture/air sources on the %MC of plywood in single stud assembly (base) and retrofitted with double stud with Buff Matt clay as exterior brick. R2=0.07.

Table 4-6 summarizes the biodegradation risks of the double-stud assembly under different simulation scenarios i.e. moisture loads, types of brick veneer, and rain deposition factors based on the MC (decay indicator) and RHT (mold growth indicator) criteria under the current climatic conditions. The MC and RHT are calculated based on the simulation results obtained from the second year.

Table 4-6. Number of hours that plywood in double stud assembly would be within biochemical risk defined by 20% of MC, 30% of MC, and RHT criteria over the second year of simulation under current climatic condition at Montreal International Airport.

		<i>NO Source</i>			<i>Air Leak</i>			<i>Rain Leak</i>		
		Decay		Mold	Decay		Mold	Decay		Mold
		%MC >20%	%MC >30%	T>5 & RH>80	%MC >20	%MC >30%	T>5 & RH>80	%MC >20%	%MC >30%	T>5 & RH>80
<i>BUFF</i>	0.07	0	0	427	0	0	4349	8761	4260	5190
<i>MATT</i>	0.35	0	0	524	0	0	4678	8761	8761	5171
<i>CLAY</i>	0.7	0	0	322	0	0	4828	8761	8761	5174
<i>RED MATT</i>	0.07	0	0	550	0	0	4804	8761	5486	5177
<i>CLAY</i>	0.35	0	0	324	0	0	4973	8761	8761	5168
	0.7	0	0	382	0	0	4397	8761	8761	5166
<i>Calcium</i>	0.07	0	0	598	0	0	4759	8761	7952	5157
<i>Silicate</i>	0.35	0	0	530	0	0	4916	8761	8761	5153
	0.7	0	0	581	0	0	4825	8761	8761	5153
<i>Old Brick</i>	0.07	1345	0	5085	8610	0	5123	8761	8761	5083
	0.35	6286	0	5021	8761	0	5052	8761	8761	5011
	0.7	7849	0	5016	8761	0	5048	8761	8761	5004

Similar to what have been observed from *Figure 4-17* for buff matt clay brick assembly, the plywood sheathing remains under 20%MC without rain leakage for assemblies except for the old brick. Due to the high water absorption coefficient of the old brick, the brick veneer may not be dried quickly enough and results in high level of MC in plywood sheathing. As shown in *Table 4-6*, with the increase of rain deposition factor, the number of hours with MC above 20% increases and when air leakage introduced to the assembly, the plywood in old brick assembly remains above 20% all year round. When 1% rain leakage introduced into the assembly, the MC of plywood stays above 20% all year round for all assemblies. With a rain factor of 0.07, over 50% of the time the

MC of plywood is above 30%. When the rain factor is increased to 0.35 and 0.70, the plywood stays above 30% all year round.

It seems that the mold growth risk defined by the RHT criteria is more stringent. As shown in *Table 4-6*, all assemblies would have mold growth risk defined by the RHT criteria when no air or rain leakage is introduced. The number of hours is significantly increased when air leakage is introduced and further increases with the introduction of rain leakage for assemblies except for the old brick. As shown in *Figure 4-18*, for all air-moisture sources the plywood in double stud assembly comprised of old brick has above 80% of RH. The introduction of rain leakage does not change much of the temperature and the number of hours meeting the RHT criteria governed by the number of hours with temperature above 5°C although plywood stays at a higher RH level, almost 100%.

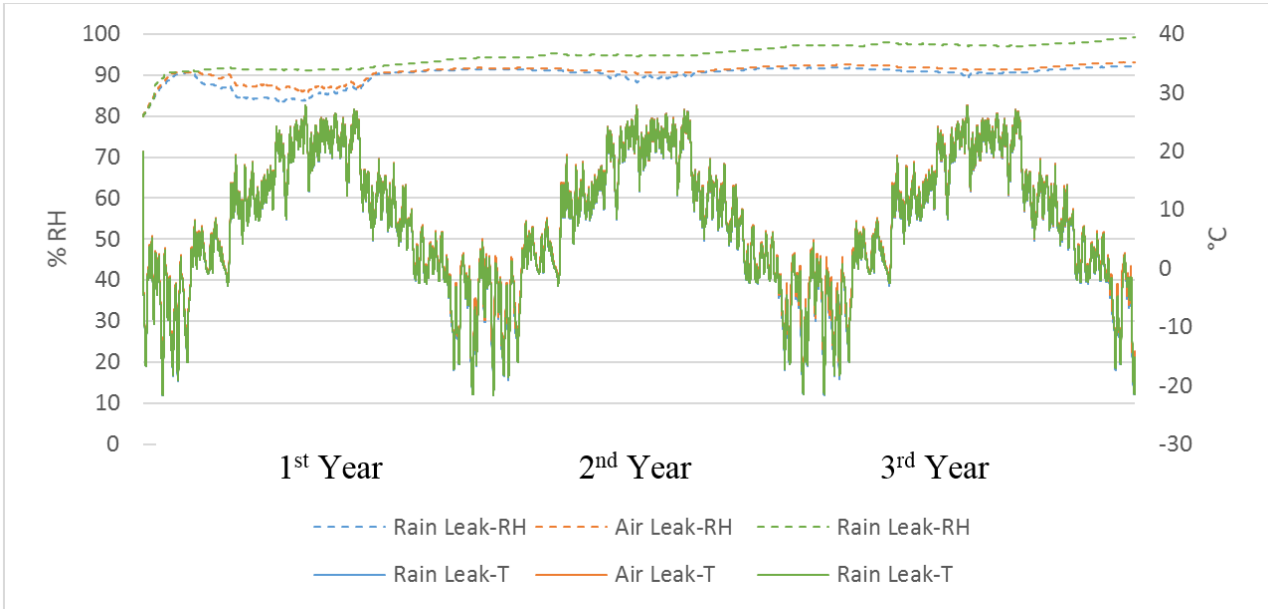


Figure 4-18. Impact of the moisture/air sources on the %RH and T of plywood in double stud assembly with old brick as the exterior brick. R2=0.07

Table 4-7 summarizes the biodegradation risks in double-stud assembly under different moisture loads with a rain deposition factor of 0.07 based on the MC and RHT criteria under the current and future climatic conditions. The MC and RHT are calculated based on the simulation results obtained from the second year.

Table 4-7. Number of hours that plywood would be within biochemical risk defined by 20% of MC, 30% of MC, and RHT criteria over the second year of simulation years under current and future climate of Montreal.

		<i>NO Source</i>			<i>Air Leak</i>			<i>Rain Leak</i>		
		<i>%MC >20%</i>	<i>%MC >30%</i>	<i>T>5 & RH>80</i>	<i>%MC >20</i>	<i>%MC >30%</i>	<i>T>5 & RH>80</i>	<i>%MC >20%</i>	<i>%MC >30%</i>	<i>T>5 & RH>80</i>
<i>Buff Matt Clay</i>	Retrofitted current	0	0	427	0	0	4349	8761	4260	5190
	Retrofitted 2020	0	0	567	0	0	4403	8226	0	5335
	Retrofitted 2050	0	0	1026	0	0	4719	6145	0	5676
	Retrofitted 2080	0	0	1501	0	0	5244	5193	0	6147
<i>Red Matt Clay</i>	Retrofitted current	0	0	550	0	0	4804	8761	5486	5177
	Retrofitted 2020	0	0	597	0	0	4880	8358	0	5328
	Retrofitted 2050	0	0	2816	0	0	5463	6283	0	5662
	Retrofitted 2080	0	0	3714	0	0	5712	5217	0	6147
<i>Calcium Silicate</i>	Retrofitted current	0	0	598	0	0	4759	8761	7952	5157
	Retrofitted 2020	0	0	2016	0	0	4947	8761	2080	5302
	Retrofitted 2050	0	0	3747	0	0	5505	6459	0	5609
	Retrofitted 2080	0	0	4464	0	0	5817	5276	0	6201
<i>Old Brick</i>	Retrofitted current	1345	0	5085	8610	0	5123	8761	8761	5083
	Retrofitted 2020	1089	0	5196	6034	0	5241	8761	8761	5188
	Retrofitted 2050	425	0	5455	4297	0	5507	8761	8761	5453
	Retrofitted 2080	0	0	5954	124	0	5996	8761	8761	5951

Table 4-7 shows that the mold growth risk defined by the RHT criteria would increase over the future climatic conditions for the retrofitted case under all simulation scenarios. The decay risk defined by MC decreases over the future climatic conditions for assemblies except for the old brick when rain leakage is introduced. For the old brick assembly, with rain leakage, the MC of plywood sheathing stays above 30% all year round. The different trends in biodegradation risk defined by these two criteria may be explained as that over the future climatic conditions higher rainfall is

expected therefore higher MC due to rain leakage, however, the higher temperature and solar radiation increases drying of the assembly as well, as a result of increased wetting and increased drying, most of the assemblies have lower MC except for the old brick assembly. In the old brick assembly, the increase in wetting is more significant than the increase in drying capacity, therefore, the number of hours above 30%MC is the same. As for the RHT criteria, the balance between wetting and drying still results in higher number of hours with meeting the RHT criteria.

Mold growth risk in plywood is also investigated for three consecutive years using the widely used mold growth model proposed by Hukka and Viitanen (1999). *Figure 4-19* shows the mold growth index of plywood sheeting in double stud assemblies with a rain deposition factor of 0.07. Results *Figure 4-19* of are based on the deduction of decreasing values in unfavourable conditions. It is seen that under air leak and rain leak source the mold growth would likely increase. *Table 4-8* shows the impact of rain deposition factors of 0.07, 0.35, and 0.7 on the mold growth index of plywood sheeting in the single stud (Base assembly) and retrofitted to double stud assembly. The results are based on three years of simulation under base climate (year 1973) at Montreal International Airport. It is observed that upgrading of the base assembly (single stud) to the retrofitted option (double stud) would increase the mold growth risk. Increasing of the rain deposition factor from 0.07 to 0.7 would likely increase the mold growth intensity from 0 to 5.71.

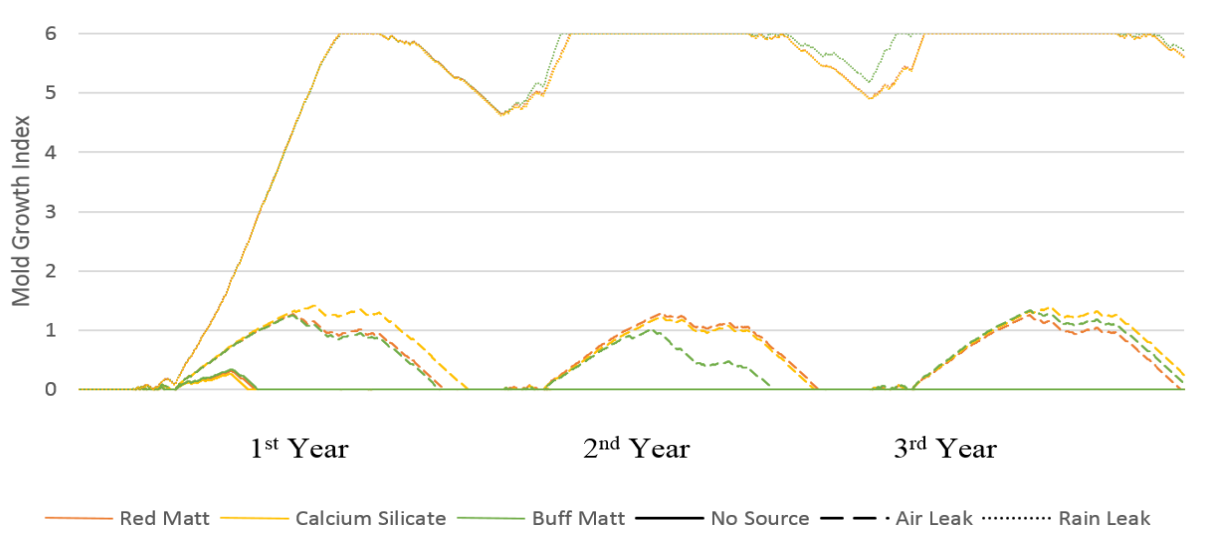


Figure 4-19. Mold growth index of plywood sheathing in double stud assembly over three years of simulation under base weather data (1973) at Montreal International Airport. With decreasing consideration.

Table 4-8. Impact of rain deposition factor on the mold growth index of plywood sheathing over three years of simulation under current climate of Montreal International Airport.

	<i>No source</i>		<i>Air Leak</i>		<i>Rain Leak</i>		
	Rain Deposition	Base Case	Retrofitted	Base Case	Retrofitted	Base Case	Retrofitted
Buff Matt	0.07	0	0	0	0.10	5.21	5.66
	0.35	0	0	0	0.25	5.27	5.66
	0.7	0	0	0	0.41	5.31	5.71
Red Matt	0.07	0	0	0	0	5.20	5.62
	0.35	0	0	0	1.16	5.28	5.66
	0.7	0	0	0	5.71	5.35	5.66
Calcium Silicate	0.07	0	0	0	0.25	5.19	5.60
	0.35	0	0	0	2.32	5.26	5.66
	0.7	0	0.01	0	5.70	5.37	5.66

Table 4-9 investigates the impact of climate change on mold growth index of both base case and retrofitted assemblies exposed to rain deposition factor of 0.07 under three years of simulation at Montreal International Airport. Results show that under future climates at Montreal International Airport the mold growth risk of plywood sheathing in retrofitted assemblies would decrease. Mold growth index in the base assemblies would peak by 2050 and would likely decrease onwards.

Among all moisture-air sources the rain leakage scenario would cause more mold growth index whereas except by 2080 plywood in all assemblies with rain source would be within level 5 of mold index.

Table 4-9. Impact of climate change on the mold growth index of plywood sheeting over three years of simulation under current climate of Montreal International Airport.

		<i>No source</i>		<i>Air Leak</i>		<i>Rain Leak</i>	
		<i>Base Case</i>	<i>Retrofitted</i>	<i>Base Case</i>	<i>Retrofitted</i>	<i>Base Case</i>	<i>Retrofitted</i>
<i>Buff Matt</i>	<i>Base weather</i>	0	0	0	0.1	5.21	5.66
	<i>2020</i>	0	0	0	0	5.32	5.46
	<i>2050</i>	0	0	0	0	5.48	5.38
	<i>2080</i>	0	0	0	0	3.29	5.36
<i>Red Matt</i>	<i>Base weather</i>	0	0	0	0	5.20	5.62
	<i>2020</i>	0	0	0	0	5.31	5.47
	<i>2050</i>	0	0	0	0	5.49	5.35
	<i>2080</i>	0	0	0	0	3.55	5.16
<i>Calcium Silicate</i>	<i>Base weather</i>	0	0	0	0.25	5.19	5.60
	<i>2020</i>	0	0	0	0	5.30	5.68
	<i>2050</i>	0	0	0	0	5.47	5.32
	<i>2080</i>	0	0	0	0	4.21	5.25

CHAPTER 5. Conclusion

5. 1. Summary of Research

This study investigates the building performance of a typical Canadian single-family house retrofitted to the PassiveHaus standard under the current and future climates. Building performance is determined in terms of the energy consumption, thermal comfort, and durability. Weather data for future years are generated using HasCM3 general circulation model with the A2 emission scenario. IES is used for the whole building energy simulations. Thermal comfort is evaluated for the free running south oriented room using two methods of temperature of greater than 26°C and thermal comfort limits defined by the adoptive model for naturally ventilated single-family houses proposed by peeters et al. (2013). Five different shading scenarios were proposed for the PH to assess both thermal comfort and energy consumption.

Durability analysis is done in terms of the potential of freeze thaw risk in the 1cm of the most exterior layer of the exterior brick and the potential of biochemical risk in plywood using WUFI Pro. For the freeze thaw analysis single stud assembly and solid masonry are considered as above grade walls in the base case. These assemblies are also considered to be retrofitted to meet the requirements of the PassiveHaus standard and then freeze thaw risk in the base case assemblies and the retrofitted options are compared under the current and future climates. Moreover, the impact of various changing parameters including the different exterior bricks including Buff Matt Clay, Red Matt Clay, Calcium Silicate, and Old Brick; different moisture/air sources including “No source”, “Infiltration”, and “Rain Source”; and various rain deposition factors of 0.07, 0.35, and 0.7 are investigated under the current climate (1973 as the base climate), 2020, 2050 and 2080

climates at Montreal International Airport. Biochemical risk of the plywood is also investigated for the single stud assembly (base above grade wall) and retrofitted to double stud assembly which meets the PH requirements.

5. 2. Research Contributions and Conclusions

5. 2. 1. Energy Consumption

Simulation results also show that in 2013 the annual energy required to moderate internal temperature of QEC and PH retrofitted option would be approximately 45MWh and 8.6MWh, respectively. Nevertheless in 2080, these amounts would likely decrease to about 35MWh and 8.2MWh, respectively. Therefore, the total energy consumption in QEC house would decrease by 21% from the current year to 2080, while the total energy consumption in the retrofitted house decreases by 9% from the current year to 2020 then slightly increases afterwards.

The trend in the energy consumption of PH house over future climates implies that the insulation level of building envelopes may need to be optimized over the predicted future climates. For conditioned PH houses in Montreal the impact of shading devices on the energy consumption is negligible.

5. 2. 2. Thermal Comfort

Results show that compared to the base case, the PH retrofitted option has higher risks of overheating. It is observed that in the house built to the QEC with natural ventilation the overheating (indoor temperature greater than 26°C) is around 0.1% and 10.0% of the time within a year in 2013 and year 2080, respectively. However, for the same house retrofitted to the

PassiveHaus standard, the overheating risks would increase to 5.2% and 31.4% in 2013 and 2080, respectively.

Moreover, it was concluded that the total number of hours in QEC house in compliance with 90% acceptability would be 1883 hours, which is 23% and 3% higher than the PH with no shading and the PH with shading D under current weather conditions, and 51% and 42% higher in 2080. Results also indicated that having any of the shading configurations A, B, C and D in the free running house would increase the number of acceptable hours for PH house, among which shading D provides the most. It was observed that the total number of hours in PH with shading D in compliance with 90% acceptability would be around 21% and 16 % higher than that in PH house with no shading in 2013 and 2080 respectively.

5. 2. 3. Durability

Weather data analysis shows that the number of crossing points that is expected to occur for Montreal would peak by 2020. FDEI shows that the frost decay exposure potential would likely increase from 1973 to 2020. It is predicted that from 2020 onward this risk would likely decrease. Simulation shows that upgrading of the base cases (except for the old brick in solid masonry assemblies with R2 of 0.35 and 0.7 and in double stud with R2 of 0.07) to retrofitted strategies (except for the old brick in retrofitted with XPS and foam) would not only increase the frost decay risk by the current climate but also by 2080. However, this risk would significantly decrease by 2080.

It is concluded that Buff Matt Clay brick performs better with no hour in the frost decay risk zones compared to other bricks by the current climate and 2080. Old brick has the most number of hours in frost decay risk. Red Matt Clay and Calcium Silicate might be within the freeze thaw risk zone

by the current climate. However, there would be likely no frost decay risk for the Red Matt Clay in 2080.

Results show that retrofitting of the single assembly to double stud would significantly increase the biodegradation risk on plywood, except for the old brick. Results also showed that when “No Source” is introduced into the assemblies the number of hours in biodegradation risk would be less than the “Air Leak” and the “Rain Leak”.

Study shows that the number of hours that plywood would be in decay risk defined by MC would likely decrease from the current climate to 2080. However, when RHT criteria is used as determination of the risk the mold growth on plywood would be more by 2080 than the current climate. Mold growth risk of plywood in assemblies comprised of any brick veneer, except with old brick, would likely decrease over the future climate.

5. 3. Limitations

In this study IPCC’s A2 storyline was chosen to create the future climate. Investigation on other CO2 emission storylines and a wider range for the prediction of the future rain would increase the accuracy of the research; which due to time limitation it was not assessed in this research.

References

- Aarle, M. V., Schellen, H. & Schijndel, J. V., 2015. *Hygro Thermal Simulation to Predict the Risk of Frost Damage in Masonry; Effects of Climate Change*. Torino, IBPC.
- Aguiar, R., Oliveira, M. & Goncalves, H., 2002. Climate change impacts on the thermal performance of Portuguese buildings Results of the SIAM study. *Build, Serv, Eng, Technol*, 44(12), pp. 223-231.
- Alfano, F. R., Lanniello, E. & Palella, B. I., 2013. PMV-PPD and acceptability in naturally ventilated schools. *Building and Environment*, Volume 67, pp. 129-137.
- Al-Tamimi, N. A. & Fadzil, S. F. S., 2011. The potential of shading devices for temperature reduction in high rise residential buildings in the tropics. *Procedia Engineering*, Volume 21, pp. 273-282.
- Asadi, E., Da Silva, M. G., Antunes, C. H. & Dia, L., 2012. Multi-objective optimization for building retrofit strategies: A model and an application. *Energy and Buildings*, Volume 44, pp. 81-87.
- ASHRAE, 2010. *Standard for the design of high – performance green buildings except low-rise residential buildings*, Atlanta: American Society of Heating, Refrigerating and Air Conditioning.
- Athienitis, A. & Santamouris, M., 2002. *Thermal Analysis and Design of Passive Solar Buildings.*, London: Jame & James (Science Publishers) Ltd.,.
- Badea, A. et al., 2014. A life-cycle cost analysis of the passive house “POLITEHNICA” from Bucharest. *Energy and Buildings*, Volume 80, pp. 542-555.
- Barlow, S. & Fiala, D., 2007. Occupant comfort in UK offices—How adaptive comfort theories might influence future low energy office refurbishment strategies. *Energy and Building*, Volume 39, pp. 837-846.
- Berger, T. et al., 2014. Impacts of climate change upon cooling and heating energy demand of office buildings in Vienna, Austria. *Energy and buildings*, Volume 80, pp. 517-530.
- Bill Dunster Architects, 2005. *UK Housing and climate change. Heavyweight vs. lightweight construction*, London: Arup Research and Development.
- Bjorsell, N. et al., 1999. *IDA indoor climate and energy*. Kyoto, IBPSA Building Simulation 99 conference.

BSI, 1992. *BS8104, Code of practice for assessing exposure of walls to wind-driven rain*, s.l.: British Standard.

Canada, N. r., 2011. *Complementary Programs and Incentives for Homes*. [Online] Available at: <http://oee.nrcan.gc.ca/residential/personal/retrofit/272?attr=4> [Accessed 28 05 2013].

CANLII, 2013. *Regulation respecting energy conservation in new buildings*. [Online] Available at: <http://canlii.ca/t/11gw>

Chan, A., 2012. Effect of adjacent shading on the thermal performance of residential buildings in a subtropical region. *Applied Energy*, Volume 92, pp. 516-522.

Chowa, D. C., Li, Z. & Darkwaa, J., 2013. The effectiveness of retrofitting existing public buildings in face of future climate change in the hot summer cold winter region of China. *Energy and Buildings*, p. 176–186.

CMHC, 2004. *Renovating for Energy Savings: Case Studies*. [Online] Available at: <http://www.cmhc-schl.gc.ca/en/co/grho/reensa/index.cfm> [Accessed 15 March 2015].

CMHC, 2011. *Research Report: Near Net Zero - Energy Retrofits for Houses*, Vancouver: Canada Mortgage and housing Corporation.

CMHC, 2012. *Highly energy Efficient Building Envelope Retrofits for Houses*, Ottawa: Canada Mortgage Housing Corporation.

Coley, D., Kershaw, T. & Eames, M., 2012. A comparison of structural and behavioural adaptations to future proofing buildings against higher temperatures. *Building and Environment*, Volume 55, pp. 159-166.

Coley, D. & Kershaw, T., 2010. Changes in internal temperatures within the built environment as a response to a changing climate. *Building and Environment*, 45(1), pp. 89-93.

De Dear, R. & Brager, G., 1998. Towards an adaptive model of thermal comfort and preference. *ASHRAE transaction*, pp. 145-167.

de Wilde, P., Rafiq, Y. & Beck, M., 2008. Uncertainties in predicting the impact of climate change on thermal performance of domestic buildings in the UK. *Building Services Engineering Research and Technology*, 29(1), pp. 7-26.

Dear, R. d. & Brager, G. S., 2001. The adaptive model of thermal comfort and energy conservation in the built environment. *International Journal of Biometeorol*, Volume 45, pp. 100-108.

Department of Resources, E. a. T., 2010. *Improving the energy efficiency of commercial and government buildings*. [Online]
Available at: <http://www.climatechange.gov.au/what-you-need-to-know/buildings/commercial.aspx>
[Accessed 1 September 2013].

Djebbar, D., Mukhopadhyaya, P. & Kumaran, M. K., 2002. *Retrofit strategies for a high-rise wall system and analysis of their hygrothermal effects*, s.l.: National Research council Canada.

DOE, 2009. *DOE to Fund up to \$454 Million for Retrofit Ramp-Ups in Energy Efficiency*. [Online]
Available at: <http://energy.gov/articles/doe-fund-454-million-retrofit-ramp-ups-energy-efficiency>
[Accessed 1 September 2013].

DOECC, 2010. *Warmer homes, greener homes: a strategy for household energy management*. [Online]
Available at: <https://www.gov.uk/government/organisations/department-of-energy-climate-change>
[Accessed 2 September 2013].

Egricon, 2010-2011. *MarkSim™ DSSAT weather file generator*. [Online]
Available at: <http://gismap.ciat.cgiar.org/MarkSimGCM/>
[Accessed 06 08 2014].

EN 15026, 2007. *Hygrothermal performance of building components and building elements. Assessment of moisture transfer by numerical simulation. EN 15026:2007*, s.l.: BSI.

Environment Canada, 2008. *Canadian weather energy and engineering data files (CWEEDSfiles), canadian weather for energy calculation (CWEC files) user manual*, Canada: Environment Canada.

Environment canada, 2014. *Canada's national climate archive*. [Online]
Available at: http://climate.weather.gc.ca/index_e.html
[Accessed 03 10 2014].

Environment Canada, 2014. *Current Weather in Montréal*. [Online]
Available at: <http://montreal.weatherstats.ca/>
[Accessed 13 09 2014].

Environment Canada's National Climate Services, 2013. *historical climate data*. [Online]
Available at: http://climate.weather.gc.ca/index_e.html#access

Fedorik, F. & Illikainen, K., 2013. HAM and mould growth analysis of a wooden wall. *International Journal of Sustainable Built Environment*, Volume 2, pp. 19-26.

Fenech, A. & Comer, N., 2013. *Future Projections of Climate Change for the Atlantic Region of Canada Using Global Climate Models Used in the IPCC Fifth Assessment Report (2014)*, Charlottetown: University of Prince Edward Island.

Fraunhofer IBP, 2013. *WUFI (Version 5.2) [Software]*. [Online] Available at: www.wufi.de [Accessed 28 01 2014].

Freewan, A. A., 2014. Impact of external shading devices on thermal and daylighting performance of offices in hot climate regions. *Solar Energy*, Volume 102, pp. 14-30.

Gamtessa, S. & L.Ryan, D., 2007. *Utilization of energy saving retrofit programs in Canada. Who? What? Why?*, Edmonton: Canadian Building Energy End-use data and analysis centre.

Gaterell, M. & McEvoy, M., 2005. The impact of climate change uncertainties on the performance of energy efficiency measures applied to dwellings. *Energy and Buildings*, 37(9), pp. 982-995.

Ge, H. & Krpan, R., n.d. *Wind-driven Rain Study in the Coastal Climate of British Columbia*, Burnaby: British Columbia Institute of Technology.

George Brown College, 2013. *ARGILE retrofit Guide*, Toronto: George Brown College.

Grossi, C. M., Brimblecombe, P. & Harris, L., 2007. Predicting long term freeze-thaw risks on Europe built heritage and archeological sites in a changing climate. *Science of The Total Environment*, 377(2), pp. 273-281.

Gupta, R. & Gregg, M., 2012. Using UK climate change projections to adapt existing English homes for a warming climate. *Building and Environment*, pp. 8-17.

Gupta, R. & Gregg, M., 2012. Using UK climate change projections to adapt existing English homes for a warming climate. *Building and Environment*, Volume 55, pp. 20-42.

Halawa, E. & Van Hoof, J., 2012. The adaptive approach to thermal comfort: Critical overview. *Energy and Buildings*, pp. 101-110.

Halawa, E. & Van Hoof, J., 2012. The Adaptive Approach to Thermal Comfort: A Critical Overview. *Energy and Buildings*, pp. 101-110.

Haojie, W. & Chen, Q., 2014. Impact of climate change heating and cooling energy use in buildings in the United States. *Energy and Building*, Volume 82, pp. 428-436.

Haupt, K., Jurk, K. & Petzold, H., 2003. *Inside thermal insulation for historical facades*, Lisse: Balkema Publishers.

Huang, Yu; Niu, Jian-lei; Chung, Tse-ming, 2013. Study on performance of energy-efficient retrofitting measures on commercial building external walls in cooling-dominant cities. *Applied Energy*, Volume 103, p. 97–108.

Huang, Y., Niu, J.-l. & Chung, T.-m., 2012. Energy and carbon emission payback analysis for energy-efficient retrofitting in buildings_ overhang shading options. *Energy and Buildings*, p. 94–103.

Hughes, R. & Bargh, B., 1982. *The weathering of brick: Causes, assessment and measurement.*, Champaign: Report of the joint Agreement between the US. Geological Survey and the Illinois State Geological Survey.

Hukka, A. & Viitanen, H., 1999. A mathematical model of mould growth on wooden material. *Wood Sci Technol*, 33(6), pp. 475-85.

Hulme, M. et al., 2002. *Climate Change Scenarios for the United Kingdom: The UKCIP02 Scientific Report*, Norwich: Tyndall Centre for Climate Change Research, University of East Anglia.

Humphreys , M. & Hancock, M., 2007. Do people like to feel ‘neutral’? Exploring the variation of the desired thermal sensation on the ASHRAE scale. *Energy Build*, Volume 39, pp. 867-878.

IBP, 2011. *WUFI Pro Version 5.1*, Holzkirchen: Fraunhofer Institute for Building Physics.

IEA Annex 14 Final Report, 1991. *Condensation and Energy, Sourcebook*, K.U.Leuven: International Energy Agency, Energy Conservation in Buildings.

IEA, 2011. *Annex 50, Prefabricated Systems for Low Energy Renovation of Residential Buildings*. [Online]
Available at: <http://www.ecbcs.org/annexes/annex50.htm>
[Accessed 20 05 2015].

IEA, 2015. *Annex 55-Reliability of Energy Efficient Building Retrofitting-Probability Assessment of Performance and Cost (RAP-RETRO)*, Gothenburg: Department of Civil and Environmental Engineering, CHALMERS UNIVERSITY OF TECHNOLOGY.

Institute for Catastrophic Loss Reduction, 2011. *Climate change information for adoption*. [Online]
Available at: http://www.iclr.org/images/Bruce_climate_change_info_march_2011.pdf
[Accessed 09 09 2014].

IPCC, 2007. *The Physical Science Basis. Working Group I Contribution to the Fourth Assessment Report of the Intergovernmental Panel on Climate Change*, Cambridge: Cambridge University.

IPHA, 2010. *Passive House Guidelines*. [Online] Available at: http://www.passivehouse-international.org/index.php?page_id=80 [Accessed 19 12 2013].

ISO, 2009. *Hygrothermal performance of buildings – Calculation and presentation of climatic data – Part 3: Calculation of a driving rain index for vertical surfaces from hourly wind and rain data*. ISO 15927-3:2009, s.l.: International Organization for Standardization.

Jacob, D. et al., 2008. *Klimaauswirkungen und Anpassung in Deutschland—Phase 1: Erstellung regionaler Klimaszenarien für Deutschland*, UBA, Roßlau: Umweltbundesamt.

Jentch, M., Bahaj, A. & James, P., 2008. Climate change future proofing of buildings generation and assessment of building simulation weather files. *Energy and Buildings*, 40(12), pp. 2148-2168.

Johns, T. C. et al., 2003. Anthropogenic climate change for 1860 to 2100 simulated with the HadCM3 model under updated emissions scenarios. *Climate dynamics*, Volume 20, pp. 583-612.

Jonas, T., Marty, C. & Magnusson, J., 2009. Estimating the snow water equivalent from snow depth measurements in the Swiss Alps. *Journal of Hydrology*, 378(2009), pp. 161-167.

Jylha, K. et al., 2015. Energy demand for the heating and cooling of residential houses in Finland in a changing climate. *Energy and Buildings*, Volume 99, pp. 104-116.

Jylha, K. et al., 2009. *The changing climate in Finland: estimates for adaption studies*. ACCUM project report 2009, Helsinki: Finnish Meteorological Institute.

Karimpour, M. et al., 2015. Impact of Future Climate change on the Design of energy Efficient Residential Building Envelopes. *Energy and Buildings*, Volume 87, pp. 142-154.

Kesik, T. & Saleff, I., 2009. *Tower Renewal Guidelines; For the Comprehensive Retrofit of Multi-Unit Residential Buildings in Cold Climates*, Toronto: University of Toronto.

Köliö, A., Pakkala, T. A., Lahdensivu, J. & Kiviste, M., 2014. Durability demands related to carbonation induced corrosion for Finnish concrete buildings in changing climate. *Engineering Structures*, Volume 62-63, pp. 42-52.

Konstantinou, T. & Knaackb, U., 2013. An approach to integrate energy efficiency upgrade into refurbishment design process, applied in two case-study buildings in Northern European climate. *Energy and Building*, pp. 301-309.

Kwong, Q. J., Adam, N. M. & Sahari, B., 2014. Thermal comfort assessment and potential for energy efficiency enhancement in modern tropical buildings: A review. *Energy and Building*, pp. 547-557.

- Laefer, D., Boggs, J. & Cooper N, 2004. Engineering properties of historic brick - variability considerations as a function of stationary versus nonstationary kiln type.. *Journal of American Institute of conservation of Historic and Artistic Works*, 4(3), pp. 255-272.
- Levy, P. E., Cannel, M. G. & Friend, A. D., 2004. Modelling the impact of future changes in climate, CO₂ concentration and land use on natural ecosystems and the terrestrial carbon sink. *Global Environmental Change*, Volume 14, pp. 21-30.
- Lis, K. M. et al., 2007. A frost decay exposure index for porous, mineral building materials. *Building and Environment*, Volume 42, pp. 3547-3555.
- Lomas, K. & Giridharan, R., 2012. Thermal comfort standards, measured internal temperatures and thermal resilience to climate change of free running buildings : A case study of hospital wards. *Building and Environment*, Volume 55, pp. 57-72.
- Lomas, K. & Giridharan, R., 2012. Thermal comfort standards, measured internal temperatures and thermal resilience to climate change of free-running buildings: a case-study of hospital wards. *Building and Environment*, Volume 55, pp. 57-72.
- Maeyens, J., Janssens, A. & Breesch, H., 2001. *Ontwerpregels voor zomercomfort in woningen*, Belgium: Division of Architecture, Department of applied Science, University of Gent.
- Mavrogianni, A. et al., 2012. Building characteristics as determinants of propensity to high indoor summer temperatures in London dwellings. *Building and Environment*, Volume 55, pp. 117-130.
- Ma, Z., Cooper, P., Daly, D. & Ledo, L., 2012. Existing building retrofits: Methodology and state-of-the-art. *Energy and Buildings*, pp. 889-902.
- McLeod, R. S., Hopfe, C. J. & Kwan, A., 2013. An investigation into future performance and overheating risks in Passivhaus dwellings PassiveHaus dwellings. *Building and Environment*, pp. 189-209.
- Ministry of Energy, 2013. *Conservation First: A Renewed Vision for Energy Conservation in Ontario*. [Online]
Available at: <http://www.energy.gov.on.ca/en/conservation-first/>
[Accessed 20 05 2015].
- Morelli, M. et al., 2012. Energy retrofitting of a typical old Danish multi-family building to a “nearly-zero” energy building based on experiences from a test apartment. *Energy and Buildings*, Volume 54, pp. 395-406.
- Nakicenovic, N. & Swart, R., 2007. *IPCC Special Report on Emmission Scenarios*, Geneva: International Panel on Climate Change.

National Research Council, 2010. *Canadian Centre for Housing Technology*. [Online] Available at: [ccht-cctr.gc.ca: http://www.ccht-cctr.gc.ca/eng/index.html](http://www.ccht-cctr.gc.ca/eng/index.html) [Accessed 02 01 2014].

Nijland, T. G., Adan, O. C., Van Hees, R. P. & Van Etten, B. D., 2009. Evaluation of the effects of expected climate change on the durability of building materials with suggestions for adoption. *HERON*, Volume 54, pp. 1-37.

Nikoofard, S., Ugursal, I. & Beausoleil-Morrison, I., 2014. Technoeconomic assessment of the impact of window shading retrofits on the heating and cooling energy consumption and GHG emissions of the Canadian stock. *Energy and Buildings*, Volume 69, pp. 354-366.

Nik, V. M. & Kalagasidis, A. S., 2013. Impact study of the climate change on the energy performance of the building stock in Stockholm considering four climate uncertainties. *Building and Environment*, Volume 60, pp. 291-304.

Nik, V. M., Kalagasidis, A. S. & Kjellstrom, E., 2012. Assessment of hygrothermal performance and mould growth risk in ventilated attics in respect to possible climate changes in Sweden. *Building and Environment*, Volume 55, pp. 96-109.

Orme, M., Palmer, J. & Irving, S., 2003. *Control of overheating in well-insulated housing housing*. In: *Building sustainability*. [Online] Available at: <http://www.cibse.org/pdfs/7borme.pdf>

Orosa, J. A. & Oliveira, A. C., 2011. A new thermal comfort approach comparing adaptive and PMV models. *Renewable Energy*, Volume 36, pp. 951-956.

Oseland, N. A., 1994. comparison of the predicted and reported thermal sensation vote in homes during winter and summer. *Energy Build*, Volume 21, pp. 45-54.

Palmero-Marrero, A. & Oliveira, A. C., 2010. Effect of louver shading devices on building energy requirements. *Applied Energy*, Volume 87, pp. 2040-2049.

Passive House Institute, 2011. *Quality Approved Passive House Certification-Criteria for Residential Passive Houses*. [Online] Available at: www.passiv.de [Accessed 15 01 2015].

Passive House Institute, 2012. *Passive House Requirements*. [Online] Available at: http://passiv.de/en/02_informations/02_passive-house-requirements/02_passive-house-requirements.htm

Passive House Institute, 2012. *What is a Passive House?*. [Online] Available at: http://www.passiv.de/en/02_informations/01_whatisapassivehouse/01_whatisapassivehouse.htm

Peeters, L., Dear, R. D., Hensen, J. & D'haeseleer, W., 2009. Thermal Comfort in Residential Buildings: comfort Values and Scale for Building Energy simulation. *Applied Energy*, Volume 86, pp. 772-780.

Ren, Z., Chen, Z. & Wang, X., 2011. Climate change adaptation pathways for Australian residential buildings. *Building and Environment*, 46(11), pp. 2398-412.

Robert, A. & Kummert, M., 2012. Designing net-zero energy buildings for the future climate, not for the past. *Building and environment*, pp. 150-158.

Roy, L., Leconte, R., Brissette, F. & Marche, C., 2001. The Impact of Climate Change on Seasonal Floods of a Southern Quebec River Basin. *Hydrological Processes*, Volume 15, pp. 3167-3179.

Sahlin, P. et al., 2004. Whole building simulation with symbolic DAE equations and general purpose solvers. *Building and Environment*, Volume 39, pp. 949-958.

Sajjadian, S., Lewis, J. & Sharpless, S., 2013. *Risk and Uncertainty in Sustainable Building Performance*. Berlin, Springer, pp. 903-912.

Santamouris, M. & Hestnes, A., 2002. Office—passive retrofitting of office buildings to improve their energy performance and indoor working conditions. *Building and Environment*, pp. 555 - 556.

SDC, 2007. *Stock Take: Delivering Improvements in Existing Housing*. Sustainable Development Commission. [Online] Available at: [http://www.sd-www.sd-commission.org.uk/publications/downloads/Stock Take UK Housing.pdf](http://www.sd-www.sd-commission.org.uk/publications/downloads/Stock_Take_UK_Housing.pdf) [Accessed 24 05 2013].

SEDLBAUER, K., 2002. Prediction of Mould Growth by Hygrothermal Calculation. *Thermal Environment and Building Science*, pp. 321-335.

SEI, 2009. *Retrofitted Passive Homes- Guideline for upgrading existing dwellings to the PassiveHaus Standard*, Clonakilty: Sustainable Energy Ireland (SEI).

Sharpless, S., 2009. *Use of climate change scenarios for building simulation: the CIBSE future weather years*, London: CIBSE.

Simons, R., 2008. Altering existing buildings in the UK. *Energy Policy*, p. 4482–4486.

Solomon, S. et al., 2007. *Contribution of Working Group I to the fourth Assessment Report of the Intergovernmental Panel on Climate Change*, Cambridge: Cambridge University Press.

Straaten, R. V., 2014. *Improving access to the frost dilatometry methodology for assessing brick masonry freeze thaw degradation risk*. Waterloo, Building Science Consulting Inc.

Straube, J., 2009. *The Passive House (Passivhaus) Standard: A comparison to other cold climate low-energy houses*. [Online]
Available at: <http://www.buildingscience.com/documents/insights/bsi-025-the-passivhaus-passive-house-standard>

Straube, J. & Schumacher, C., 2007. *Interior Insulation Retrofits of Load-Bearing Masonry Walls in Cold Climates*, Toronto: Building Science Press.

Straube, J., Schumacher, C. & Mensigna, P., 2010. *Assessing the FreezeThaw Clay Brick for Interior Insulation Retrofit Projects*. Florida, s.n.

Sustainable Energy Research Group, 2009. *Climate change Weather File Generator (CCWeatherGen) manual*, Southampton: Department of Civil Engineering and the Environment, University of Southampton.

Tobias, L. & Vavaroutsos, G., 2009. *Retrofitting Office Buildings to be Green and Energy-Efficient: Optimizing Building Performance, Tenant Satisfaction, and Financial Return*, Washington DC: Urban Land Institute ULI.

TRCCG, 2008. *Your Home in a Changing Climate. Retrofitting Existing Homes for Climate Change Impacts*. [Online]
Available at: <http://www.london.gov.uk/trccg/docs/pub1.pdf>
[Accessed 09 07 2013].

U.S. Department of Energy, 2012. *Energy Plus Energy Simulation Software*. [Online]
Available at: http://apps1.eere.energy.gov/buildings/energyplus/cfm/weather_data3.cfm/region=4_north_and_central_america_wmo_region_4/country=3_canada/cname=CANADA
[Accessed 23 07 2014].

Ueno, K., Straube, J. & Straaten, R. V., 2013. *Field monitoring and simulation of a historic mass masonry building retrofitted with interior insulation*. Florida, In Proceeding of the Performance of the Exterior Envelopes of Whole Buildings.

University of Waterloo, 2012. *Waterloo News*. [Online]
Available at: <https://uwaterloo.ca/news/news/climate-change-warm-canada-increased-temperatures-2c-2020>
[Accessed 14 September 2014].

Van Den, H. B. et al., 2006. *KNMI climate change scenarios 2006 for the Netherlands*, De bilt: KNMI.

van der Linden, A., Boerstra, A., Kurvers, S. & De Dear, R., 2006. Adaptive etemperature limits: a new guideline in The Netherlands. A new approach for the assessment of building performance with respect to thermal indoor climate. *Energy Build*, Volume 38, pp. 8-9.

Vereecken, E., Van Gelder, L., Janssen, H. & Roels, S., 2015. Interior insulation for wall retrofitting – A probabilistic analysis of energy savings and hygrothermal risks. *Energy and Buildings*, Volume 89, pp. 231-244.

Viitanen, H. & Ojanen, T., 2007. *Improved Model to Predict Mold Growth in Building Materials, Paper based on the VTT Projects “Building Biology” and “Integrated Prevention of Moisture and Mould Problems”*, Finland: Building Biology.

Wang, F. et al., 2014. Developing a weather responsive internal shading system for atrium spaces of a commercial building in tropical climates. *Building and Environment*, Volume 71, pp. 259-274.

Wang, H. & Chen, Q., 2014. Impact of climate change heating and cooling energy use in buildings in the United States. *Energy and Buildings*, Volume 82, pp. 428-436.

Wang, X., Chen, D. & Ren, Z., 2010. Assessment of climate change impact on residential building heating and cooling energy requirement in Australia. *Building and Environment*, 45(7), pp. 1663-1682.

Wan, L., Li, D., Pan, W. & Lam, J., 2012. Impact of climate change on building energy use in different climate zones and mitigation and adaptation implications. *Applied Energy*, Volume 97, pp. 274-282.

Warner, M., 2012. *Climate change to warm Canada with increased temperatures of up to 2C by 2020 and 4C by 2050.* [Online] Available at: <https://uwaterloo.ca/news/news/climate-change-warm-canada-increased-temperatures-2c-2020>

Wilkinson, J., Rose, D., Sullivan, B. & Straube, J., 2009. Measuring the Impact of Interior Insulation on Solid Masonry Walls in a Cold Climate. *Journal of Building Enclosure Design*, Summer, Volume Summer 2009, pp. 11-17.

Wytrykowska, H., Uneo, K. & Straaten, V., 2012. *Byggmeister test home: Cold Climate multifamily masonry building condition assessment and retrofit analysis.*, Golden: Building America Report, US Department of Energy.

Zmeureanu, R. & Renaud, G., 2008. Estimation of potential impact of climate change on the heating energy use of existing houses. *Energy Policy*, 36(1), pp. 303-310.